Loma Linda University Electronic Theses, Dissertations & Projects

9-2015

Palmitic Acid Activation of Dendritic Cells: Implications for Type 2 Diabetes

Dequina Angelina Nicholas

Recommended Citation

Nicholas, Dequina Angelina, "Palmitic Acid Activation of Dendritic Cells: Implications for Type 2 Diabetes" (2015). *Loma Linda University Electronic Theses, Dissertations & Projects*. 302.
https://scholarsrepository.llu.edu/etd/302

LOMA LINDA UNIVERSITY
School of Medicine
in conjunction with the
Faculty of Graduate Studies

————————————

Palmitic Acid Activation of Dendritic Cells: Implications for Type 2 Diabetes

by

Dequina Angelina Nicholas

————————————

A Dissertation submitted in partial satisfaction of
the requirements for the degree
Doctor of Philosophy in Biochemistry

————————————

September 2015

Each person whose signature appears below certifies that this dissertation in his/her opinion is adequate, in scope and quality, as a dissertation for the degree Doctor of Philosophy.

_____, Co-Chairperson
William H.R. Langridge, Professor of Biochemistry

_____, Co-Chairperson
Marino De Leon, Professor of Physiology

_____
Anthony Firek, Chief of Endocrinology and Diabetes, JL Pettis VA Medical Center and Loma Linda University Medical Center

_____
Kimberly Payne, Associate Professor of Pathology & Human Anatomy

_____
Christopher Perry, Assistant Professor of Biochemistry

_____
Ubaldo Soto, Assistant Research Professor of Microbiology and Molecular Genetics

_____
Nathan Wall, Assistant Professor of Biochemistry

ACKNOWLEDGEMENTS

CONTENTS

TABLES

FIGURES

ABBREVIATIONS

Ab	Antibody
ANOVA	Analysis of Variance
APC	Antigen Presenting Cell
BCE	Before the Common Era
Breg	B Regulatory Cell
BSA	Bovine Serum Albumin
ACN	Acetonitrile
CARD	Caspase activation and recruitment domains
CCL	Chemokine (C-C motif) Ligand
CD	Cluster of Differentiation
CLS	Crown Like Structures
CTL	Cytotoxic T lymphocyte
CXCL	Chemokine (C-X-C motif) Ligand
DAMP	Danger Associated Molecular Pattern
DAPI	4',6-diamidino-2-phenylindole
DC	Dendritic Cell
DIO	Diet Induced Obesity
DMSO	Dimethyl Sulfoxide
DPBS	Dulbecco's Modified Phosphate Buffered Saline
EtOH	Ethanol
FA	Fatty Acid
FBS	Fetal Bovine Serum

FSC	Forward Scatter
GFP	Green fluorescent protein
GM-CSF	Granulocyte Macrophage Colony Stimulating Factor
H	Histone
HSA	Human Serum Albumin
HbA1c	Hemoglobin A1c
HCD	Higher-energy Collisional Dissociation
IFN	Interferon
IgA	Immunoglobulin A
IgG	Immunoglobulin G
IL	Interleukin
iNOS	Inducible Nitric Oxide Synthase
IO	Ionomycin
IPA	Ingenuity Pathway Analysis
K	Lysine
KCl	Potassium Chloride
LRR	Leucine Rich Repeat
MCP-1	Monocyte Chemoattractant Protein 1
MHC	Major Histocompatibility Complex
MIP	Macrophage Inflammatory Proteins
MoM	Multiple of the Median
MS	Mass Spectometry
NADPH	Nicotinamide Adenine Dinucleotide Phosphate-oxidase

NFκB	Nuclear Factor Kappa-light-chain-enhancer of Activated B Cells
NK cell	Natural Killer Cell
NLRP	NOD or NACHT, LRR and PYD Domains-containing Protein
NOD	Nucleotide-binding Oligomerization Domain
NOX	Nitrogen Oxide
PA	Palmitic Acid
PAMP	Pathogen Associated Molecular Pattern
PBMC	Peripheral Blood Mononuclear Cell
PBS	Phosphate Buffered Saline
PCA	Principal Component Analysis
PMA	Phorbal 12-myristate 13-acetate
PRR	Pattern Recognition Receptor
PTM	Post translational modification
RANTES	Regulated on Activation, Normal T Cell Expressed and Secreted (also known as CCL5)
RPLC	Reverse Phase Liquid Chromatography
SCX	Strong Cation Exchange
SFA	Saturated Fatty Acid
SSC	Side Scatter
Th	T helper
TLR	Toll-like Receptor
TMT	Tandem Mass Tag
TNF	Tumor Necrosis Factor

TRAM	TRIF-related Adaptor Molecule
Treg	T regulatory Cell
TRIF	TIR-domain-containing Adapter-inducing Interferon-β
TXNIP	Thioredoxin-interacting Protein
TXR	Thioredoxin
VAT	Visceral Adipose Tissue

PREFACE

My journey to writing this dissertation began as child who watched her mother prick her finger every single day to check her blood sugar levels. As I grew to be a graduate student, I felt it was my purpose to research type 2 diabetes and contribute to improved therapies not only for my mother and other family members with the disease, but also for all people who continue to suffer from type 2 diabetes.

My primitive research goals involved understanding how inflammation contributed to diabetes. With great mentoring and more focus, I have spent the last 5 years researching the role of palmitic acid, a common saturated fatty acid derived from the diet, in the progression of inflammatory mechanisms in type 2 diabetes. Based on current knowledge in the fields of lipid biology, immunology, and type 2 diabetes the objective of this dissertation is to present the data I have been able to gather in support of the hypotheses underlying construction of the following diagram (Figure i). After presentation of the data in this dissertation, Figure i will be presented a second time as a working model for describing the role of palmitic acid in the stimulation of type 2 diabetes inflammation.
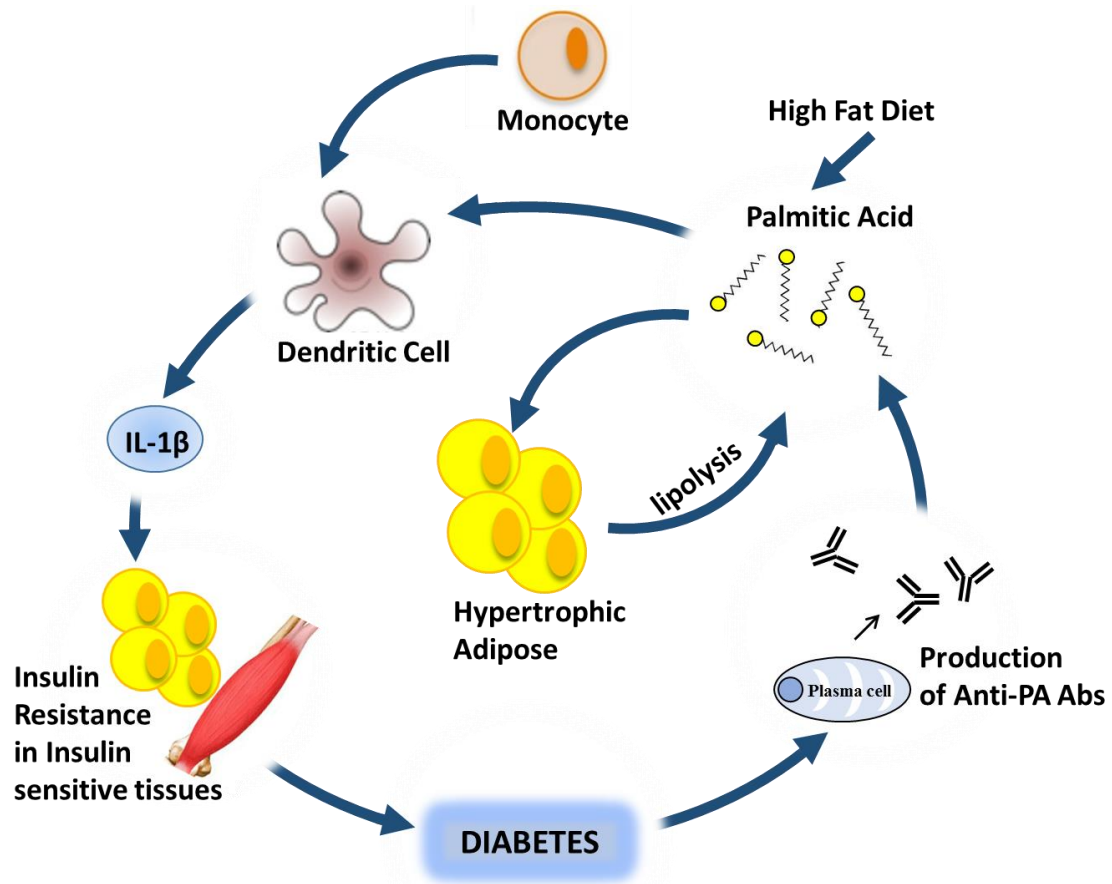
Figure i. Outline of Hypotheses tested in this dissertation. Hypotheses: (1) The differentiation of dendritic cells from monocytes is regulated by epigenetic changes, (2) palmtic acid activates dendritic cells, and (3) anti-palmitic acid antibodies are present in human serum.

This dissertation should be of interest to endocrinologists, immunologist, and lipid scientist, as well as dietitians and public health professionals who desire a more complete understanding of the etiology of type 2 diabetes. For me, completion of this dissertation has been a gratifying journey. Please enjoy the experience of my journey as you read.

ABSTRACT OF THE DISSERTATION

Palmitic Acid Activation of Dendritic Cells: Implications for Type 2 Diabetes

by

Dequina Nicholas

Doctor of Philosophy, Graduate Program in Biochemistry
Loma Linda University, September 2015
Drs. William Langridge and Marino De Leon, Co-Chairpersons

Infiltration of immune cells into visceral adipose tissue is observed in type 2 diabetes development. Monocytes are recruited to obese visceral adipose tissue in large numbers and retain the ability to differentiate into dendritic cells, important antigen presenting cells in the immune system. Differentiation of monocytes into dendritic cells likely accounts for the increased number of dendritic cells observed in the adipose tissue of type 2 diabetic patients. We have demonstrated this differentiation process is regulated in part by a major reduction of linker histone proteins. In adipose tissue, dendritic cells are exposed to high levels of saturated fatty acids. Increased saturated fatty acid levels derived from high fat diets are strongly associated with chronic adipose tissue inflammation. Palmitic acid, the most abundant of saturated fatty acids, is pro-inflammatory and has been linked to insulin resistance. However, the mechanisms underlying palmitic acid induction of inflammation remain unknown. We have confirmed palmitic acid binding to Toll-like receptor 4 (TLR4) on human dendritic cells. In response to palmitic acid activation of TLR4, dendritic cells were shown to secrete pro-inflammatory cytokines that may lead to insulin resistance. In addition, we identified anti-palmitic acid IgG antibodies in the serum of patients with unmanaged type 2 diabetes. In conclusion, diet-derived saturated fatty acids may act as mediators of chronic

inflammation associated with type 2 diabetes. Together, the experimental data presented

support the hypothesis that palmitic acid is an inducer of dendritic cell induced

inflammation and is an important target for type 2 diabetes therapy.

CHAPTER ONE

INTRODUCTION: FATTY ACIDS, INFLAMMATION, AND TYPE 2 DIABETES

Abstract

Approximately 285 million people worldwide have type 2 diabetes, and it is

projected that this number will more than double by the year 2030. Thus, it is imperative

to advance our understanding of diabetes pathogenesis. Regulation of diet, obesity, and

inflammation is thought to play a significant role in improving insulin sensitivity and

reducing the risk of diabetes onset. Visceral adipose tissue is a major site of inflammation

in type 2 diabetes, and dyslipidemia is a major factor in the recruitment of activated

immune cells including macrophages, dendritic cells, T cells, NK cells, and B cells to

visceral adipose tissue. The Immune cells in adipose tissue are a major source of pro-

inflammatory cytokine production thought to stimulate insulin resistance. In this review

of the literature, the role of increased dietary free saturated fatty acids and cellular and

molecular mediators linked to insulin resistance in the initiation of obesity-induced

inflammation are identified. In addition, novel concepts in diet-induced inflammation

and type 2 diabetes are discussed.

Introduction

Diabetes mellitus is a group of metabolic disorders characterized by high blood

glucose levels extending over a long period of time. Historically, this group of metabolic

diseases was first described in an Egyptian manuscript called the Ebers papyrus, dated to

1550 BCE (Bryan 2010). Egyptian historians noted that this disease was characterized by

polyuria (frequent urination). In addition, ants were attracted to the urine of people with

this disease because it was sweet (Bryan 2010). In the first century AD, the Greek physician Arateus described "siphon" (diabetes) as "the melting down of flesh and limbs" into urine (Engelhardt 1989). People who were suspected to have diabetes were diagnosed by "water tasters" who tasted the urine to see if it was sweet (Engelhardt 1989). By the 17-1800s the term "mellitus" or "from honey" was added to diabetes to differentiate it from diabetes insipidus (frequent urination due to dysregulation of antidiuretic hormone). In the 1900s, Frederick Banting and Charles Best discovered that a deficiency of insulin was responsible for the development of diabetes mellitus (Macleod and Banting 1923). Insulin and glucagon were found to be two major hormones responsible for regulating blood glucose levels (Cavallero, Malandra et al. 1954). Glucose induces the release of insulin, which activates insulin receptors and ultimately results in the insertion of glucose transporters into the cell membrane. These glucose transporters allow cells to use or store blood glucose, thereby removing excess glucose from the blood stream. Without effective insulin, blood glucose levels become chronically high and act as an osmotic diuretic. The diuretic property of high blood glucose levels causes the trademark symptom of frequent urination noted above.

Diabetes mellitus can be sub-classified into three major categories: type 1, type 2, and gestational diabetes. Type 1 diabetes is a well characterized autoimmune disorder which results in targeted destruction of pancreatic islet β-cells, the cells which secrete insulin. Type 2 diabetes is representative of 90-95% of all diabetes cases worldwide and is a complex metabolic disease generally resulting from insulin resistance. Insulin resistance is a state in which the body can produce insulin, but cells cannot utilize it effectively. Gestational diabetes occurs in 3-8% of pregnant women and may be caused

by hormones related to pregnancy or a shortage of insulin (Thomas and Philipson 2015). This literature review will be focused on type 2 diabetes and obesity-induced inflammatory immune mechanisms implicated in insulin resistance.

Worldwide, approximately 285 million people have been diagnosed with type 2 diabetes (Franks, Hanson et al. 2010, Hu 2011). In the U.S., healthcare costs are reported to be over 245 billion dollars annually (American Diabetes 2013). The growing incidence of type 2 diabetes is tied to a variety of risk factors. Genetic factors such as increased appetite and propensity to store abdominal fat may increase the risk of type 2 diabetes. However, modifiable factors such as a high energy or high fat diet, and reduced physical activity are believed to be the greatest contributors to disease development (Wheeler, Montgomery et al. 2012). These environmental factors appear to increase inflammation, a third major risk factor for development of type 2 diabetes. Chronic, low-grade tissue inflammation, especially in visceral adipose tissue is linked to obesity and development of type 2 diabetes (Olefsky and Glass 2010, Winer and Winer 2012). The remainder of this chapter will describe how high fat diets affect visceral fat inflammation, and its contribution to type 2 diabetes pathogenesis.

Diet, Adipose Tissue, and Type 2 Diabetes

Adipose Tissue in the Obese State

For decades, the association between poor diet and obesity in the development of type 2 diabetes has been extensively studied. Chronic-low grade inflammation is the factor that appears to link all three. Adipose tissue, now recognized as a major endocrine organ rather than simply an inert tissue for cushion and warmth, has been identified as the

major site for obesity-induced inflammation. The main function of adipocytes is to store energy in the form of lipids. Their secondary function as an endocrine organ involves the secretion of hormones such as leptin, estrogen, resistin and pro-inflammatory cytokines such as TNF-α. Recently, adipocytes have been shown to have direct immune function. They express CD40 and MHCII, which are involved in the activation of T cells in type 2 diabetes (Poggi, Jager et al. 2009, Deng, Lyon et al. 2013). Adipocytes can also secrete pro-inflammatory cytokines such as TNF-α and IL-1β, contributors to insulin resistance (Hotamisligil, Shargill et al. 1993, Hosogai, Fukuhara et al. 2007, Osborn, Gram et al. 2008). During the lean state, adipocytes synthesize IL-4 and IL-13, cytokines which have the ability to induce macrophage differentiation into the anti-inflammatory M2 phenotype (Figure 1) (Kang, Reilly et al. 2008). Alternatively, increased visceral adipose tissue results in chronic inflammation. In obese individuals, the secretion of pro-inflammatory substances such as non-esterified fatty acids (FAs) and cytokines is dramatically increased (Karpe, Dickmann et al. 2011). In the insulin resistant state, adipocytes undergo high levels of lipolysis and release free fatty acids (Figure 1). In addition, when stimulated by TNF-α (i.e. during obesity-induced inflammation), adipocytes produce and secrete the chemokine CCL5, a chemoattractant molecule which can recruit T cells to fat tissue (Wu, Ghosh et al. 2007).

Dietary Fatty Acids and Type 2 Diabetes

As previously mentioned, a large risk factor for type 2 diabetes is a diet high in fat. In particular, diets high in saturated fats provide a source of long chain saturated FAs. Increased levels of these dietary saturated FAs like palmitic and stearic acids have been

associated with the onset of inflammation and type 2 diabetes (Storlien, Jenkins et al.

1991, Kolb and Mandrup-Poulsen 2010, Oliver, McGillicuddy et al. 2010). Palmitic acid

(PA) is a highly abundant FA and is found primarily in palm oils, meats, and dairy

products. Because this FA is abundant in the Western diet, dietary FA composition

contributes significantly to the relative bio-availability and storage of PAs in body tissues

(Riserus, Willett et al. 2009). The conveience of processed foods coupled with high

caloric intake may result in obesity which subsequently leads to elevated serum and

tissue FAs that may be responsible for the onset of insulin resistance (Riserus, Willett et

al. 2009).

Increased levels of non-esterified FAs in serum are linked to metabolic

dysfunction, obesity, and an increased risk for development of type 2 diabetes (Paolisso,

Tataranni et al. 1995, Charles, Eschwege et al. 1997, Pankow, Duncan et al. 2004, Salgin,

Ong et al. 2012). Across several studies, non-esterified FAs have been shown to induce

insulin resistance in liver and skeletal muscle (Boden, Chen et al. 1995, Boden, Cheung

et al. 2002, Belfort, Mandarino et al. 2005). Too much serum non-esterified FAs are also

known to induce inflammation responsible for generating systemic insulin resistance

(Tripathy, Mohanty et al. 2003, Liang, Tantiwong et al. 2013). The mechanism by which

this pathology may occur is discussed in the following sections.

Saturated Fatty Acid Stimulation of Immune Cells

Although overall increased free FA levels negatively affect metabolic

homeostasis, not all non-esterified FAs are created equal. Non-esterified saturated fatty

acids derived from triglycerides in the diet or from lipolysis from adipose tissue are

generally considered pro-inflammatory. The most prominent mechanism emerging to explain how saturated FAs could impact immunity is focused on activation of the pathogen recognition receptor (PRR) Toll-like receptor 4 (TLR4) (Shi, Kokoeva et al. 2006). Several studies have shown TLR4 to be a link between innate immunity and fatty acid-induced insulin resistance (Shi, Kokoeva et al. 2006). Saturated FAs have been shown to activate macrophages through TLR4 (Lee, Sohn et al. 2001, Nguyen, Favelyukis et al. 2007, Suganami, Yuan et al. 2009). This observation is important because TLR4 signaling promotes the maturation of M1 macrophages, a macrophage phenotype responsible for secretion of TNF-α, IL-1, IL-6, IL-12, iNOS, monocyte chemoattractant protein 1 (MCP-1), and RANTES in inflamed adipose tissue during type 2 diabetes (Winer and Winer 2012). Saturated FAs have also been shown to activate adipocytes and microglia through TLR signaling (Song, Kim et al. 2006, Suganami, Tanimoto-Koyama et al. 2007, Wang, Liu et al. 2012). Further, our laboratory has shown that PA activates dendritic cells via TLR4 and induces secretion of IL-1β (Chapter 3). In further support of this concept, mice with a mutation in or deficient in TLR4 are protected from the inflammatory effects of a high-fat diet rich in PA (Suganami, Mieda et al. 2007, Davis, Gabler et al. 2008). Lastly, TLR4 in hematopoietic cells is critical for development of insulin resistance in adipose tissue (Shi, Kokoeva et al. 2006, Saberi, Woods et al. 2009). Although FA interference with TLR4 signaling has been clearly demonstrated, the mechanism of how saturated FAs interact with components of the TLR4 pathway have only recently been clarified (Chapter 3).

Visceral Fat Inflammation in Type 2 Diabetes

Visceral adipose tissue (VAT) has proven to be a key site for inflammation associated with type 2 diabetes (Winer and Winer 2012). There are several views regarding how adipose tissue inflammation begins. However, it is generally believed that a high fat diet and a subsequent increase in visceral adipose tissue are the underlying culprits for attraction of immune cells. Obesity results in apoptotic centers of hypertrophic adipocytes (Hosogai, Fukuhara et al. 2007, Rausch, Weisberg et al. 2008), leptin secretion, unfolded protein responses activated by ER stress (Hummasti and Hotamisligil 2010), secretion of MCP-1 from hypoxia activated macrophages and lipolysis that releases free FAs which ultimately lead to immune cell infiltration, inflammation, and insulin resistance (Halberg, Khan et al. 2009). Infiltration of visceral adipose tissue by immune cells results in low-grade chronic inflammation and secretion of pro-inflammatory cytokines which can induce insulin resistance both locally and systemically (Figure 1). Although the order of immune cell infiltration is disputed, it is becoming well understood that a variety of immune cells are involved in visceral fat inflammation (Winer and Winer 2012). In the following section, we will describe the major subsets of immune cells implicated in type 2 diabetes as well as deal with the emerging roles of lesser studied immune cell types.
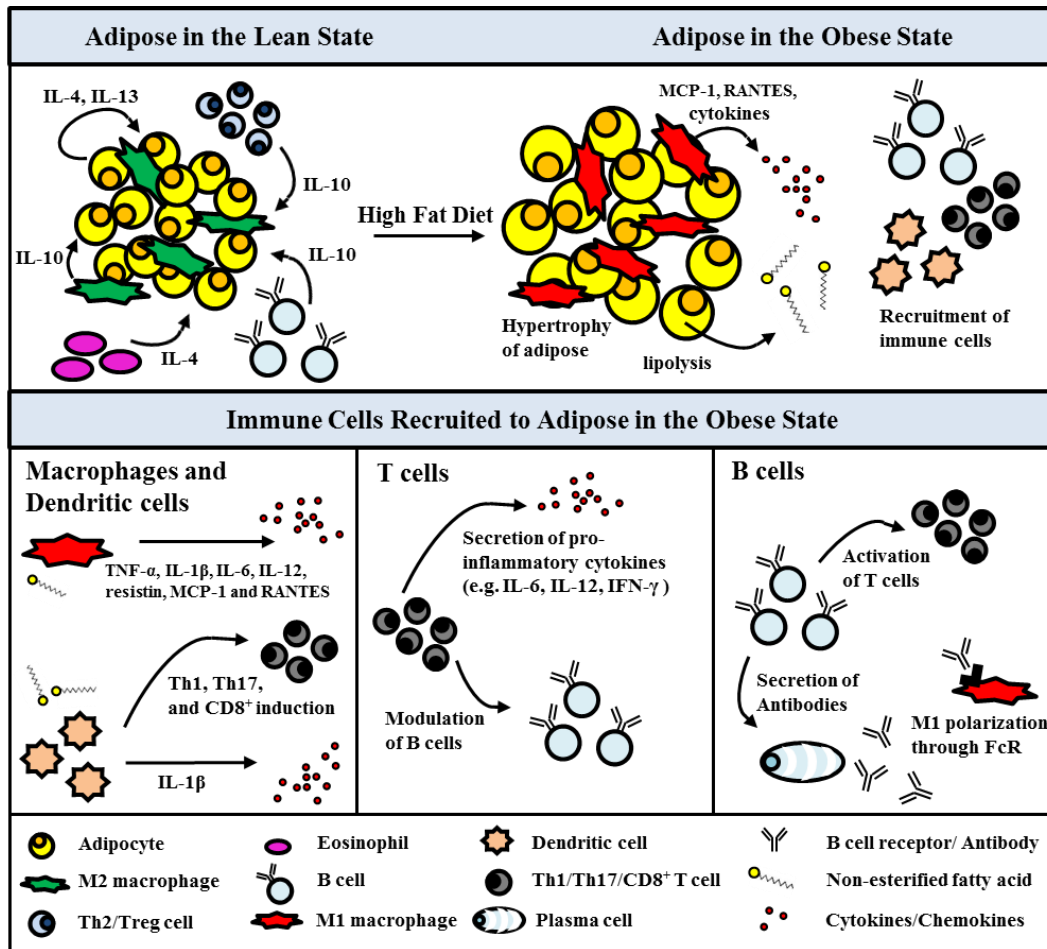
Figure 1. Overview of Obesity-induced Inflammation. In the lean state, resident macrophages are maintained in the M2 phenotype. A combination of IL-10 from Treg and Breg cells, IL-4 from eosinophils and adipocytes, and IL-13 from adipocytes polarize macrophages to M2, which also secrete IL-10. In the obese state, adipocytes become hypertrophic, form necrotic centers due to hypoxia, and undergo increased lipolysis. These conditions polarize macrophages to the M1 phenotype which results in the production of pro-inflammatory cytokines and chemoattractant molecules that recruit immune cells to the adipose tissue. Likely, increased saturated fatty acids from lipolysis activate macrophages and dendritic cells through TLR signaling. Activated M1 macrophages secrete cytokines that favor the maintenance of Th1, Th17, and CD8+ T cells. Dendritic cells secrete IL-1β which contributes to insulin resistance and directs differentiation of naïve T cells into pro-inflammatory subsets. Th1, Th17, and CD8+ T cells secrete classic pro-inflammatory cytokines which also polarize macrophages to the M1 phenotype. In addition, T helper cells provide stimulation to B cells which result in maximal antibody responses. B cells can act as antigen presenting cells and activate pro-inflammatory T cell subsets. After T cell help, B cells can differentiate into antibody secreting plasma cells. Antibodies from these B cells have the ability to polarize macrophages to the M1 phenotype and activate macrophages by binding Fc receptors.

Monocytes / Macrophages

Macrophages are presently the most studied immune cells in VAT inflammation. Macrophages are antigen presenting cells (APCs) deemed responsible for secreting the majority of cytokines during chronic inflammation. During the lean state, M2 (alternatively activated or anti-inflammatory) macrophages are present in VAT (Winer and Winer 2012). It is generally accepted that M2 macrophages survey the tissue, aid in remodeling, and help maintain VAT insulin sensitivity. M2 polarization is induced by IL-4, IL-10, and IL-13 (Lumeng, Bodzin et al. 2007). M2 macrophages secrete IL-10 and IL-1 receptor antagonist which are anti-inflammatory and protect against insulin resistance (Lumeng, Bodzin et al. 2007).

Resident macrophages recognize dead adipocytes and can be activated by FAs through TLR2 and TLR4 (Cinti, Mitchell et al. 2005). TLR4 induces M1 (classical activation) polarization of macrophages. These M1 macrophages differentiate from monocytes recruited to VAT during obesity-induced inflammation (Kraakman, Murphy et al. 2014). The infiltration of M1 macrophages disrupts the balance of M1/M2 (pro-/anti-inflammatory) macrophages which results in inflammation. The secretion of TNF-α, IL-1β, IL-6, IL-12, resistin, MCP-1 and RANTES by M1 macrophages recruit more monocytes and inhibit insulin signaling often through serine phosphorylation (Mantovani, Sozzani et al. 2002, Olefsky and Glass 2010). This infiltration of macrophages to the VAT plays a key role in obesity-induced inflammation. Inhibiting the infiltration of CD11b myeloid cells, namely macrophages, prevents the adverse effects of a high fight diet in mice (Wueest, Rapold et al. 2010). In further support, ablating M1 macrophages by targeting diphtheria-sensitive CD11c$^+$ cells with diphtheria toxin improved glucose

tolerance in diet-induce obese (DIO) mice (Patsouris, Li et al. 2008). Overall, the general role of macrophages in VAT inflammation is well defined (Kraakman, Murphy et al. 2014). However, the initial insult that induces the recruitment of monocytes to VAT is still under investigation.

Dendritic Cells

Dendritic cells (DCs) are professional antigen presenting cells which play a dominant role in linking the innate immune response to the adaptive immune response by presenting antigen on MHCII molecules to naïve T cells. The role of DCs in obesity-induced inflammation remains relatively unknown (Lee and Lee 2014). However, studies have shown a potential role for both the adaptive immune response and for DCs in obesity-induced inflammation (Winer and Winer 2012). A study aimed at examining the effect of depleting CD11c$^+$ adipose tissue macrophages in obese diabetic mice indicated DCs may play a key role in obesity-induced insulin resistance (Patsouris, Li et al. 2008). The authors of this study found that depletion of CD11c$^+$ cells in mice improved obesity-induced insulin resistance and reduced pro-inflammatory cytokines in the adipose tissue. Although these results were attributed to the adipose tissue macrophages, ablation of cells positive for CD11c, a classical dendritic cell marker, also depleted circulating DCs, which outnumber adipose macrophages (Hashimoto, Miller et al. 2011). Therefore, this study also indicates that circulating CD11c$^+$ DCs may contribute to obesity-induced-inflammation. In support of this conclusion, two laboratories have shown that the numbers of DCs in VAT in mice increase during obesity (Bertola, Ciucci et al. 2012, Stefanovic-Racic, Yang et al. 2012). Not only that, CD103 DCs, a subset known to be

10

important in the differentiation of Treg cells, is decreased in VAT of obese mice (Jaensson, Uronen-Hansson et al. 2008). Interestingly, Bertola et al, showed that DCs isolated from VAT of obese mice induced naïve T cells to differentiate *in vitro* into Th17 cells, a T cell subset which antagonizes Treg function (Bertola, Ciucci et al. 2012). However, changes in Th17 populations in VAT *in vivo* have not yet been identified. In addition to macrophages and B cells, resident DCs recognize dying adipocytes. Mechanistic studies from our laboratory and others have indicated how the innate functions of DCs may play a role in obesity-induced inflammation. Due to obesity-induced hypoxia and increased lipolysis in adipose tissue, DCs are activated by apoptotic debris and free fatty acids via Toll-like receptors (TLRs) (Cinti, Mitchell et al. 2005) (Chapter 3). The activation of DCs through TLRs induces secretion of pro-inflammatory cytokines linked to adipose inflammation and insulin resistance. Although there is sufficient evidence for the innate function of DCs in obesity-induced inflammation, increased research efforts are needed to understand how the adaptive function of DCs might influence B and T cells during this chronic inflammatory response.

T Cells

T cells were identified in VAT almost 15 years ago (Bornstein, Abu-Asab et al. 2000). T cells regulate macrophage polarization and are thought to regulate inflammation during insulin sensitive/resistant states (Winer and Winer 2012). In addition, depletion of $CD3^+$ T cells reduced VAT inflammation, glucose intolerance, and insulin resistance in diet-induced obese (DIO) mice (Nishimura, Manabe et al. 2009). Believed to infiltrate VAT after B cells, T cells and their role in type 2 diabetes inflammation has now been

extensively studied (Lee and Lee 2014). Like B cells, T cells are divided into various subsets depending on their phenotype and function. T regulatory cells (Tregs) are an anti-inflammatory subset of T cells which help mediate VAT homeostasis during the lean state in mice. Tregs can reduce VAT inflammation and insulin resistance, secrete IL-10 to polarize macrophages to the anti-inflammatory M2 phenotype, and block TNF-α induced pro-inflammatory cytokines such as IL-6 (Lumeng, Bodzin et al. 2007, Winer and Winer 2012). Additionally, the percentage of Tregs in VAT directly correlate with insulin sensitivity (Feuerer, Herrero et al. 2009). Normally, Tregs comprise 30-50% of T cells in VAT and hyper-express IL-10 (Feuerer, Herrero et al. 2009). On the other hand, the proportion of Treg cells in VAT decrease during the obese state (Feuerer, Herrero et al. 2009, Nishimura, Manabe et al. 2009, Winer, Chan et al. 2009), likely due to the increase in recruited pro-inflammatory cells. This same decrease has also been found in humans (Zeyda, Huber et al. 2011).

The pro-inflammatory T cell subsets most implicated in type 2 diabetes inflammation are Th1 cells and CD8^{+} T cells. In general, DIO mice have three times more VAT T cells than mice fed a standard diet, indicating increased T cell recruitment (Wu, Ghosh et al. 2007). These T cells are found co-localized with clusters of macrophages and dying (apoptotic/necrotic) adipocytes called crown like structures (CLS) (Olefsky and Glass 2010) (Rausch, Weisberg et al. 2008).The importance of T cells in obesity stimulated insulin resistance is highlighted by the fact that the inhibition of T cell migration to VAT prevents insulin resistance in DIO mice (Kendall and Hupfeld 2008). Both the percentage and total number of IFN-γ producing Th1 cells are increased in VAT of mice fed a high fat diet (Rocha, Folco et al. 2008, Winer, Chan et al. 2009,

Strissel, DeFuria et al. 2010) . This scenario has also been found to occur in humans (O'Rourke, Metcalf et al. 2009, Winer, Chan et al. 2009). IFN-γ aids in the polarization of macrophages to the M1 phenotype. Th1 cells also secrete IL-12. Th1 deficient IL-12p35 null mice on a high fat diet have improved insulin sensitivity (Winer, Chan et al. 2009). Th1 cells are not the only T cell subset implicated in obesity-induced inflammation. CD8^{+} T cells are found to increase in VAT of DIO mice after 2 weeks (Nishimura, Manabe et al. 2009). Most are activated and they co-localize with CLS (Nishimura, Manabe et al. 2009). CD8^{+} T cells help to recruit M1 macrophages as indicated by the reduction of M1 macrophages, IL-1, IL-6, TNF-α, MIP-α, and RANTES in VAT when CD8^{+} T cells were abolished (Nishimura, Manabe et al. 2009). Lastly, CD8^{+} T cells may also function in supporting monocyte differentiation (Nishimura, Manabe et al. 2009).

B Cells

B cells have recently been shown to play a role in type 2 diabetes. They consist of two major subsets, B-1 and more commonly, B-2 cells (Winer and Winer 2012). B-1 cells are further divided into B-1a cells which produce the majority of natural IgM and B-1b cells which are involved in the T cell-independent antigen humoral response (Rothstein, Griffin et al. 2013). B-2 cells, on the other hand, respond to T cell dependent antigens. Another subset of B cells, the B-10 cells are IL-10 producing B cells which are part of a larger subset called B regulatory cells (Bregs) (Iwata, Matsushita et al. 2011). Much of what is known regarding the role of B cells in type 2 diabetes and visceral fat inflammation is derived from DIO mice studies. B cells are known to be involved in type 2 diabetes because B cell deficient DIO mice have increased insulin sensitivity (Winer,

13

Winer et al. 2011). In the lean state, adipose natural B regulatory cells (Breg and B-10), in addition to spleen derived B-10 and B-1a cells are known to secrete IL-10 and protect against insulin resistance (Nishimura, Manabe et al. 2013, Shen, Yen Chng et al. 2014, Wu, Parekh et al. 2014). However, during obesity, the total number of B cells increases in VAT, as well as the amount of pro-inflammatory B-2 cells (Duffaut, Galitzky et al. 2009, Winer, Winer et al. 2011). Transfer of B-2 cells from DIO mice to DIO B cell null mice deteriorates metabolic status (Winer, Winer et al. 2011). It has been shown that there is increased class switching of B cells to IgG and that transfer of IgG from DIO mice, but not from lean mice, worsens insulin resistance (Winer, Winer et al. 2011). In addition, B cells induce MHC dependent secretion of cytokines from T cells such as IFN-γ, which can polarize macrophages to a pro-inflammatory M1 phenotype. Although less about the role of B cells in type 2 diabetes in humans is known, Winer et al.. has shown that distinct profiles of autoantibodies are associated with insulin resistance (Winer, Winer et al. 2011, Winer and Winer 2012). Additionally, B cells from type 2 diabetics secrete less IL-10 in response to TLR2, 4, or 9 stimulation (Jagannathan, McDonnell et al. 2010). However, B cells do not induce insulin resistance on their own. Transfer of B cells from DIO mice to DIO mice lacking both T and B cells has little effect on glucose tolerance (Winer, Winer et al. 2011). Therefore, much of B cells' role in type 2 diabetes may be mediated through T cell dependent mechanisms.

Other Immune Cells

The immune system is very complex, and although much research regarding obesity-induced inflammation has been focused on B cells, T cells, and macrophages, a

host of other cellular players have been implicated. Neutrophils have been shown to transiently migrate into VAT and inhibition of neutrophils improves obesity-induced insulin resistance and macrophage accumulation (Elgazar-Carmon, Rudich et al. 2008, Talukdar, Oh da et al. 2012). In addition, obesity in response to a high fat diet increases neutrophil infiltration within a week (Talukdar, Oh da et al. 2012). These results suggest that, similar to a classic immune response, neutrophils are one of the first cells recruited to the site of "infection" (Lee and Lee 2014). Eosinophils produce the majority of IL-4 in VAT during the lean state. This IL-4 has been shown to be critical in polarizing macrophages to the M2 phenotype in M2-GFP reporter mice (Wu, Molofsky et al. 2011). Conversely, obesity decreases the number of eosinophils in the adipose tissue indicating that this cell type may be involved in regulating macrophages during obesity-induced inflammation. Mast cells, although strongly associated with allergy and asthma, have been shown to be important in obesity-induced insulin resistance. Deletion of mast cells in a high fat diet mouse model improves insulin resistance and reconstitution of mast cells worsens it. However, reconstitution of mast cells in IL-6 or IFN-γ knock out DIO mice did not worsen insulin resistance. This data indicates that IL-6 or IFN-γ made by mast cells in VAT are important to the development of insulin resistance (Liu, Divoux et al. 2009). NKT cells, which generally recognize lipid antigens presented on CD1d molecules, are found to be increased in VAT in response to a high fat diet in mice within 6 weeks (Ohmura, Ishimori et al. 2010). However, CD1d deficient mice present no differences in insulin resistance and glucose intolerance (Mantell, Stefanovic-Racic et al. 2011). Several studies have published contradictory results regarding the role of NKT cells in obesity-induced inflammation. Therefore, more research is necessary to

15

investigate the role of NKT cells and other cellular players in the development of VAT inflammation.

Systemic Inflammation in Type 2 Diabetes

Chronic inflammation due to obesity does not only affect the VAT. Increased secretion of pro-inflammatory cytokines by immune cells in the adipose tissue also causes systemic inflammation and insulin resistance in muscle tissue. A summary of these cytokines changes are presented in Figure 2. Although many cytokines and chemokines are involved in obesity-induced inflammation, TNF-α, IFN-γ, IL-6, and especially IL-1β have been closely linked to systemic insulin resistance.

TNF-α

TNF-α was the first pro-inflammatory cytokine to be associated with obesity and insulin resistance (Hotamisligil, Shargill et al. 1993). TNF-α is known to inhibit triglyceride deposition and induce lipolysis (Kim, Tillison et al. 2006, Yang, Zhang et al. 2011, Jin, Sun et al. 2014). Similar to non-esterified free fatty acids, TNF-α inhibits insulin stimulated IRS-1 tyrosine phosphorylation and glucose uptake by GLUT4 (Lumeng, Bodzin et al. 2007).

Immune Cell Changes in T2D	
↑ B cells	↔ δγT cell
↑ CD8$^+$ T cells	? NK
↑ Th1 cells	
↑ Th17 cells	↓ Treg cells
↑ NKT cells	↓ Eosinophils
↑ Mast Cells	↓ Th2 cells
↑ M1 macrophages	↓ M2 Macrophages

Cytokine Changes in T2D	
↑ IL-1	↓ IL-4
↑ IL-6	↓ IL-10
↑ IL-8	↓ IL-13
↑ IL-18	
↑ TNF-α	
↑ NO	
↑ IFN-γ	

Figure 2. Summary of cellular and cytokine changes during obesity-induced inflammation.

Two studies in patients with rheumatoid arthritis undergoing infliximab (monoclonal antibody against TNF-α) therapy showed a rapid beneficial effect on insulin resistance and sensitivity (Gonzalez-Gay, Gonzalez-Juanatey et al. 2010, Stagakis, Bertsias et al. 2012). However, several follow up studies and other studies using neutralizing anti-TNF-α antibodies such as Etanercept did not show any improvement in insulin sensitivity (Bernstein, Berry et al. 2006, Ferraz-Amaro, Arce-Franco et al. 2011). Although conflicting results have been found using TNF-α as a target for the treatment of type 2 diabetes and obesity-induced inflammation, this cytokine is important because it introduced a link between inflammation, obesity, and insulin resistance.

IFN-γ

IFN-γ is another pro-inflammatory cytokine shown to be related to insulin

resistance. Glucose intolerance and insulin sensitivity is increased in IFN-γ deficient DIO

mice (Rocha, Folco et al. 2008). In addition, IFN-γ reduces insulin-induced uptake of

glucose in adipocytes and can polarize macrophages to the M1 phenotype (Nathan,

Murray et al. 1983, Martinez, Sica et al. 2008, McGillicuddy, Chiquoine et al. 2009).

Lastly, IFN-γ, can induce the expression of T cell and monocyte chemoattractant proteins

such a RANTES and MCP-1 and 2 from an adipocyte cell line (Rocha, Folco et al. 2008).

IL-6

IL-6 is a classical pro-inflammatory cytokine that has also been implicated in

metabolic inflammation. In obesity, IL-6 is increased (Pal, Febbraio et al. 2014). This

increased IL-6 is associated with increases in systemic Th17 cells in DIO mice (Winer,

Paltser et al. 2009). Although the role of IL-6 in insulin resistance is controversial, it has

been targeted as potential treatment for metabolic inflammation. For example,

rheumatoid arthritis patients with diabetes experienced an HbA1c drop when treated with

anti-IL-6 antibody Tocilizumab (Ogata, Morishima et al. 2011).

IL-1β

IL-1β has recently become the most prominent cytokine attributed with inducing

insulin resistance. Once IL-1β is produced, it must be processed into its mature form by

caspase-1, which is activated by the NOD-, LRR- and pyrin domain-containing 3

(NLRP3) inflammasome. IL-1β expression is upregulated during obesity and is strongly

related to a high fat diet (Table 1). Our laboratory has shown that it is positively

correlated to the amount of saturated FA intake, specifically dietary PA (Table 1).

Table 1. Serum IL-1β from Hispanic patients with type 2 diabetes (n =7) correlates with dietary fat intake. IL-1β was measured in serum samples obtained from participants in the *En Balance* diabetes intervention program and correlated with dietary intake via the University of Arizona Southwest Food Frequency Questionnaire (Ojo, Beeson et al. 2010, Salto, Cordero-MacIntyre et al. 2011). P-value <0.05 is a significant correlation.

Variables	Spearman Correlation	p-value
Total dietary fat intake (g)	0.821	0.023
Energy (kcal)	0.929	0.003
Dietary Cholesterol (mg)	0.786	0.036
Fatty acids saturated (g)	**0.857**	**0.014**
10:0 Capric acid (g)	0.786	0.036
16:0 Palmitic acid (g)	**0.893**	**0.007**
18:0 Stearic acid (g)	0.821	0.023
Fatty acids monounsat.(g)	0.821	0.023
18:1 Oleic Acid (g)	0.821	0.023

Additionally, we have shown that PA directly induces the secretion of IL-1β from

dendritic cells by binding TLR4 (Chapter 3). Free FAs may also directly activate the

NLRP3 inflammasome (Legrand-Poels, Esser et al. 2014). High concentrations of

glucose promote the dissociation of thioredoxin-interacting protein (TXNIP) from its

inhibitor thioredoxin (TXR) which results in the activation of NLRP3 and the secretion of

IL-1β from β-cells (Donath and Shoelson 2011). IL-1β induces the production of a wide

range of cytokines and chemokines implicated in insulin resistance and type 2 diabetes

such as CC-chemokine ligand 2 (CCL2), CCL3 and CXC-chemokine ligand 8 (CXCL8)

(Donath and Shoelson 2011). These chemokines lead to the recruitment of macrophages. Because of IL-1β's role in insulin resistance and obesity-induced inflammation, it has become the target of several clinical trials. Therapeutics against IL-1β show promise for treating type 2 diabetes. Patients with type 2 diabetes who were treated with Anakinra, Interleukin-1 receptor antagonist (IL-1Ra), for 13 weeks had reduced HbA1c, reduced systemic IL-6, IL-17, and C-reactive peptide, and increased secretion of C-peptide (Larsen, Faulenbach et al. 2007). These effects lasted up to 39 weeks post withdrawal from the medication (Larsen, Faulenbach et al. 2009). However, insulin sensitivity did not change, although blocking IL-1 improved β-cells function and reduced markers of systemic inflammation.

Novel Concepts in Diet-induced Inflammation and Type 2 Diabetes

It is now widely accepted that type 2 diabetes is more than just a metabolic disease. Insulin resistance seems to be driven by high fat diets and obesity in an inflammation dependent manner. The involvement of adipocyte MHCII and Fc receptors (FcRs), autoantibody signatures, and restricted T cell repertoires in obese VAT suggests that inflammation associated with insulin resistance is not non-specific (Palming, Gabrielsson et al. 2006). Clearly, the net pro-inflammatory environment in obese VAT (IL-1β, IL-12, IL-18, and TNF-α) favors a Th1 response. Th1 and CD8^{+} T cells induce and perpetuate macrophage activation during obesity-induced inflammation and B cells support this inflammation by secreting antibodies which can activate macrophage FC receptors (Winer, Winer et al. 2011, Winer and Winer 2012). The emerging role of

specific responses from the adaptive immune system suggests that antigen presenting cells may play a key role in the development of obesity-induced inflammation.

Dendritic cells, professional antigen presenting cells which activate naïve T cells, have been used to demonstrate how constituents of a high fat diet, namely palmitic acid, could directly contribute to insulin resistance and obesity-induced inflammation. Palmitic acid was shown to elicit a robust IL-1β response from dendritic cells in a TLR4 dependent manner (Chapter 3). The pro-inflammatory cytokine IL-1β can induce insulin resistance by affecting insulin receptor phosphorylation and insulin receptor substrate 1 expression (Jager, Gremeaux et al. 2007). In addition, there is now evidence that FAs could directly stimulate the inflammasome, also important in the development of insulin resistance and type 2 diabetes (Esser, Legrand-Poels et al. 2014, Legrand-Poels, Esser et al. 2014, Moon, Lee et al. 2015).

Until recently, the mechanism by which saturated FAs activate TLR4 has been elusive. Our laboratory has recently demonstrated that PA is an actual TLR4 ligand (Chapter 3). Further research will be necessary to determine which other saturated FAs can bind TLR4 in addition to understanding how polyunsaturated fatty acids block TLR4 signaling (Lee, Sohn et al. 2001, Legrand-Poels, Esser et al. 2014). Lastly, the emerging role of B cells and antibodies in obesity-induced inflammation leads to the concept that diet and lipids may affect B cell function in type 2 diabetes (Winer, Winer et al. 2011). Our laboratory recently identified IgG antibodies in human serum that can recognize non-esterified saturated FAs (Chapter 5). These antibodies appear to be elevated and more frequent in populations with unmanaged diabetes. Although the role of these antibodies

are unknown, their presence indicates lipids may somehow be involved the immune

responses seen in type 2 diabetes.

.

Summary and Conclusion

It has long been understood that a high fat diet plays a large role in the

pathogenesis of type 2 diabetes. More recently, we are beginning to understand that diet

and obesity can have a direct effect on inflammation associated with type 2 diabetes.

However, interactions between the constituents of the foods we eat and our immune

system are poorly understood. Non-esterified long chain saturated FAs such as PA are

associated with obesity, insulin resistance, and inflammation. It is now clear that

saturated fatty acids have the potential to act directly on immune cells and induce a

cascade of events that ultimately contributes to insulin resistance. It is imperative to

better understand the mechanisms by which free fatty acids interact with the immune

system in order to design effective therapeutics for obesity-induced inflammation and

type 2 diabetes.

CHAPTER TWO

A ROLE FOR EPIGENETIC REPROGRAMMING DURING HUMAN MONOCYTE DIFFERENTIATION TO DENDRITIC CELLS (PUBLISHED IN THE JOURNAL OF CELLULAR AND MOLECULAR PROTEOMICS, 2015)

Abstract

Recruitment of monocytes to visceral adipose tissue and their subsequent differentiation is an important event in obesity-induced inflammation. Epigenetic reprogramming is thought to play an important role during monocyte differentiation into dendritic cells. To further understand the regulators of this differentiation process, we characterized monocytes and monocyte-derived dendritic cells with mass spectrometry based protein/histone expression profiling. Our data show that linker histone H1 proteins are significantly downregulated during monocyte differentiation. While highly enriched H3K9-methyl/S10-phos/K14-acetyl tri-modification forms of histone H3 were identified in monocytes, they were dramatically reduced in dendritic cells. In contrast, histone H4 K16 acetylation was found to be markedly higher in dendritic cells than in monocytes. We also found that global hyperacetylation generated by the nonspecific histone deacetylase HDAC inhibitor Apicidin induces monocyte differentiation. Together, our data suggest that specific regulation of inter- and intra-histone modifications including H3 K9 methylation, H3 S10 phosphorylation, H3 K14 acetylation, and H4 K16 acetylation must occur in concert with chromatin remodeling by linker histones for differentiation of human myeloid cells into dendritic cells. Understanding this process may lead to therapeutics which can manipulate monocyte differentiation and the obesity-induced inflammatory response.

Introduction

In type 2 diabetes, the number of dendritic cells (DCs) in adipose tissue is increased (Lee and Lee 2014). This increase in DCs is likely due to the recruitment of monocytes and subsequent differentiation in response to adipose tissue inflammation, similar to what occurs during colitis (Rivollier, He et al. 2012). Differentiation of monocytes from human peripheral blood mononuclear cells (PBMC) into dendritic cells using GM-CSF + IL-4 has frequently been used as a model for understanding the process of dendritic cell immune responses to inflammatory stimuli, viral infection, and environmental cues (Takashiba, Van Dyke et al. 1999, Baek, Haas et al. 2009, Fangradt, Hahne et al. 2012). In human bone marrow, myeloid progenitors give rise to macrophage/dendritic cell progenitor cells from which are derived monocytes, macrophages, and dendritic cells. However, epigenetic regulation or reprogramming in this complex differentiation system is not yet fully understood.

Previous studies demonstrated that histone H1s are differentially expressed and incorporated into chromatin during embryonic stem cell differentiation and reprogramming to pluripotency (Terme, Sese et al. 2011). The linker histone H1s "beads-on-a-string" structure aids chromatin folding into highly compacted 30 nm chromatin fibers (Misteli, Gunjan et al. 2000). In addition, the three histone H1 isoforms, H1.3, H1.4 and H1.5, are required for embryonic stem cell differentiation as demonstrated by *in vivo* H1.3/H1.4/H1.5 triple null experiments (Zhang, Cooke et al. 2012). Histone H1 null cells exhibit altered nucleosome architecture (Hashimoto, Takami et al. 2010) which may cause epigenetic reprogramming (Terme, Sese et al. 2011), specific changes in gene regulation including repression of pluripotency gene Oct4

expression (Fan, Nikitina et al. 2005, Zhang, Cooke et al. 2012), and cell growth (Fan, Nikitina et al. 2003, Sancho, Diani et al. 2008). In our experiments, CD14$^+$ monocytes were treated with GM-CSF + IL-4. After treatment, monocyte differentiation into dendritic cells was assessed by mass spectrometry and bioinformatics analyses.

In this chapter, we describe unique protein expression profiles, specifically the linker histones, between monocytes and dendritic cells. We identified H3K9-methyl/S10-phos/K14-acetyl tri-modification forms in monocytes, but not in dendritic cells. In addition, histone H4 K16 acetylation was low in monocytes but significantly higher in dendritic cells. Our findings suggest that monocyte-to-dendritic differentiation involves a switch from H3 tri-modification and high linker histone expression to histone H4 K16 acetylation and reduced histone H1.

Materials and Methods

Monocyte Isolation, Differentiation, and Flow Cytometry Analysis

Peripheral blood from healthy adult donors (age 18+) were collected from plasma apheresis filters from Lifestream blood bank, San Bernardino, CA, according to Loma Linda University IRB requirements. Leukocytes were obtained by lysing the red blood cells using ACK lysis buffer (8.3g/L NH4CL, 1.0g/L KHCO3, 3.7mg/L EDTA Na) according to standard protocol (Life Technologies). CD14$^+$ cells were isolated from the leukocyte fractions with anti-CD14 micro beads (MACS, Miltenyi biotech).

Monocytes were cultured in RPMI 1640 supplemented with 10% FBS at a density of 10^6 cells per 1 mL. In parallel, monocytes were cultured in RPMI 1640 media with

50ng/mL GM-CSF + 10ng/mL IL-4 for 6 days to obtain dendritic cells, respectively

(Figure 3). Monocytes were also cultured in 1μM Apicidin (Santa Cruz Biotechnology).
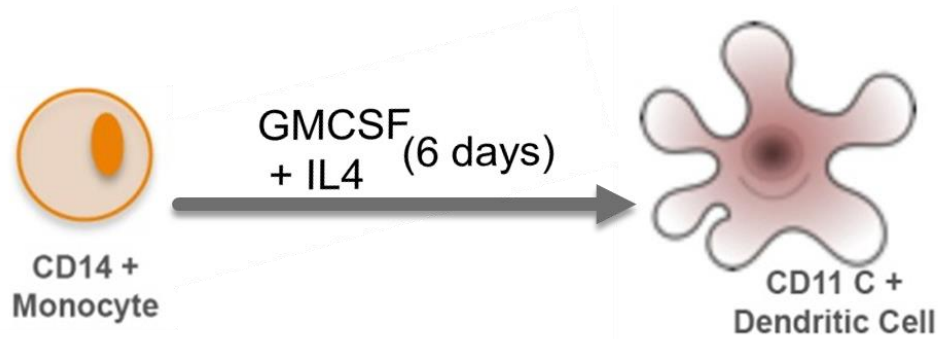
Figure 3. A brief outline of the myeloid cell differentiation process and the differentiation strategies adopted in this study.

Cells were stained for flow cytometry with the following antibodies (Ab): anti-CD14 APC (Miltenyi), anti-CD11b PE, anti-H1.5 (Abcam), anti-H4K16Ac (Abcam), anti-H3K9Me3, anti-H3S10p, anti-H3K9Me3S10pK14Ac, anti-Rabbit IgG FITC (Biolegend), anti-HLA-DR PerCP (Beckton Dickenson), and fixable viability dye eFlour 450 (eBioscience) according to standard protocol. For intracellular histone staining, cells were fixed with 4% paraformaldehyde for 10 min, permeabilized with Odyssey blocking buffer (Licor Inc.) + 0.2% Triton-X 100, then stained with 1°Ab followed by the 2°Ab at room temperature for 45 min each. Cells were then washed with PBS and resuspended in 195 μl PBS + 5 μl Propidium Iodide (eBioscience) + 50μl/mL RNAse. Cells were run on a MACSQuant flow cytometer and data was analyzed using FlowJo software v.7.6 (Tree Star, Ashland, OR).

Sample Preparation and Mass Spectrometry Analysis

The cell pellet was lysed in RIPA lysis buffer (Santa Cruz Biotechnology, CA) with additionally added 1% Nonidet P40, PMSF (0.2mM), and protease inhibitor cocktail (Roche, one tablet per 10 mL) with the assistance of sonication (3 x 30 strokes) and incubation on ice for 2 hours. The protein mixture was centrifuged and the supernatant transferred into a clean tube. This extraction procedure was carried out twice and the supernatants were combined. The protein concentration in the supernatant was determined by BCA assay. Approximately 60 µg of each protein sample was resuspended in 25mM triethylammonium bicarbonate, pH 7.8. The protein solution was reduced by addition of 10 mM DTT and incubation at 50 $^{\circ}$C for 30 min, followed by carbamidomethylation with 25 mM iodoacetamide in the dark for 1 hr. The proteins were precipitated by addition of 4 volumes of -20 $^{\circ}$C precooled acetone and stored at -20 $^{\circ}$C overnight. The protein was pelleted by centrifugation at 14,000 rpm for 10 minutes and the supernatant was discarded. The protein pellet was dissolved in 25 mM triethylammonium bicarbonate buffer and digested by trypsin at a protein/trypsin enzyme ratio of 25:1 (by mass) for 10 hours at 37 $^{\circ}$C.   The TMT (Tandem Mass Tag) isobaric Mass Tagging Kit (Thermo-Fisher Scientific) was used to label the peptides following the manufacturer's recommended conditions. Each TMT-labeled protein pool was acidified with 0.1% formic acid and fractionated with strong cation-exchange (SCX) chromatography on a Toptip column (Poly LC, MD). For fractionation, the matrix was equilibrated with 0.1% formic acid in 20% acetonitrile (ACN) to facilitate peptide binding. After collection of the flow-through, 1 mL of each subfraction was sequentially eluted with 20% ACN, 0.05M KCl, 0.2M KCl, 0.35 M KCl, 0.5M KCl, and 5%

ammonium hydroxide in 20% ACN. Next, the fractions were dried under vacuum to remove ACN, reconstituted in 1% formic acid, and then desalted using a Toptip column with C18/hypercarb mixed materials (Poly LC, MD). The eluted peptides were once again vacuum-dried, reconstituted in 30 μl of 0.1% formic acid, and then subjected to LC-MS/MS analysis. Quantitation of SCX fractionated TMT-6 labeled peptides was carried out on the Thermo LTQ-Orbitrap Velos Pro mass spectrometer. Peptides were separated by online reverse phase liquid chromatography (RPLC) using an Easy-nLC equipped with an autosampler (Thermo Scientific). A 10 cm, 75 μm id (internal diameter of the column), 3-μm particle size, C18-A2 analytical column (Thermo) was used for the RPLC separations. Approximately 2 μg of peptide sample was injected. A precolumn (Thermo, 0.1 × 2 cm, 5 μm C18-A1) was brought in line with the analytical column and a 250-min gradient (solvent A, 0.1% FA in water; solvent B, 0.1% FA in ACN) from 5–30% solvent B was used for separating the peptides. The Orbitrap mass analyzer was set to acquire data at 60,000 FWHM resolution for the parent full-scan mass spectrum followed by data-dependent high collision-energy dissociation (HCD) MS/MS spectra for the top 12 most abundant ions acquired at 7500 resolution.

Data Analysis

Proteins were identified and quantified through the Proteome Discoverer 1.3 platform (Thermo) by using both Mascot searching engine (Mascot Darmon 2.2.2; Matrix Science, London, UK) and Sequest HT (employing the International Protein Index (IPI) *Homo Sapiens* database (version 3.73, June 2010, containing 89739 entries). Mascot (or Sequest) searching parameters were used as follows: Carbamidomethylation of cysteine

and TMT-6 modification of peptide N-terminus and lysine were set as fixed

modifications and oxidation of methionine and deamination of asparagine and glutamine

were set as variable modifications, trypsin was the protease selected and up to two missed

cleavages was used. Mass tolerance for the precursor ions was 10 ppm and for the

MS/MS 0.2 Da. Only peptides with minimal length of four amino acids were considered

and peptides were filtered for maximum false discovery rate of 1%. At least one unique

peptide with posterior error probability of less than 0.05 was accepted for quantification

using the TMT-reporter ions and proteins were grouped.

Bioinformatic Analysis

Multivariate statistics analysis using the "R" program has previously been utilized

for metabolic profiling (Reitman, Jin et al. 2011). We have adapted this method for

protein expression statistics analysis. Multivariate statistics and associated graphics were

performed in R, version 64.25.1. Heat maps were drawn using the heatmap.2 function

found in the gplots package. Ingenuity Pathway Analysis (IPA) of protein

functions/pathways or upstream regulators was performed using individual or the

combined protein expression dataset from two monocyte GM-CSF treatment

experiments. The activation z-scores (a numerical value representing the strength of the

relationship between a set of proteins and a function/disease) of "Cell movements" and

"Functions for Hematological System Development" from IPA analysis were extracted

for multivariate statistics analysis to determine cell motility patterns associated with cell

differentiation. Principal component analysis (PCA) was performed using the prcomp

function in R and the calculation was based upon a singular value decomposition of the

centered and scaled data matrix. The first two principal components, PC1 and PC2, which contributed to the majority of the variance in the dataset, were plotted using the built-in biplot function.

Statistical Analysis

Determination of statistical significance of histone H1 expression among treatment groups was completed using two-way ANOVA in GraphPad Prism v6. For TMT measurement of Histone H1s, five biological replicates were performed. A web based Java code based on the Sattherwaite equation (Zhang, Schrag et al. 2012) was written for calculation of the degrees of freedom (v or DF) and t-values that were used for calculation of p-values. Significance was accepted at $p = 0.05$. In figures, $* = p < 0.05$, $** = p < 0.01$, $*** = p < 0.001$, and $**** = p < 0.0001$.

Antibody Generation

A rabbit polyclonal antibody against histone H3 K9Me3S10pK14Ac was made as described (Xu, Zhang et al. 2005) using a synthetic peptide containing histone H3 sequence: KQTAR(K-Me3)(S-Pho)TGG(K-Ac)APRKQC. Specificity of this anti-H3 tri-modification antibody was further tested by ELISA (data not shown). K9Me3S10pK14Ac peptide was conjugated to KLH as described by the manufacturer (Pierce) and coated to the microtiter plates. The specific or nonspecific H3 competitor peptides were tested in the competition assay for their ability to inhibit binding of anti-H3 tri-modification antibody to K9Me3S10pK14Ac-KLH conjugate.

Results

Analysis of Protein Expression in Differentiated Monocytes

Monocytes isolated by CD14$^+$ magnetic beads were differentiated into dendritic

cells (DC) in culture using interleukin-4 (IL-4) (10ng/mL) + GM-CSF (50ng/mL) for 6

days (Figure 3). The cells were stained for flow cytometry with anti-CD14 and anti-

CD11b (integrin alpha M) to ensure greater than 97% CD14$^+$ monocyte isolation purity

and the success of differentiation (Figure 4).
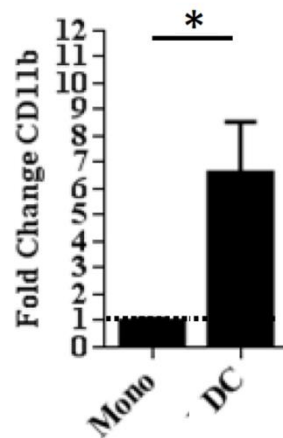
Figure 4. Quantification of surface CD11b on treated monocytes by flow cytometry. Fold
change in MFI was determined by subtracting out the background fluorescence and
normalizing data to monocyte surface expression. N=4.

Next, whole cell lystates of monocytes and DCs were made for analysis by mass

spectrometry. The whole cell lysates were rich in nuclear proteins due to stringent

extraction conditions. These conditions included the use of RIPA buffer with additional

1% NP-40 and extensive sonication to shear chromatin. Under these conditions, nearly

complete extraction of nuclear proteins was achieved as attested by the presence of

histone H1.5 in the whole cell protein extracts but not in the remaining pellets which underwent acid-precipitation (Figure 5A). Histone proteins were abundant in the cell extracts and sequence coverage by mass spectrometry for most histones was over 90% (Figure 5B).

Equal amounts of proteins extracted from the cell lysates were digested by trypsin and labeled with TMT reagents. About 1551 proteins were identified and quantified in two sets of monocytes and DCs. Because there are distinctive surface marker/cytokine gene or protein expression profiles detected for GM-CSF + IL-4-treated monocytes (dendritic cells) as indicated by previous genomic or flow-cytometric (FC) analysis (Le Naour, Hohenkirk et al. 2001, Seager Danciger, Lutz et al. 2004), we assessed markers typically used for characterization of human monocyte-derived dendritic cells. Our mass spectrometry data revealed that protein expression of CD209 (DC-SIGN) and CD1a was increased by 12.0 and 2.9 folds in GM-CSF + IL-4-treated monocytes while the expression of CD14 was decreased by 2.9 fold. The protein expression profiles of these three proteins measured by mass spectrometry were in agreement with previously demonstrated FC and gene expression data of GM-CSF + IL-4 induced dendritic cells. After confirming with flow cytometry and mass spectrometry that the differentiated cells were dendritic cells, we then used Ingenuity Pathway Analysis (IPA) to evaluate proteome differences between monocytes and dendritic cells. IPA indicated that pathways involving cell movement and hematological system development and function are differentially regulated for dendritic cells as compared to monocytes.

A

RIPA   AP

Anti-H1.5
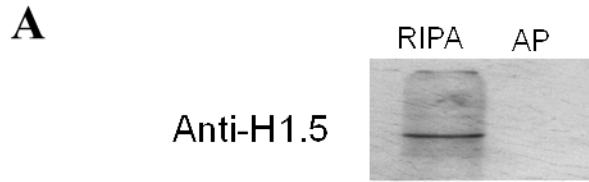
B

Histones	GI	Sequest Score	Sequence Coverage
H1.0	4885371	62.45	98.45
H1.2	4885375	1011.65	98.59
H1.3	4885377	998.76	76.47
H1.4	4885379	1107.70	98.17
H1.5	4885381	923.77	91.15
H1X	5174449	138.00	90.14
H2A	24496292	2917.45	100
H2A.Z	4504255	944.32	91.41
Macro-H2A.1	20336746	460.47	75.00
H2B	510991	7344.64	98.41
H3.1	4504285	2023.21	97.06
H3.3	4885385	1674.69	97.06
H4	4504321	1868.29	100

Figure 5. Extraction efficiency of histone proteins from whole cell lysates by modified RIPA buffer. (A) Western-blot analysis of histone H1.5 in the RIPA cell lysates as compared with extraction of histones extracted by acid-precipitation (AP) from the cell pellets which remained after RIPA extraction. The volume of acid-extraction solution was adjusted to the same volume of RIPA extraction. Two separate extraction experiments were performed and U937 cells were used as a test. (B) Typical protein sequence coverage of major histone proteins were achieved from the proteomics experiments carried out in this study.

Since the proteins regulated in these two pathways are related to cell motility, the

activation z-scores from IPA analysis from these two pathways were extracted to create a

heat map (Figure 6). Analysis of this sub-dataset suggests that monocyte-derived

dendritic cells showed less adhesion of immune cells, neutrophils, and phagocytes, but

faster cell movement and migration, and higher levels of phagocytosis of myeloid cells in

comparison with monocytes (Figure 6A). Therefore, activation z-scores of cell motility

could be used to distinguish between monocytes and DCs. These results support findings

that suggest differentiation from monocytes into DCs is accompanied by a significant

change in the expression of genes related to cell structure and motility (Hashimoto,

Suzuki et al. 1999).

In addition to DC markers, other proteins implicated in monocyte-to-dendritic cell

differentiation were quantified by mass spectrometry. Fatty acid binding protein 4

(FABP4) was significantly up-regulated (4 fold) in GM-CSF + IL-4-treated monocytes.

Other significantly increased upstream regulators specific to GM-CSF + IL-4-treated

cells include immunoglobulin, β-estradiol, PPARγ, TGFβ, and TP53. These transcription

factors have been shown to act cooperatively in the regulation of cell cycle progression

and monocyte-derived DC differentiation (Nagy, Szanto et al. 2012, Zietara, Lyszkiewicz

et al. 2013).
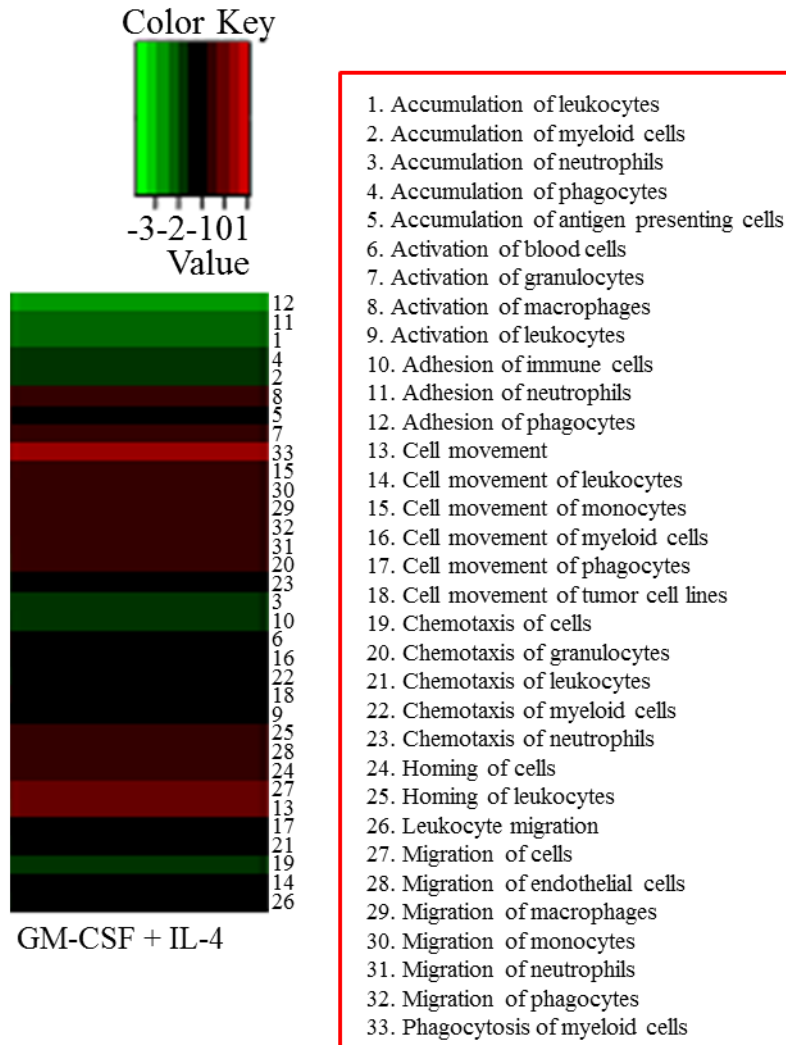
Figure 6. Selective protein expression profile in cell motility of DCs compared to monocytes. Heat map of the z-scores of 33 types of cellular functions related to cell motility. Datasets from IPA analysis of GM-CSF + IL-4-treated monocytes are plotted.

Correlation between Histone H1 Expression and Cell Lineage

Principal component analysis of changes in the dendritic cell proteome identified six proteins which negatively correlated with monocyte differentiation (data not shown). These proteins include histone H1.4, histone H1.5, and high mobility group protein HMG-17. As detected by mass spectrometry, these proteins were representative of the

most significantly downregulated proteins in response to differentiation. Since extremely altered expression of HMG-17 and H1.4/H1.5 linker proteins was observed in differentiated cells, we extracted the quantified expression levels of all the linker histone proteins.

We found that HMG-17 and histone H1 isoforms (H1.0, H1X, H1.2, H1.3, H1.4, and H1.5) were significantly downregulated in GM-CSF + IL-4-differentiated cells (Figure 7). The data suggest that DCs have a unique histone H1 expression profile which possibly affects the degrees of plasticity of chromatin structures confined by the linker histone proteins. Presumably, cells with low levels of histone H1 expression have loosely confined chromatin structures that could affect cell morphology and potentially cell motility. Loosely confined chromatin would have increased chromatin accessibility to transcription factors and histone modification enzymes including histone acetyltransferases.

Changes in Histone Modifications during Monocyte-to-Dendritic Cell Differentiation

Due to the observed changes in histone H1 expression levels, we set out to determine whether histone modifications were affected. The same set of mass spectrometry data for protein expression analysis was reanalyzed by resetting the searching parameters including removal of TMT-6 labeling to lysine but addition of dynamic modification of acetylation and methylation to lysine and phosphorylation to serine and threonine. Under these new search parameters, protein acetylation and phosphorylation sites were identified and specific attention was paid to histone modifications. We found that most of the major histone proteins were identified and

quantified with higher than 90% sequence coverage (Figure 4B). Mascot searching

reported the identification of two H3 peptide sequences with K9-dimethylation/S10-

phosphorylation/K14-acetylation and K9-trimethylation/S10-phosphorylation/K14-

acetylation (H3K9-dimethyl, H3K14-acetyl, and H3S10-phos). Significant amounts of

H3K9-dimethyl/K14-acetyl di-modification and H3K9-acetyl/K14-acetyl forms were also

detected. After detecting these and other post-translational modifications (PTMs), we

assessed their relative levels in monocytes and dendritic cells.
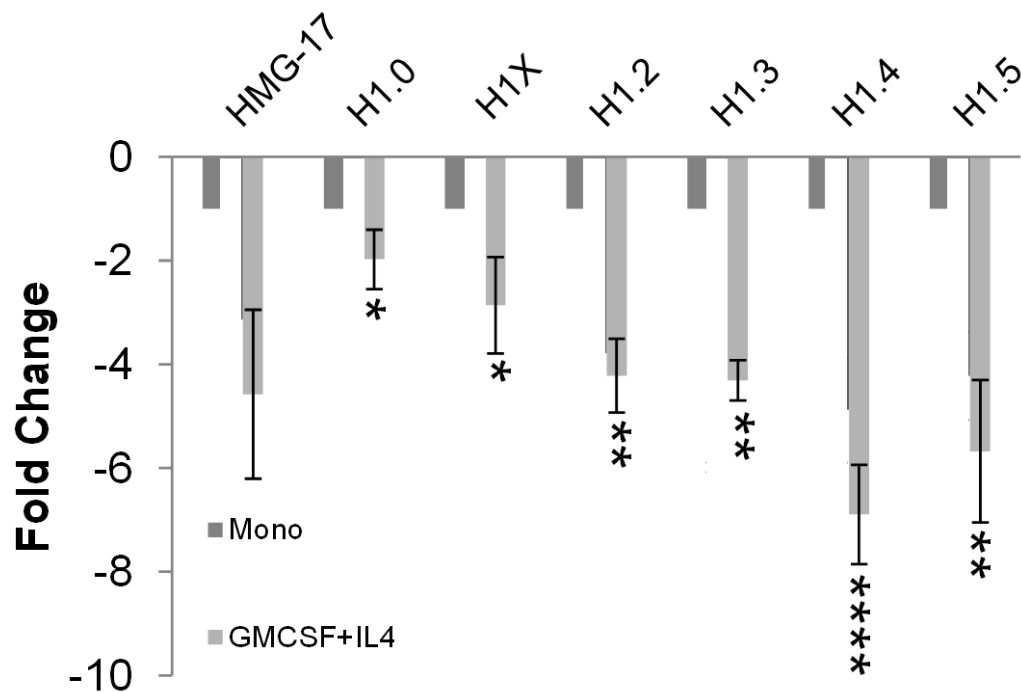
Figure 7. Comparison of relative histone expression between monocytes and dendritic cells (GM-CSF + IL-4 treated monocytes) N=5. Statistical analysis - Determination of statistical significance among treatment groups was completed using Two Way ANOVA in GraphPad Prism v6. Significance was accepted at p = 0.05. In figures, * = p < 0.05, ** = p < 0.01, *** = p < 0.001, and **** = p < 0.0001.

As indicated in Figure 8, histone H4K16Ac was significantly higher in dendritic

cells than in monocytes (Figure 8). We used intracellular staining and flow cytometry to

validate this PTM in addition to other PTMs identified by mass spectrometry.
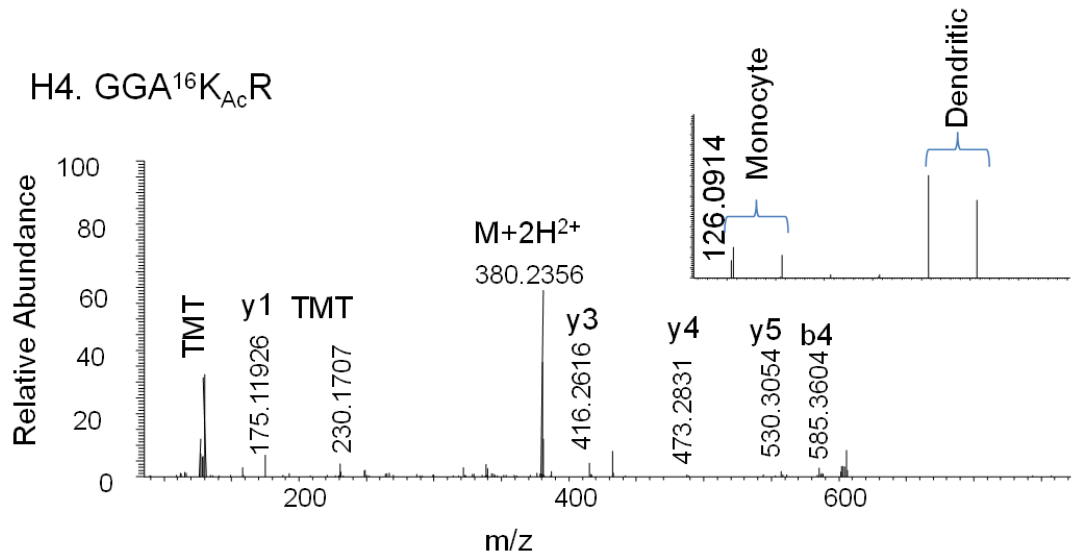
Figure 8. Higher-energy collisional dissociation (HCD) spectra of TMT tagged H4K16Ac peptide. HCD spectrum of the precursor ion at *m/z* 380.2356 (2+) corresponding to H4 K16 acetylated peptide. Tryptic peptides of monocyte proteins were labeled with TMT-126 and -127 and dendritic cells (GM-CSF+IL-4 treatment) were TMT-130 and -131.

Using an antibody we generated against the H3K9$_{Me3}$S10$_p$K14$_{Ac}$ tri-modification

(data not shown), along with commercial antibodies against H3K9Me3 (H3 lysine 9 tri-

methylation), H3S10p (H3 serine 10 phosphorylation), H4K16Ac (H4 lysine 16

acetylation), and histone H1.5, we did FC experiments in order to verify the quantitative

histone data obtained by mass spectrometry. As shown in Figure 9, H1.5 was highly

enriched in monocytes (97.5% cells positive) and dramatically reduced in dendritic cells

(4.82%) displaying a pattern similar to our mass spectrometry data (data not shown).

Similarly to H1.5, H3S10p was also highly enriched in monocytes (98.3% cells positive)

and dramatically reduced in dendritic cells (2.28%). The same decreasing pattern was

seen for H3K9Me3 from monocytes (24.8%) to dendritic cells (1.61%). Consistent with

the mass spectrometry data, H3K9Me3S10pK14Ac tri-modification was enriched in monocytes (8.82%) and dramatically reduced in dendritic cells (0.7%). In contrast to histone H3 methylation and phosphorylation, H4 lysine K16 acetylation (H4K16Ac) was slightly increased in dendritic cells (1.34%) as compared with in monocytes (0.35%), which showed the same pattern as the mass spectrometry data (Figure 8). The data revealed that a switch from H3 methylation, phosphorylation, and high linker histone expression to histone acetylation occurred during monocyte-to-dendritic cell differentiation.
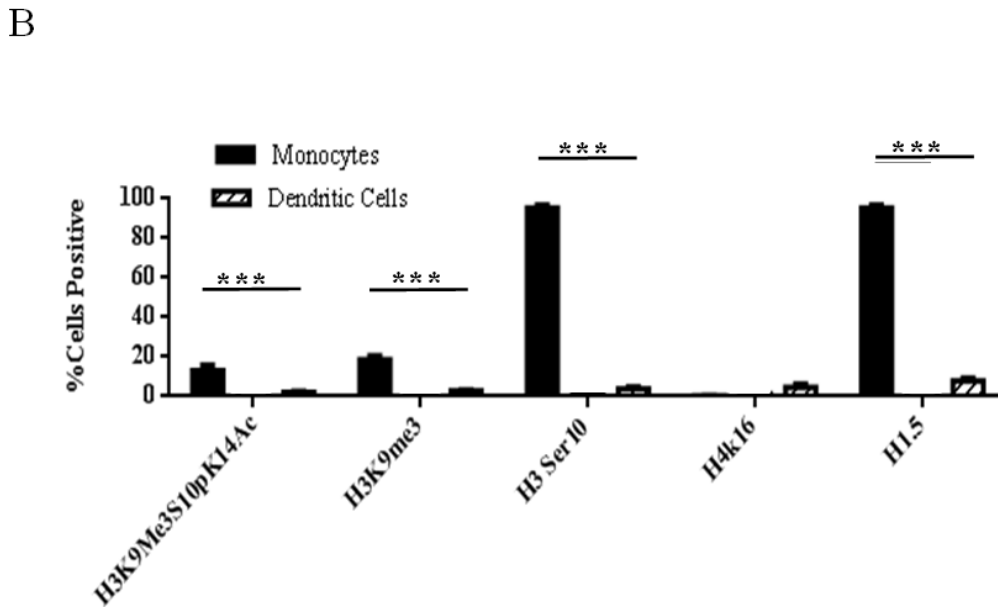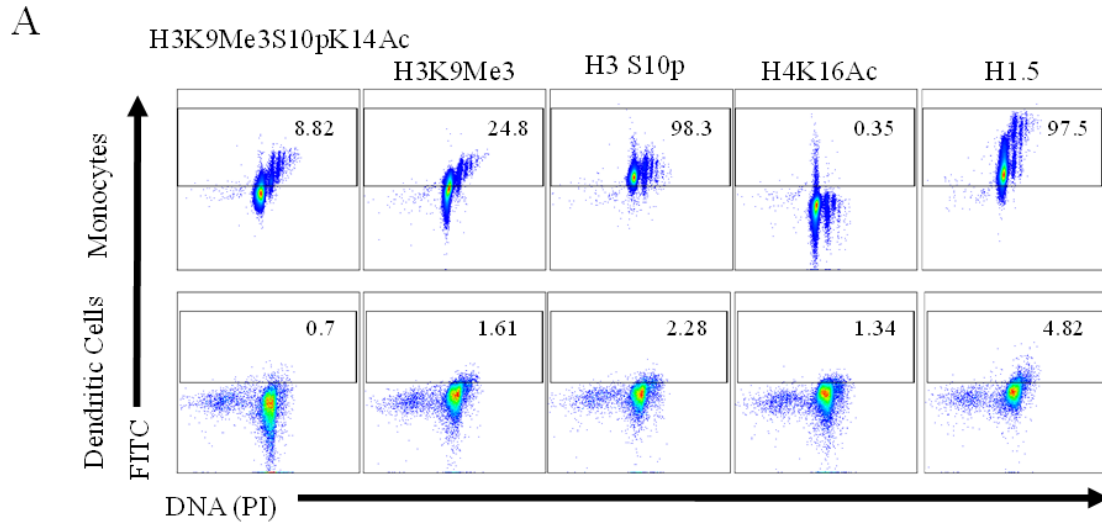
Figure 9. Flow Cytometric analysis of cell cycle and expression of histone H1.5 and histone modifications in monocytes and dendritic cells generated with GM-CSF +IL-4. (A) Dot plots represent the expression of histone modifications. The x-axis represents propidium iodide staining for genomic DNA. The cell population to the left are in G1/G0 phase, and the cell population to the right are in G2/M phase with cells in between in S phase. The y-axis is the fluorescence of $2°$ Ab against the indicated $1°$ Abs. (B) Bar graph (mean ± SEM) of the percent of cells positive for histone H1.5 or histone modifications. N=3, samples run in duplicates. Statistical analysis was performed using Two-way Anova.

Proper Regulation of Histone Acetylation is Required for Monocyte Differentiation

into Dendritic Cells

Because we observed that H4 K16 acetylation increased during monocyte differentiation with GM-CSF + IL-4 (Figures 7 and 8), we investigated the role histone H4 K16 acetylation plays in monocyte differentiation to DCs by treating monocytes with 1 μM Apicidin in order to manipulate histone acetylation. Apicidin is a specific HDAC3/NCoR histone deacetylase inhibitor (Mazitschek, Patel et al. 2008). When monocyte HL60 cells were incubated with 100 nM Apicidin, global histone acetylation increased to the maximum level at 48 hours (Hong, Ishihara et al. 2003). As expected, we detected hyperacetylation of histone H4K16 by both flow cytometry analysis (Figure 10A) and Western-blot analysis (Figure 10B) until the cells became arrested at the G0/G1 phase after a six-day incubation (Figure 11) (Han, Ahn et al. 2000). Brightfield microscopy clearly showed that the morphology of Apicidin-treated monocytes was distinct from DCs (Figure 12A). The monocyte surface marker CD14 was reduced and the macrophage/dendritic cell surface marker CD11b was increased (Figure 12B). However, the surface marker CD11c decreased significantly in Apicidin-treated monocytes (Figure 12B) revealing a phenotype of CD14^{med}CD11b^{hi}CD11c^{lo} which is distinguishable from the phenotype of CD14^{lo}CD11b^{hi}CD11c^{hi} belonging to GM-CSF + IL4 (DC) treated monocytes (Figure 12B). Judged by the cell morphology and the expression of cell surface markers (Figure 12), the Apicidin-treated monocytes observed in this experiment seemed to begin differentiation but did not completely differentiate from monocytes into dendritic cells.
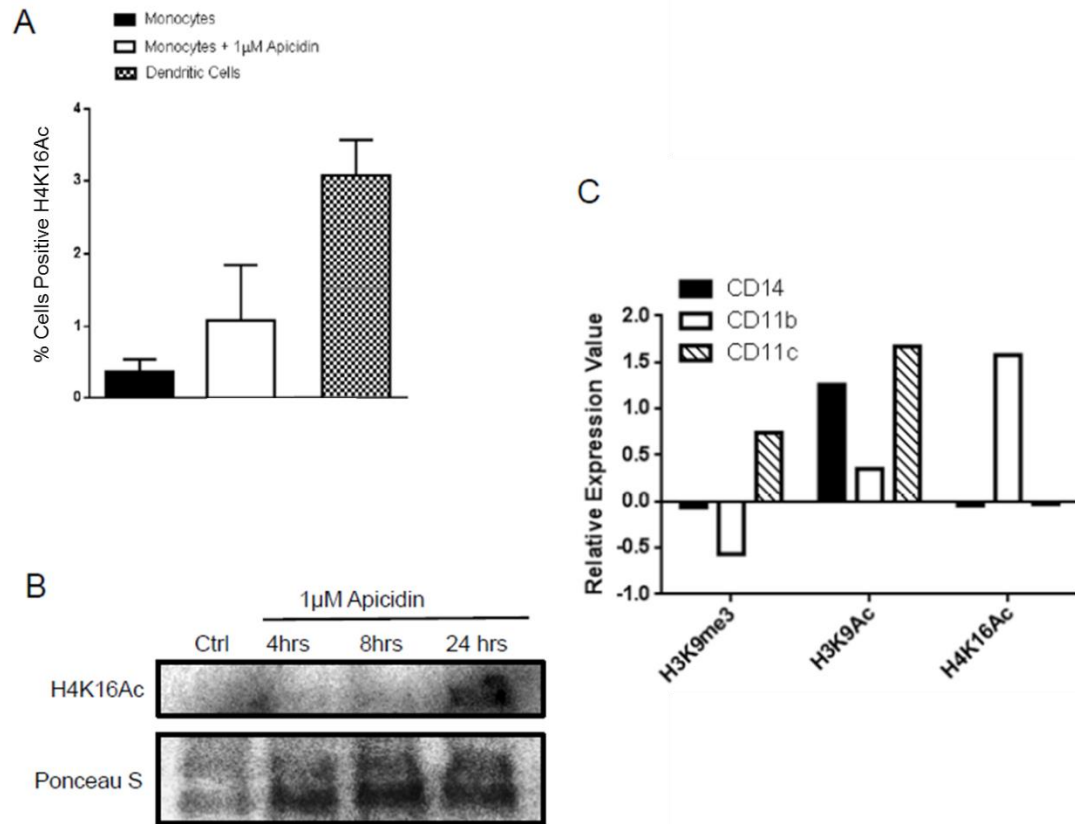
Figure 10. Histone acetylation and differentiation. (A) H4 K16 acetylation is involved in monocyte differentiation. Bar graph (mean ± SEM) of the percent of cells positive for H4 K16 acetylation (N=4). Statistical analysis was performed using Two-way Anova. (B) Western blot of increasing acetylation at H4K16 in monocytes in response to 1μM Apicidin treatment. Approximately 20μg of nuclear lysate as determined by A280 was loaded per lane. (C) Acetylation and methylation is associated with CD14, CD11b, and CD11C gene expression by analysis of public Geo Expression Omnibus data set (Accession number GSE36402). Primary normal adult lymphocytes were used for a ChIP- chip assay. After DNA to protein crosslinking, the chromatin was immunoprecipitated with either anti-H3K9me3, H3K9Ac, or H4K16Ac. Next, the crosslinking was reversed and the DNA subjected to tiling DNA array. The control input was sample with no antibody.
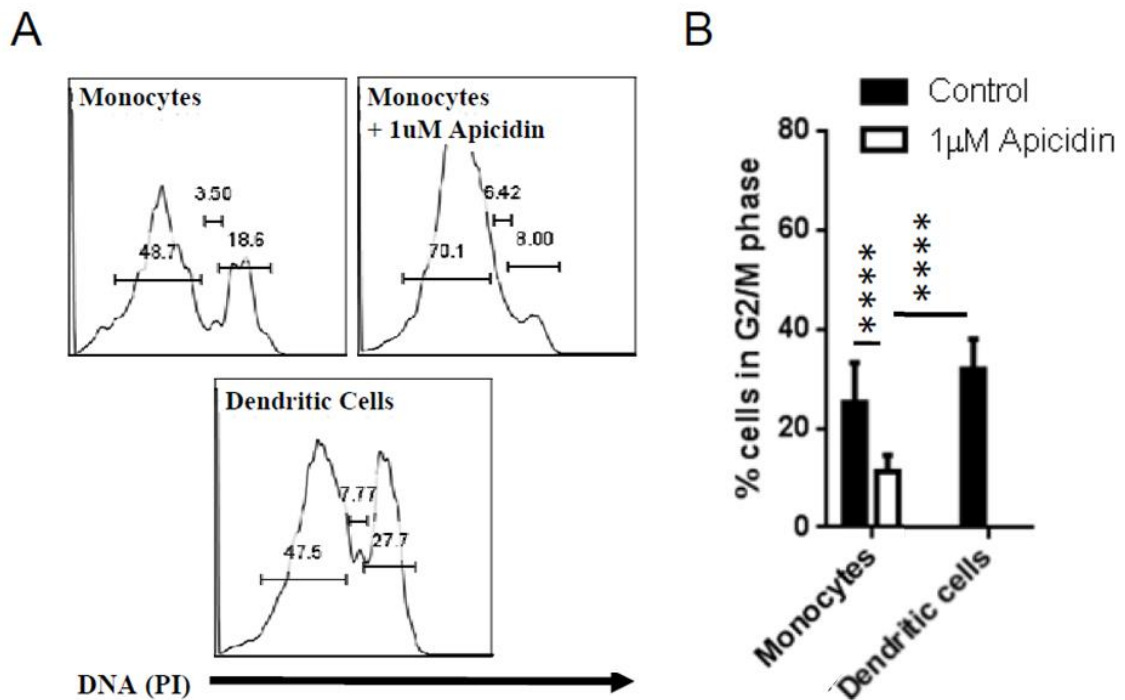
Figure 11. Inhibition of HDACs arrests differentiating monocytes in the G1/G0 phase of cell cycle. (A) Flow cytometry analysis of PI staining of dendritic cells and monocytes in the presence or absence of Apicidin after 6 days of differentiation. Histograms represent the cell cycle profile. The furthest peak to the left represents G1/G0 phase, the second peak represents G2/M phase, and the space in between the peaks represents S phase. (B) Quantification of cells in the G2/M phase from panel A. Bar graphs (mean ± SEM) are representative of 20 replicates. Statistical analysis was performed using Two-way Anova.
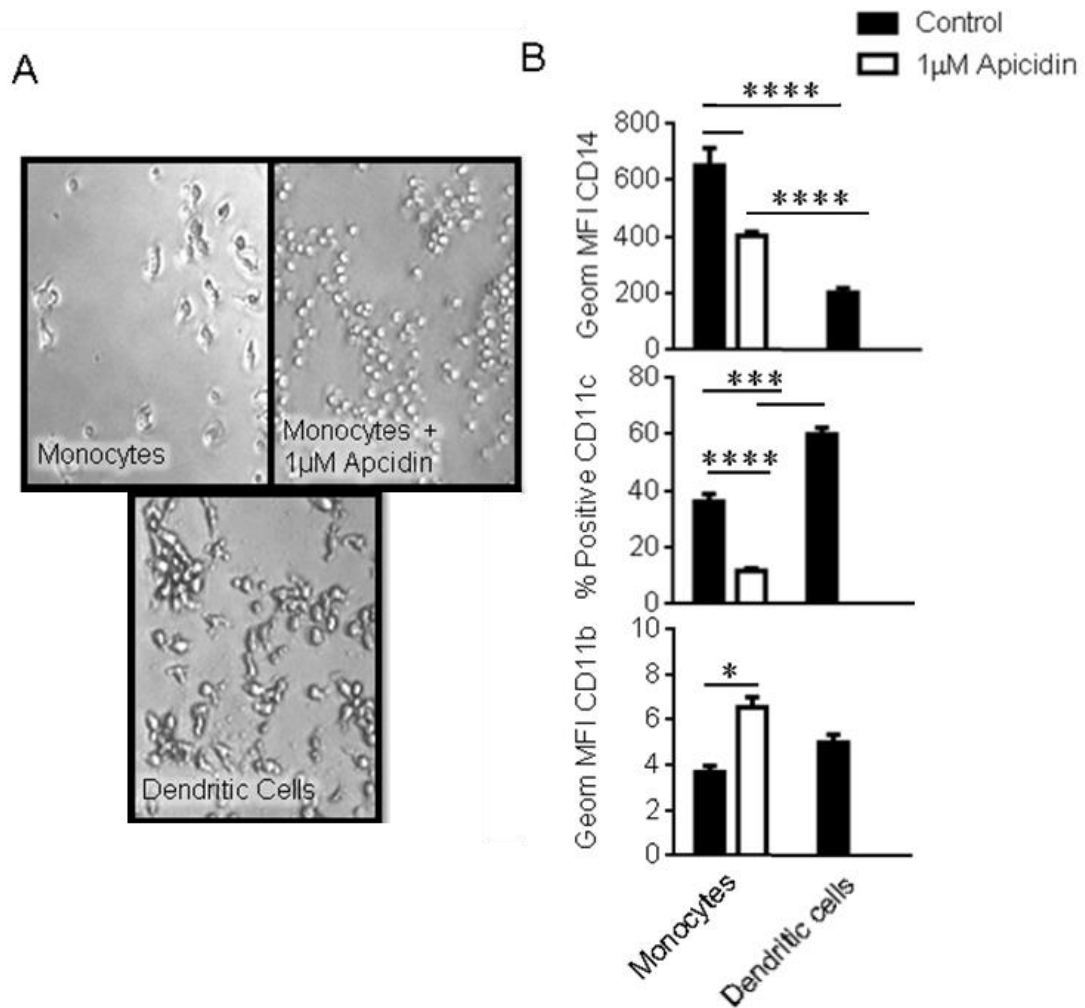
Figure 12. Histone hyperacetylation is necessary for proper monocyte differentiation. (A) Brightfield 100x microscopy images of dendritic cells and monocytes after 6 days of differentiation in the presence or absence of Apicidin. (B) Cells were stained for CD14, CD11c, and CD11b. The amount of surface expression of each marker is displayed as the geometric mean fluorescence intensity (Geom. MFI) or as percent of cells positive for the indicated marker. Bar graphs (mean ± SEM) and microscopy images are representative of 4 different patient samples in sextuplicate. Statistical analysis was performed using Two-way Anova.

Because hyperacetylation induced by Apicidin seemed to regulate expression of

DC surface markers, we investigated the association of PTMs with CD11c, CD11b and

CD14 expression. Analysis of public ChIP-chip microarray data of lymphocytes using

anti-H4K16Ac, H3K9Ac, and H3K9me3 showed that these three PTMs differentially regulated transcription of CD14, CD11c, and CD11b (Miao, Chen et al. 2012). Acetylation of H4K16 specifically increases transcription at the CD11b gene, acetylation of H3K9 specifically increases transcription at the CD14 and CD11c genes, and tri-methylation of H3K9 represses transcription at the CD11c gene but is not tightly associated with the CD11b gene (Figure 10C). An equilibrium among H3K9 tri-methylation, H3K9 acetylation, and H4K16 acetylation determines the expression levels of CD14, CD11b and CD11c (Figure 12) during monocyte differentiation. Because Apicidin non-specifically induces global hyperacetylation of H3 (including K9, K18, and K23) and H4 (including K5, K8, K12, and K16) (Han, Ahn et al. 2000), it does not induce proper monocyte to dendritic cell differentiation. Therefore, a drug that specifically acetylates H4 K16 but deacetylates at the other H3 and H4 sites would be a promising agent for monocytes to be differentiated to dendritic cells with the phenotype of CD14^{lo}CD11b^{hi}CD11c^{hi} .

Conclusion and Discussion

Using TMT-6 labeling and mass spectrometry analysis, we have compared the protein expression profiles of human monocytes with dendritic cells generated using GM-CSF + IL-4. Clustering analysis using the activation z-scores obtained from IPA revealed that monocytes differed substantially from GM-CSF + IL-4 induced dendritic cells based upon their cell motility patterns (Figure 6). These differences may be due to differential expression of linker histone proteins, typically histone H1.4 and H1.5 (Figure 7). H1.4/H1.5 expression was markedly decreased in dendritic cells differentiated from

45

monocytes, suggesting that expression of these proteins might be a dynamic process (Figure 7). The linker histone proteins (H1s) define chromatin structures and are normally considered to be chromatin repressors (Misteli, Gunjan et al. 2000, Clausell, Happel et al. 2009). Chromatin in monocytes was associated with highly expressed H1s and differed from chromatin in dendritic cells which was associated with low levels of histone H1 expression. This effect might be related to chromatin plasticity with a tightly confined structure found in the monocytes in comparison with loosely confined structures in dendritic cells that might affect cell morphology and cell motility. In macrophages the loss of H1 proteins facilitate the chemotactic response to inflammatory stimuli (De Toma, Rossetti et al. 2014). Therefore, down-regulation of H1s may play a similar role in DCs and be necessary for optimal DC function.

Unique tri-modification forms, H3K9-dimethyl/S10-phos/K14-acetyl and H3K9-trimethyl/S10-phos/K14-acetyl, was identified in human monocytes but was absent in dendritic cells (Figure 9). This undeniable identification by mass spectrometry was consistent with previous identifications of these modifications during mitosis (Garcia, Barber et al. 2005), suggesting that H3S10 phosphorylation and H3K9 methylation could naturally occur simultaneously (Mateescu, England et al. 2004, Eberlin, Grauffel et al. 2008, Papamokos, Tziatzos et al. 2012). Histone H4 K16 acetylation, a key switch for turning heterochromatin into euchromatin (Millar, Kurdistani et al. 2004), was low in monocytes while significantly increased in dendritic cells (Figure 8 and 7). Clearly, the cross-talk between inter- and intra-histone modifications that include H3 K9 methylation, H3 S10 phosphorylation, H3 K14 acetylation, and H4 K16 acetylation in concert with chromatin remodeling by linker histones is one of the major epigenetic regulatory

machineries that regulate the processes of cell cycle progression and differentiation of human myeloid cells (Hass, Gunji et al. 1992). Inhibition of histone deacetylase HDAC3 by Apicidin increased the acetylation of histone H4 K16 and decreased histone H3 K9 methylation, S10 phosphorylation, and H1.5 expression (data not shown), resulting in partial monocyte differentiation (Figure 12). This PTM pattern suggests histone acetylation is required for initial monocyte differentiation. Apicidin inhibits the expression of CD11c (Figure 12B). Therefore Apicidin is not a proper small molecule to be used to obtain dendritic cells from monocytes. However, Apicidin could be of benefit in the treatment of inflammatory diseases such as type 2 diabetes by arresting cell growth.

The information generated by proteomics analysis on histone modifications and the expression of linker histones during human monocyte-to-dendritic cell differentiation is a foundation for elucidating epigenetic remodeling/reprogramming mechanisms that underlie human myeloid cell differentiation. Here, we have provided a basis for understanding the epigenetic mechanisms that control normal differentiation. Future research should focus on PTMs associated with high fat diets, obesity, and type 2 diabetes to understand the role of epigenetic factors that regulate immune cell differentiation during chronic obesity-induced inflammation. Studies that assess induction of gene expression of key inflammatory cytokines such as TNF-α (Lee, Kim et al. 2003, Iwamoto, Iwai et al. 2007) may uncover epigenetic targets that facilitate the development of therapeutic agents for the treatment of disorders of the human immune system such as type 2 diabetes. Continued development of epigenetic drugs, such as histone acetyltransferase activators or histone deacetylase inhibitors that specifically

modulate histone H4 K16 acetylation, can open up a new avenue for dendritic cell immune therapy.

Acknowledgements

CHAPTER THREE

PALMITIC ACID INDUCES DENDRITIC CELL MATURATION AND TLR4

DEPENDENT SECRETION OF IL-1B

Abstract

Palmitic acid (PA) stimulates pro-inflammatory responses in human professional antigen presenting cells such as dendritic cells (DCs). Here we show PA stimulates human DC maturation and activation as determined by the upregulation of CD86 and CD83. Using isothermal titration calorimetry, we show that PA binds to Toll-like receptor 4 (TLR4). The binding of PA stimulates TLR4 endocytosis, confirming that PA is a TLR4 ligand. In addition, we show that PA induces TLR4 and caspase-1 dependent secretion of active IL-1β. Lastly, our data show that the activation of NFκB by PA is regulated by both TLR4 signaling and PA generated reactive oxygen species. These experiments demonstrate for the first time that activation of TLR4 depends on molecular interactions between PA and TLR4. These findings provide a mechanism for PA action on cells of the innate immune system.

Introduction

Fatty acids (FAs) are potent regulators of immune function. For example, omega 3/6 polyunsaturated FAs are anti-inflammatory while saturated FAs stimulate inflammation (Weatherill, Lee et al. 2005) . Although lipids influence inflammation, mechanisms defining how FAs modulate immune cells remain unknown. Current theories include active FA metabolites, alteration of cell membrane composition, FA peroxidation, and more recently, receptor responses (Hirasawa, Hara et al. 2008,

Leonarduzzi, Gamba et al. 2012, Shaikh, Jolly et al. 2012). Although much progress has been made in understanding FA-induced inflammation, research regarding FA effects on immune cells, specifically dendritic cells (DCs), is sparse.

Dendritic cells are responsible for conveying innate immune signals to lymphocytes. Because DCs are professional antigen presenting cells which bridge innate and adaptive immunity, it is important to understand how they process various classes of stimuli. In innate immunity, the DC response to inflammation comprises secretion of TNF-α and NO to aid in the clearing of pathogens (Serbina, Salazar-Mather et al. 2003). DCs also activate NK cells through both contact dependent and independent mechanisms (Barreira da Silva and Munz 2011). In adaptive immunity, DC-secreted factors affect IgA production by B cells (Tezuka, Abe et al. 2007). Most importantly, DCs prime naïve T cells, stimulate Th1 and Th2 responses, cross present Ag to CD8$^+$ T cells, and regulate T cell differentiation (Nakano, Lin et al. 2009, Segura, Albiston et al. 2009).

The DCs ability to interact with T cells depends on its maturation state. Immature DCs are highly endocytic and express relatively low levels of T cell co-stimulatory markers and MHC (Steinman and Swanson 1995, Mellman and Steinman 2001). In contrast, mature DCs express proteins important for T cell activation and have reduced antigen uptake, accompanied with efficient Ag presentation (Cella, Engering et al. 1997). Phenotypically, high expression of CD83 is the best measure of DC maturity (Lechmann, Berchtold et al. 2002).

Only mature DCs interact with T cells. Whether this interaction induces tolerance or immunity depends on DC activation. Activation is a process distinct from maturation. Activated DCs can be distinguished from resting mature DCs by expression of higher

levels of MHC and co-stimulatory molecules and by production of cytokines (Probst, Lagnel et al. 2003).

Palmitic acid (PA), a long chain saturated FA prevalent in the Western diet, may activate innate immune cells through TLR4. For example, PA activation of microglia is inhibited by TLR4 neutralizing antibodies and dietary FAs activate TLR4 signaling in macrophages and increase TLR4 dimerization (Shi, Kokoeva et al. 2006, Wong, Kwon et al. 2009, Wang, Liu et al. 2012). Furthermore, Lee et al. showed that saturated FAs did not activate NFκB in TLR4 negative macrophage cell lines (Lee, Sohn et al. 2001). While there is strong evidence that PA regulates immune cells through TLR4, no studies have yet demonstrated molecular interactions between FAs and TLR4.

Evidence suggests that FAs may contribute to production of IL-1β (Grishman, White et al. 2012). IL-1β is produced as a pro-protein in response to NFκB activation through pattern recognition receptor (PRR) signaling. However, translation of IL-1β is not sufficient for secretion. A second signal from a PAMP or DAMP, such as reactive oxygen species (ROS) or TRIF/TRAM dependent TLR signaling, must induce pro-protein cleavage. This second signal induces the formation of the inflammasome, a multimeric protein complex. Inflammasomes typically consist of a sensor molecule, an adaptor protein (ASC), and caspase-1(Latz, Xiao et al. 2013). The sensor molecule for most inflammasomes is a NOD-like receptor (NLR) such as NLRC4 (NOD-, LRR- and CARD-containing 4) (Ting, Lovering et al. 2008). When pro-caspase-1 is recruited to the ASC via homotypic binding of CARDs (caspase activation and recruitment domains) (Lopez-Castejon and Brough 2011), autolytic cleavage occurs, producing active caspase-1. Caspase-1 then cleaves pro-IL-1β into active of IL-1β (Latz, Xiao et al. 2013).

Because DCs express TLR4 and play key roles in both innate and adaptive immune responses, PA has the potential to exert broad immune effects. Therefore, our goal was to characterize PA-induced DC maturation and activation. We hypothesized that PA ligation to TLR4 causes DCs to adopt a pro-inflammatory phenotype. Our isothermal titration calorimetry (ITC) data show that PA binds TLR4 via the adaptor protein MD-2. The TLR4 signal induced by PA results in the activation and maturation of DCs accompanied with a robust IL-1β response. These data suggest DCs recognize PA through PAMP associated mechanisms. Thus, PA may serve as a dietary immune modifier (DIM) resulting in the induction of chronic inflammation.

Materials and Methods

Monocyte Isolation and DC Culture

Human monocyte-derived DCs were generated as previously described (Kiertscher and Roth 1996). Peripheral blood from healthy adult donors (age 18+) was provided by the Lifestream blood bank, San Bernardino, CA, according to Loma Linda University IRB requirements. After red blood cell lysis, CD14$^+$ cells were isolated with anti-CD14 magnetic bead MACS separation (Miltenyi biotech) and cultured for 6 days in RPMI 1640 medium +10% FBS with GM-CSF and IL-4.

Preparation of PA

Palmitic acid (Sigma, St. Louis, MI), was dissolved in 100% EtOH and diluted (final conc. EtOH 0.1% v/v) in a range from 300 to 50 μM in a 2:1 molar ratio with endotoxin low FA-free BSA (Gemini Bio-products) in media containing defatted-FBS

(no experimental differences were observed between using FBS and defatted-FBS). DCs treated with physiological doses of PA (300μM, 150μM, and 50μM) were viable within 48hrs of treatment (data not shown).

Reagents

The ROS scavenger, MCI-186 (Biomol Research Laboratories) was dissolved in DMSO and diluted in a range from 1mM or 50μM. DCs were pre-treated with MCI-186 for 1hr. The TLR4 inhibitor CLI-095 (Invivogen) was used according to manufacturer protocol. The caspase-1 inhibitor peptide (ICE Inhibitor V, Z-Asp-[(2,6-dichlorobenzoyl)oxy]methane, Z-D-CH2-DCB from Calbiochem) was used at a concentration of 100μM. Vehicle control contained equimolar amounts of BSA, EtOH, or DMSO as used in experimental groups.

Antibodies and Flow Cytometry

Abs and reagents used were anti-human CD11c-PE, CD80-FITC, CD80-PE, CD83-FITC, HLA-DR-PerCP, CD11c-PE-Cy7, CD83-APC, CD86-PE, CD282-FITC, CD284-PE, Donkey anti-rabbit-FITC, fixable viability dye e-flour 450, and Anti-human CD14-PE,-APC, or -VB (Biolegend, BD biosciences, or Miltenyi Biotech). Data acquisition was on a Miltenyi MACSQuant flow cytometer (Miltenyi Biotech) and analysis was performed with FlowJo 7.6.5 (Tree Star, Ashland, OR) software.
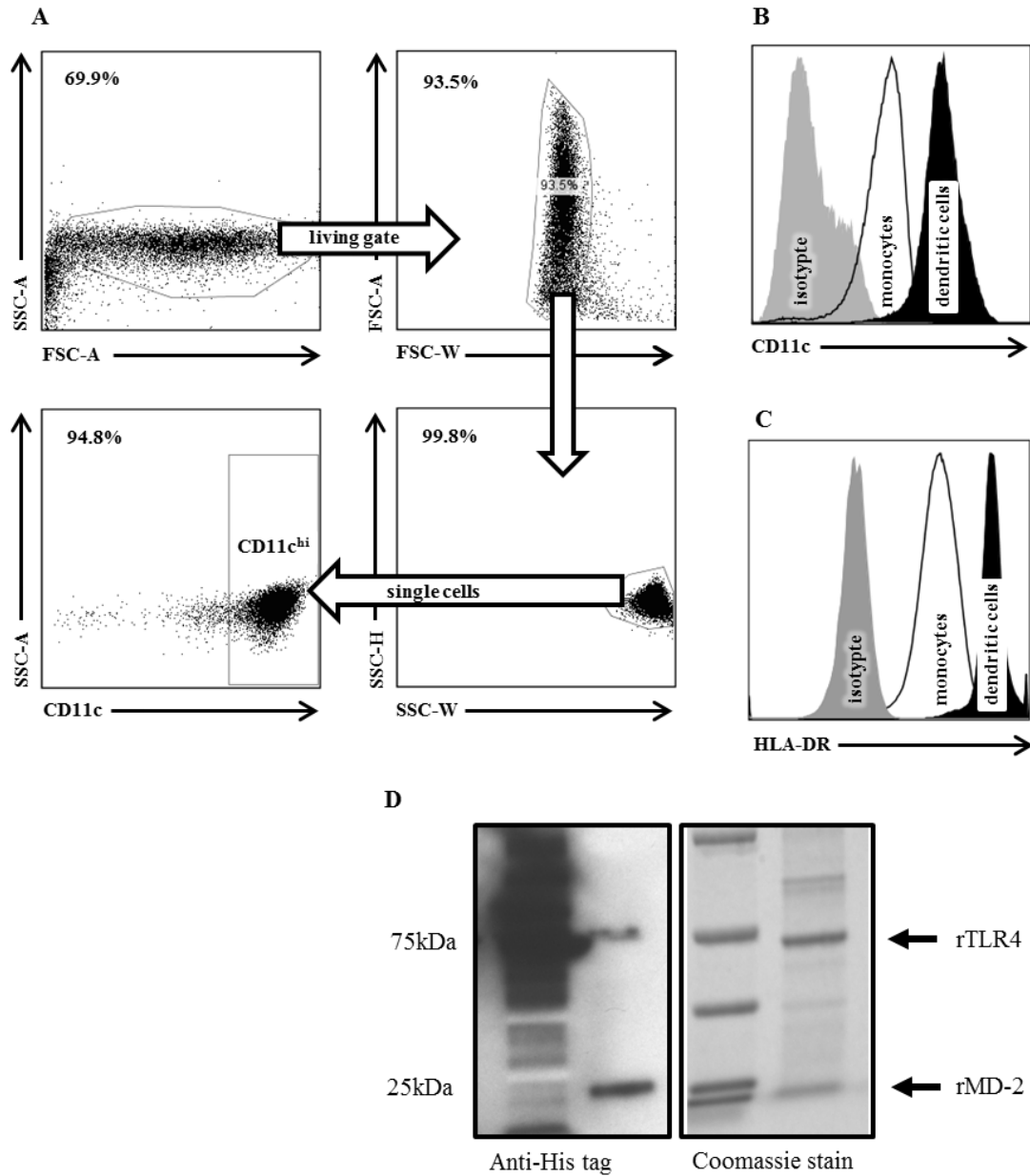
Figure 13. Basic DC Gating Strategy. (A) DCs were gated first by FSC-A and SSC-A. Doublet discrimination was performed using FSC-H vs FSC-W and SSC-H vs SSC-W. Cells with the phenotype CD11c^{hi} were gated as DCs (>94%). (B) DCs express higher levels of CD11c than their precursor monocytes. (C) DCs express higher levels of HLA-DR than their precursor monocytes. (D) Western blot and Coomassie stain of SDS-PAGE of isolated rTLR4 and rMD-2 from Hela cells.

Flow Cytometry Gating Strategy

DCs were gated by FSC-A/SSC-A. Doublet discrimination was performed using

FSC-H vs FSC-W and SSC-H vs SSC-W(Wersto, Chrest et al. 2001). Dendritic cells or

CD11c^{hi} cells (>94%) all expressed increased HLA-DR as compared to monocytes

(Figure 13A,B, and C).

qRT-PCR

Total RNA was isolated from DCs using Stat-60 reagent (Tel-Test Inc.) according

to the manufacturer's protocol. After reverse transcription with SydQuanti First Strand

cDNA Synthesis Kit (SydLabs Inc.), qRT-PCR was performed with iQ SYBR Green

Super Mix (Bio-rad) on a Bio-rad CFX96 Real-time system C1000^{tm} thermal cycler.

Values were normalized to β-actin (see Table 2).

Table 2. Primer sequences designed with NCBI primer blast for qRT-PCR

Primer	Product size (bp)	Sequence
IL-12p40 forward	107	5'- CTTGGACCAGAGCAGTGAGG -3'
IL-12p40 reverse		5'- GAACCTCGCCTCCTTTGTGA -3'
IFN-γ forward	136	5'- TCCAGTTACTGCCGGTTTGA -3'
IFN-γ reverse		5'- TGGAAGCACCAGGCATGAAA -3'
IL-1β forward	143	5'- TGAGCTCGCCAGTGAAATGA -3'
IL-1β reverse		5'- AGATTCGTAGCTGGATGCCG -3'
NLRC4 forward	59	5'- TCATCGGTGGAGTGGACCAA -3'
NLRC4 reverse		5'- TTCTGGGCAAGGTCACACAG -3'

Cytometric Bead Array

Supernatant was collected from DC cultures following PA treatment and analyzed

with multiplexed human IL-12p40, IFN-γ, IL-6, TNF, and IL-1β flex sets as described by

the manufacturer (BD biosciences) on the MACSQuant flow cytometer. Data analysis was accomplished with FACP array v3 software.

Recombinant TLR4/MD-2

Recombinant TLR4/MD-2 (Figure 13D) was isolated from stably transfected Hela cells according to published protocol (Illana and Farhaeus 2012). A plasmid (vector pD1119 cloned by DNA 2.0) encoding the TLR4 ectodomain (Accession # O00206; Glu24 - Lys631 + 10-His Tag) and MD-2 (Accession # Q9Y6Y9; Glu17 - Asn160 +10-His Tag) separated by the sequence for a viral 2A peptide was used to produce lentivirus. Transduced Hela cells were expanded in DMEM + 10% FBS and 1μM puromycin (Sigma-Aldrich).

Isothermal Titration Calorimetry

Isothermal titration calorimetry (ITC) experiments were carried out in a low volume Nano ITC (TA instruments). Electrical and chemical calibration was done according to manufacturer's instructions (Demarse, Quinn et al. 2011). 200uL of 13-30μM recombinant human TLR4/MD2 in ITC buffer (Tris/HCL pH 8, 1mM EtSH, 900μM KOH) was loaded into the cell. The syringe was loaded with 500-800 μM PA. Titrations were carried out using 22 injections of ~2.5μL each at 400s intervals, at 25°C. Data was analyzed using NanoAnalyze v2.4.1 software (TA Instruments). Data was fitted using an independent binding model.

Fluorescence Microscopy

Dendritic cells were cultured on glass slides. After 20min treatment with PA or PA+CLI-095, the cells were fixed and stained with primary anti-human phospho NFκBp65 (Cell Signaling Technologies) and secondary donkey anti-rabbit FITC (Biolegend). Slides were sealed after addition of mounting media with DAPI and 40x photos were taken on a Keyence BZ-9000 fluorescent microscope.

Electrophoretic Mobility Shift Assay

Nuclear lysates of PA treated DCs were incubated with a ^{32}P labeled DNA consensus sequence for NF-κB for 30min. The protein was subjected to gel electrophoresis. The gels were dried and exposed on X-ray film. The band density correlates to the relative amount of labeled oligonucleotide bound to NF-κB.

Western Blots

Western blots were performed on 50μg of total protein lysate from DCs treated with PA or PA+CLI-095 for reported time points to detect caspase-1 (anti-caspase-1 Cell Signaling Technologies).

Statistical Analysis

One or two way-ANOVA was performed with GraphPad Prism 6.00 software (GraphPad, San Diego, CA), and values at $P < 0.05$ were deemed significant (**=$p<0.01$, ***=$p<0.001$, ****=$p<0.0001$).

Results and Discussion

PA Binds and Induces Internalization of TLR4

To date, no one has demonstrated that PA acts as a TLR4 ligand. The crystal structure of the TLR4 ectodomain, MD-2, and LPS show that five hydrophobic carbon chains of the lipid A portion of LPS bind MD-2 (Park, Song et al. 2009). Because PA has structural similarity to the carbon chains of lipid A, up to five molecules of PA may potentially bind the hydrophobic pocket of MD-2. Our results show that PA binds to TLR4/MD-2 with an affinity (K_a) of 4.355×10^5 (Figure 14A). The PA binding to TLR4 is endothermic, exergonic, and spontaneous as evidenced by a positive ΔH, large positive ΔS, and negative ΔG respectively (Figure 14A). We validated the interaction of PA and TLR4/MD-2 by assessing DC internalization of TLR4 in response to PA. We found that PA significantly reduced surface TLR4 but not as much as LPS (Figure 14B). Of note, the kinetics of PA-induced TLR4 endocytosis is linear while LPS-induced TLR4 endocytosis is initially exponential.
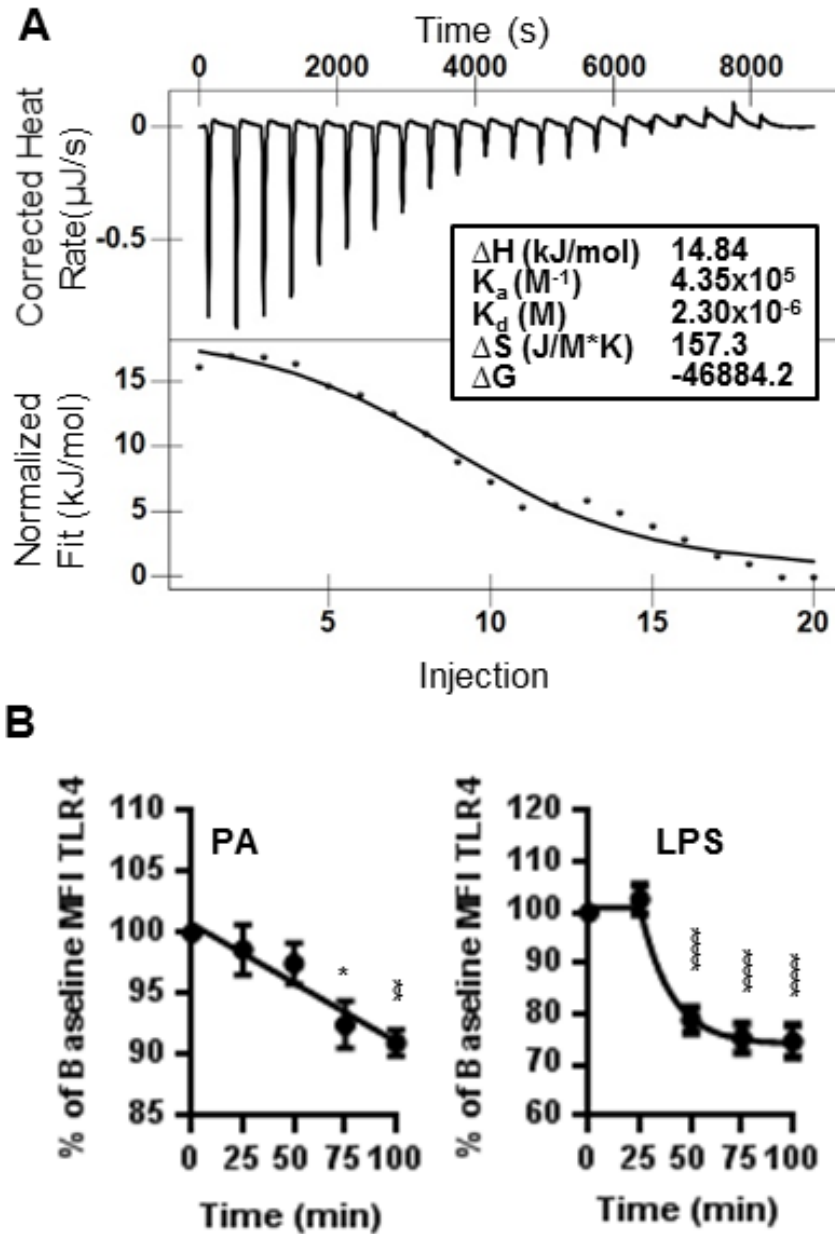
Figure 14. PA binds TLR4. (A) Isothermal titration calorimetry. Isotherms and fitted area curve of PA into TLR4/MD-2 titration. Bottom panel insert contains thermodynamic parameters for PA and TLR4/MD-2 binding interaction. (B) PA induces the internalization of TLR4. DCs were treated with 300μM PA for indicated time intervals. Cells were stained for flow cytometry. CD14⁻CD11c^hiHLA-DR^hi cells were assessed for TLR4. Data is presented as the percentage of baseline Geometric MFI. Graphs display the mean ± SEM.

The high affinity of PA for TLR4/MD-2 indicates how an increase in dietary PA may stimulate innate immune cells. PA's association with TLR4/MD-2 is an order of magnitude weaker than that of LPS interaction with MD-2 ($K_d \sim 3nM$) (Akashi, Saitoh et al. 2003). However, the K_a of PA binding to TLR4/MD-2 is greater than that of PA binding to any of the three low affinity human serum albumin binding sites (Fujiwara and Amisaki 2008). Under normal conditions, the low affinity binding sites are not occupied. However, these sites are occupied under conditions of increased lipolysis and serum FAs. Therefore, both serum PA and PA bound to low affinity sites could potentially bind TLR4/MD-2 *in vivo*.

PA Induces DC Maturation and Secretion of IL-1β

To determine if PA activates DCs through upregulation of co-stimulatory factors, naïve DCs were treated with PA and assessed for the expression of HLA-DR, CD80, CD86, and CD83 surface markers by flow cytometry (Figure 15A). PA induced the expression of CD86 as well as the maturation marker, CD83, indicating simultaneous induction of DC activation and maturation. We also examined the effects of PA on DC production of inflammatory cytokines IL-6, TNF, IFN-γ, IL-12, and IL-1β using qRT-PCR and cytometric bead array for secreted cytokines. PA seemed to increase IFN-γ secretion although this trend was not significant. There was no effect on IL-12 production and, PA also failed to increase the secretion of IL-6, TNF-α, IL-8 or IL-10, but increased IL-18 mRNA (data not shown). In contrast, PA induced robust mRNA expression of pro-IL-1β and the secretion of active IL-1β (Figure 15B and C).
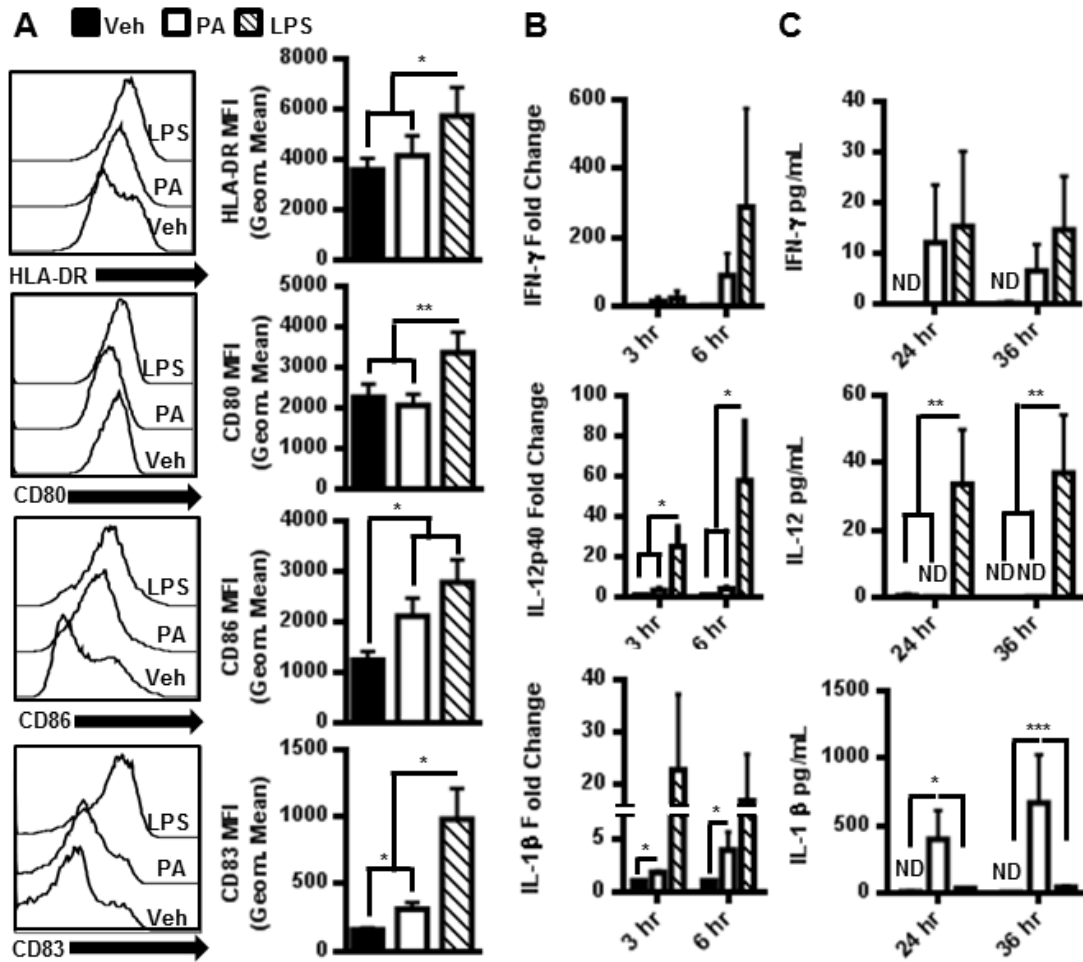
Figure 15. PA induces DC maturation and secretion of IL-1β. (A) PA upregulates DC activation and maturation markers. DCs were treated with 150μM PA for 12hrs. Representative histograms from 1 of 8 individual patient samples is presented, and the geometric MFI for the indicated marker on CD11c^{hi} cells (DCs) is graphed. (B) mRNA fold change in cytokines of DCs treated with 300μM PA. (C) Quantification of cytokines secreted from DCs treated with 300μM PA. ND = Not detectable.

Palmtic Acid Activation of NF-κB is TLR4 and ROS Dependent

TLR4 signaling results in the activation of NF-κB, an event required for transcription of

pro-IL-1β. We determined that PA induces the activation (phosphorylation) of NF-κBp65

(Figure 16A-C and Figure 17A). This activation is inhibited by blocking TLR4 with CLI-

095 (Figure 16A-B) and ROS with MCI-186 (Figure 16C). Next, we determined that

CLI-095 completely eliminated the IL-1β response to PA, but was not affected by MCI-186 (Figure 16D). Therefore, both PA ligation of TLR4 and ROS generation may be necessary for PA to exert its maximum effects.
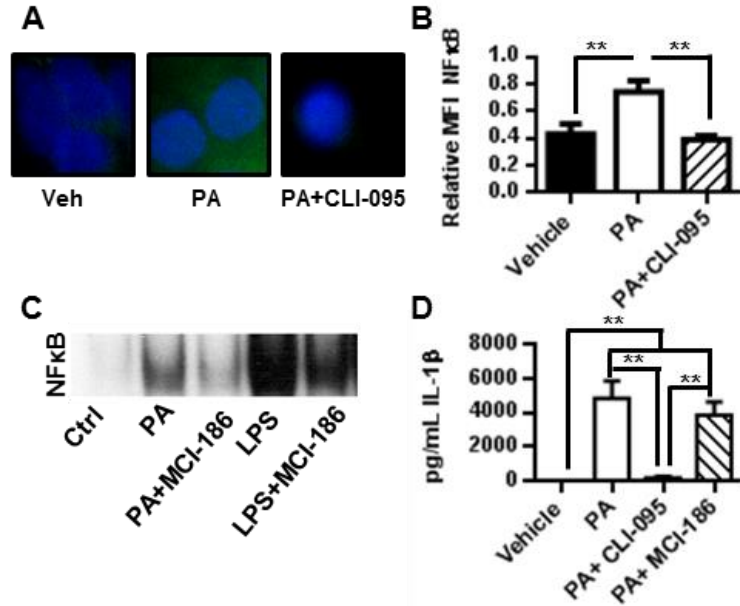
Figure 16. PA activation of NF-κB is TLR4 and ROS dependent. (A-B) PA-induced phosphorylation of NF-κBp65 is TLR4 dependent. DCs were treated with 300μM PA for 20min and analyzed for phospho NF-κBp65 (green) by fluorescence microscopy. (B) Quantitation of MFI phospho NF-κBp65 relative to DAPI (blue). (C) PA-induced activation of NF-κB is ROS dependent. DCs were treated with 300μM PA for 3hrs and analyzed by EMSA. (D) DC secretion of IL-1β is dependent on TLR4 signaling. DCs were treated with 150μM PA for 36hrs +/- CLI-095 or 50μM MCI-186. The supernatant was analyzed for concentration of IL-1β. Figure is representative of at least 3 separate patient samples.

Secretion of IL-1β is Dependent on TLR4 Induced Caspase-1 Activation

Although caspase-1 typically processes pro-IL-1β, caspase-8 which is also induced by TLR4, has the ability to cleave pro-IL-1β (Maelfait, Vercammen et al. 2008). To determine if PA-induced secretion of pro-IL-1β in DCs relies on caspase-1, we

assessed the secretion of IL-1β in the presence of a specific caspase-1 inhibitor. The

inhibition of caspase-1 knocked out almost 100% of IL-1β secretion (Figure 18B).

Since caspase-1 activity is essential for IL-1β secretion, we assessed the ability of

PA to induce activation of caspase-1 in DCs. We found that PA minimally increased the

production of active p20 caspase-1 within 2 hours with a maximum at ~30min, while

CLI-095, a TLR4 inhibitor, repressed this process (Figure 18C and 17B), indicating that

activation of caspase-1 may be dependent on TRIF/TRAM TLR4 signaling or direct

interaction with PA rather than ROS (Legrand-Poels, Esser et al. 2014).

PA Induces NLRC4 Inflammasome Transcription

Non-esterified FAs seem to have the ability to directly stimulate inflammasome

activation (Reynolds, McGillicuddy et al. 2012, Legrand-Poels, Esser et al. 2014). PA

increased NLRC4 mRNA approximately 10-fold (Figure 18A) without affecting NALP1

or NALP3 mRNA (data not shown). This result suggests it is likely that PA-induced

caspase-1 activation is via the NLRC4 inflammasome (Figure 19). Both *ex vivo* and *in

vivo* exposure of bone marrow-derived DCs to dietary saturated FAs increased NLRP3

inflammasome activation (Reynolds, McGillicuddy et al. 2012). Our studies indicate that

the NLRC4 inflammasome, rather than NLRP3, is active in processing pro- IL-1β.
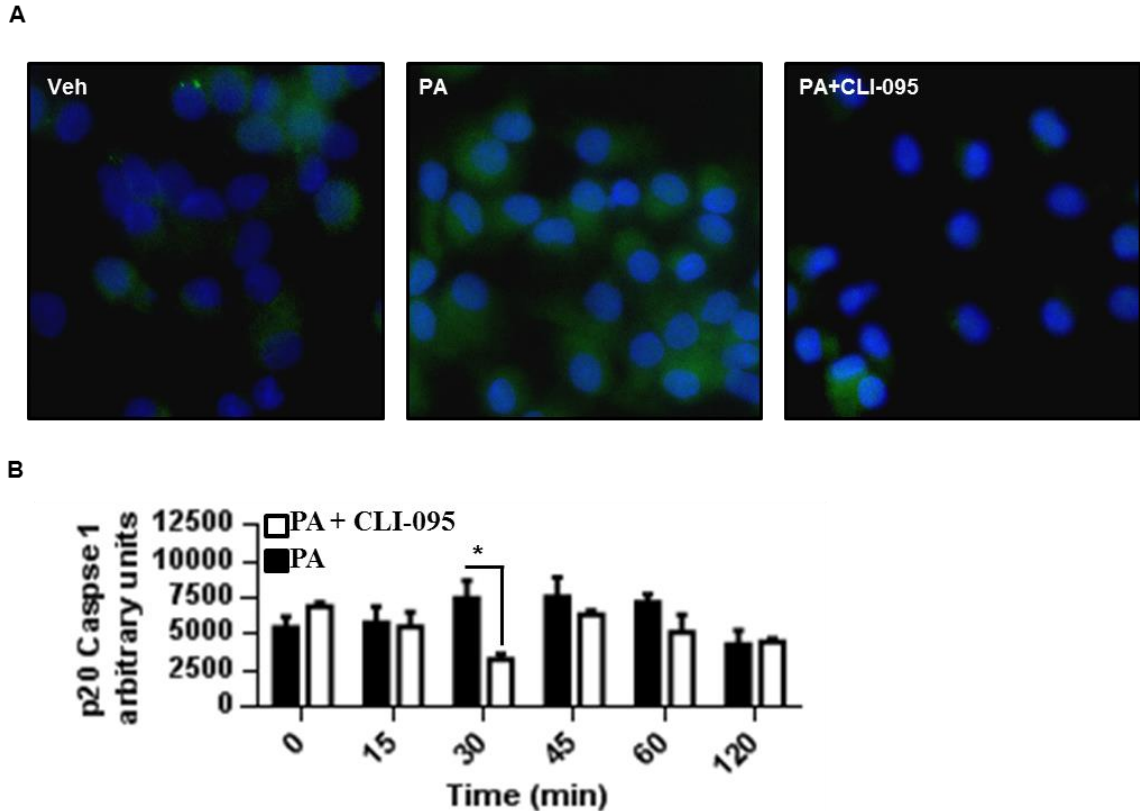
Figure 17. (A) Representative microscopy of DCs treated with PA for 20min. Green represents the presence of phospho NF-κBp65 and blue represents DAPI staining of nuclei. (B) Densitometry quantification of western blots of active caspase p20 from Figure 18C. Data was analyzed using one-way ANOVA. * = $p < 0.05$.

This difference may be due to our use of PA as opposed to a mixture of saturated FAs. However, Luo et al. demonstrated that PA specifically activates NLRC4 in HepG2 cells (Luo, Yang et al. 2012). For the first time, we show that PA initiates innate immunity in DCs by binding TLR4 and inducing IL-1β secretion. Overall, our studies suggest that dietary PA is a key metabolic stressor required for the processing of IL-1β in DCs. Understanding the mechanism of PA as a dietary immune modulator (DIM) underscores the importance of researching lipid effects on immune cells. The emergence of mechanistic data on DIMs such as FAs has the potential to provide novel molecular

targets for therapy in a host of inflammatory diseases including hypersensitivity

dermatitis, rheumatoid arthritis, and type 2 diabetes.
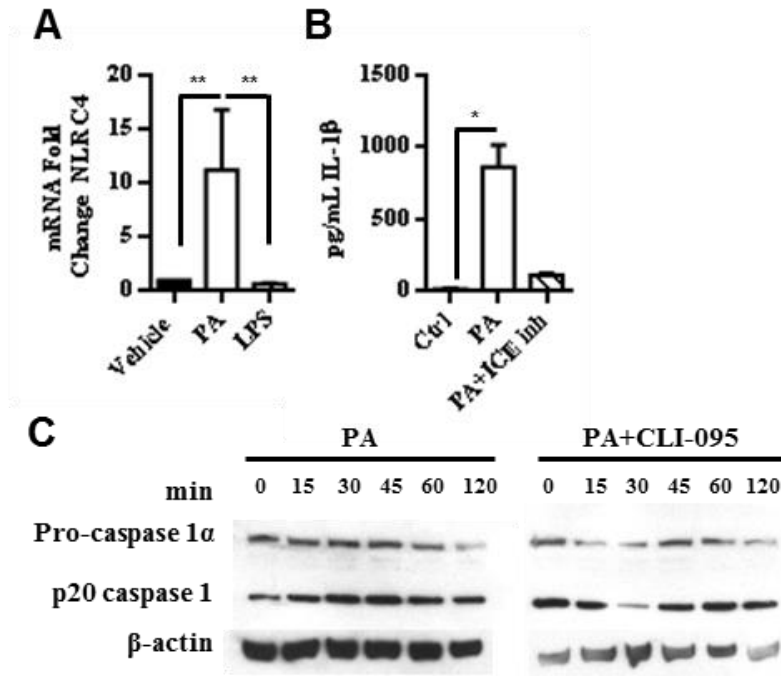
Figure 18. PA activates inflammasomes. (A) PA induces NLRC4 gene expression. DCs were incubated with 300μM PA for 6hrs and NLRC4 mRNA was analyzed by qRT-PCR. (B) PA secretion of IL-1β is caspase-1 dependent. The supernatant from DCs treated with 300μM PA for 24hrs was analyzed by cytometric bead array. (C) PA-induced caspase-1 activation is TLR4 dependent. DCs were treated with 300μM PA for increasing time points. The DC lysates were analyzed by western blot. Data is representative of 3 experiments and normalized to β-actin.
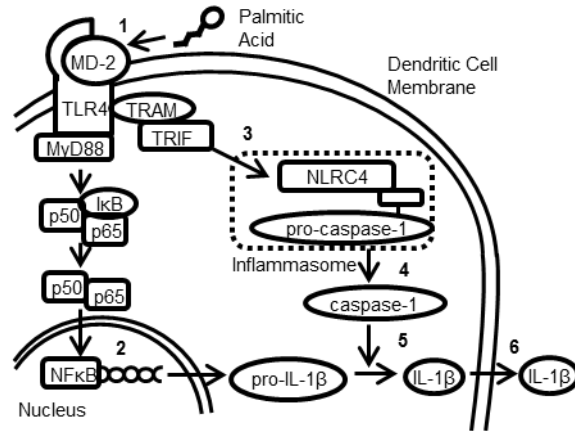
Figure 19. Mechanism of PA-induced DC secretion of IL-1β. (1) PA binds MD-2/TLR4 and induces signal transduction resulting in NF-κB activation. (2) NF-κB induces transcription of the pro-IL-1β gene which results in translation and protein expression. (3-4) PA-induced TLR4 signal transduction also results in activation of caspase-1, a process which occurs via inflammasome assembly. (5) Caspase-1 cleaves pro-IL-1β into active IL-1β. (6) With the secretory peptide signal exposed after cleavage, IL-1β is secreted from the cell.

CHAPTER FOUR

POTENTIAL MOLECULAR MECHANISMS FOR PA ACTIVATION OF

DENDRITIC CELLS

Abstract

Palmitic Acid has the ability to activate dendritic cells by binding toll-like receptor 4 (TLR4). However, the mechanisms underlying PA manipulation of DC activation remains unclear. In this chapter, we investigate potential mechanisms by which PA stimulates DC function. To achieve this goal, we employed both a focused and a broad approach. Specifically, we used the reactive oxygen species (ROS) scavenger MCI-186 and the NADPH oxidase inhibitor Apocynin to elucidate the role of ROS in PA mediated DC activation. Broadly, we also analyzed all changes in the DC proteome in response to PA treatment by mass spectrometry. We found that ROS is involved in the DC response to PA ligation of TLR4. In addition, our data suggests that PA treated DCs may have the ability to stimulate an adaptive T cell response. In conclusion, we found that ROS plays a role in PA induced DC activation, and the role of PA activated DCs on the adaptive immune system should be researched further. Determining whether PA can stimulate an adaptive immune response will shed light on how increased serum fatty acids may induce insulin resistance and subsequent type 2 diabetes.

Introduction

Dietary fatty acids (FAs) play a major role in diabetes inflammation (Pickup and Crook 1998, Halliwell 2002, Unger and Parkin 2010). Saturated FAs, e.g. palmitic acid (PA), are pro-inflammatory and have been associated with metabolic syndrome, insulin

resistance, and various immunological complications leading to type 2 diabetes (Kim, Pham et al. 2007, Riserus 2008, Titov, Krylin et al. 2011). In diabetes patients, serum saturated FAs are correlated with inflammation (Riserus 2008, Unger and Parkin 2010, Virtanen, Niinisto et al. 2010). The impact of saturated FA on the immune system can be attributed in part to their interaction with dendritic cells (DCs), the primary antigen presenting cells responsible for activating naïve T cells. While many laboratories have shown the pro-inflammatory effects of PA on DC function (Zeyda, Saemann et al. 2005, Wang, Hao et al. 2007, Igoillo-Esteve, Marselli et al. 2010, Kong, Yen et al. 2010, Piro, Maniscalchi et al. 2010), the molecular mechanisms by which PA impacts DCs remain largely unknown.

DCs are professional antigen presenting cells that function by recognizing antigens and presenting them to T lymphocytes. DCs reside in peripheral tissues until they encounter antigens that activate them. Activation through TLR signaling pathways results in DCs maturation into efficient antigen presenting cells (APCs) (Bell, Young et al. 1999). Antigen laden DCs migrate to peripheral lymph nodes, where they interact with naïve T cells to promote immune responses (Bell, Young et al. 1999). *In vitro*, DCs can be differentiated from CD14$^+$ monocytes by incubation in medium containing the cytokines GM-CSF and IL-4 (Romani, Gruner et al. 1994). The resulting immature DCs are CD14^{lo}, express MHC class II, CD1, and co-stimulatory ligands for T cell surface receptors such as B7.1 (CD80) and B7.2 (CD86), in addition to endocytic receptors such as DC-Sign and mannose receptor (MR) (Porcelli, Brenner et al. 1989, Romani, Reider et al. 1996). In addition to engagement of the T cell receptor and CD28 by dendritic cell MHC class II/CD1 and B7 proteins respectively, T cells also require cytokine signaling to

68

become active. Our laboratory has shown that PA binds TLR4 on DCs and induces secretion of the pro-inflammatory cytokine IL-1β. The aim of this study is to identify mechanisms underlying palmitic acid modulation of DC immune responses.

We hypothesized that PA induced reactive oxygen species (ROS), specifically H_2O_2, acts as a TLR4 signaling regulator (Finkel 1999, Lee, Sohn et al. 2001, Reth 2002). Different from other ROS agents that have indiscriminate chemical reactivity, H_2O_2 has specific biological targets such as proteins with an oxidizable cysteine located in an enzyme active site (Finkel 1999, Reth 2002, D'Autreaux and Toledano 2007). Protein tyrosine phosphatases are examples of enzymes susceptible to H_2O_2 regulation. *In vitro*, protein tyrosine phosphatase 1B (PTP1B) activity is reversibly inhibited by H_2O_2. (Salsman, Hensley et al. 2005). Therefore, H_2O_2 may be necessary for TLR4 signaling through inactivation of PTP1B, which negatively regulates TLR signaling (Xu, An et al. 2008). An emerging hypothesis is that antigen receptor signaling not only requires kinase activation but, more importantly, requires the inhibition of tyrosine phosphatases by H_2O_2 (Reth 2002).

We also propose that PA treated DCs stimulate pro-inflammatory T cell responses via lipid antigen presentation of PA on CD1 molecules (Schiefner and Wilson 2009). Proteins and lipoproteins are normally presented on dendritic cell MHCI and MHCII receptors, but this form of antigen presentation is not possible for lipids. Lipids are presented on a family of MHC-like proteins called CD1 molecules that are divided into two groups: group 1 (CD1a,b,and c) and group 2 (CD1d). Group 1 CD1 molecules have been shown to present foreign lipid antigens from mycobacteria to CD1 restricted T cells. Group 2 antigens are presented on CD1d to NKT cells (Cohen, Garg et al. 2009). In this

chapter, we show that PA induces ROS in DCs which may regulate PA activated TLR4 signaling. We also demonstrate that CD1b may play a role in the adaptive immune functions of PA activated DCs.

Materials and Methods

Monocyte Isolation and DC Culture

Human monocyte-derived DCs were generated as previously described (Kiertscher and Roth 1996, Mbongue, Nicholas et al. 2015). Peripheral blood from healthy adult donors (age 18+) was provided by the Lifestream blood bank, San Bernardino, CA, according to Loma Linda University IRB requirements. After red blood cell lysis, CD14$^+$ cells were isolated with anti-CD14 magnetic bead MACS separation (Miltenyi biotech) and cultured for 6 days in RPMI 1640 medium +10% FBS with GM-CSF and IL-4.

Preparation of PA

PA (Sigma, St. Louis, MI), was dissolved in 100% EtOH and diluted in a range from 300 to 50 μM in a 2:1 molar ratio with endotoxin low FA-free BSA (Gemini Bio-products) in media with defatted-FBS (EtOH 0.1% v/v).

PCR

Total RNA was isolated from DCs using Stat-60 (Tel-Test Inc.) according to the manufacturer's protocol. After reverse transcription with SydQuanti First Strand cDNA Synthesis Kit (SydLabs Inc.), RT-PCR was performed with Amplitag Gold Fast PCR

Master Mix (Applied BioSystems) on an Eppendorf Mastercyler thermal cycler.

Densitometry was performed and values were normalized to β-actin. Primers for IL-1β,

IL-12/23p40, and IFN-α were designed using NCBI primer blast.

Cytometric Bead Array

Supernatant was collected from DC cultures following 24 hours of 150μM PA

treatment and analyzed with multiplexed human IL-1β, IL-12/23p40, and IFN-α flex sets

as described by the manufacturer (BD biosciences) on MACSQuant flow cytometer.

Data analysis was accomplished with FACP array v3 software.

Antibodies and Flow Cytometry

Antibodies and reagents used were anti-human CD86-FITC, CD80-PE (BD

Pharmingen), CD11c PE, HLA-DR PerCP (Becton Dickinson), CD14-APC (Biolegend),

Annexin V FITC (ebioscience), Propidium Iodide (PI) (BD Pharmingen), 7

aminoactinomycin D (7AAD) (Biolegend). Data acquisition was on a Miltenyi

MACSQuant flow cytometer (Miltenyi Biotec) and analysis was performed with FlowJo

7.6.5 (Tree Star, Ashland, OR) software.

Flow Cytometry Gating Strategy

DCs were gated by FSC-A/SSC-A. Doublet discrimination was performed using

FSC-H vs FSC-W and SSC-H vs SSC-W. Cells with the phenotype HLA-DR^{hi}CD11c^{hi}

were gated as DCs (>94%).

Caspase 3/7 Activity Assay

To assess caspase 3/7 activity, monocytes were seeded at $2x10^5$ in a white flat

bottom 96-well plate. After DC differentiation and FA treatment, the cells were incubated

with 50μL of 3× caspase buffer [150mM Hepes pH 7.4, 450mM sodium chloride,

150mM potassium chloride, 30mM magnesium chloride, 1.2mM ethylene glycol-bis (2-

aminoethylether)-N,N,N',N'-tetraacetic acid (EGTA), 30% sucrose, 10% CHAPS, and

1.5% NP-40] and fluorogenic peptide caspase 3/7 substrate Ac-DEVD-AMC as

recommended by manufacturer (Fisher Scientific) for 2 h at room temperature in the

dark. Half of the samples were also incubated with DVED-CHO (Fisher Scientific), a

caspase 3 specific inhibitor, to ensure the efficacy of the assay. Absorbance was then read

in a MicroLumat Plus LB 96v Fluorescent Reader (EG&G Berthold) at excitation of 360

nm and emission of 460 nm.

Measurement of DC Intracellular Reactive Oxygen Species (ROS)

To measure ROS, dendritic cells, both PA treated and untreated, were incubated

with 25 μM 2',7'-dichlorofluorescein diacetate (H2DCF-DA) (Invitrogen) for 20 min at

37°C. The negative control sample was treated with 1mM MCI-186 (Biomol Research

Laboratories, Plymouth Meeting) dissolved in DMSO for 24 hrs. The positive control

samples were incubated with 10 μM H_2O_2 for 10min prior to the addition of H2DCF-DA.

The H2DCF-DA readily diffuses into the cells where it is hydrolyzed to the polar non-

fluorescent molecule 2',7'-dichlorofluorescein (H2DCF). The DCFH is readily oxidized

by ROS into the fluorescent molecule 2',7'-dichlorofluorescein (DCF) within the cell

(Hempel, Buettner et al. 1999). Following dye treatment, the DCs were harvested by

washing the cells from the wall with DPBS and then centrifuged (at 4°C at 24 x g for 5 min). Supernatant was aspirated and samples were resuspended in 200μL DPBS and analyzed via flow cytometry. Excitation/emission wavelengths for fluorescence measurements of the samples were 488 nm and 530 nm respectively.

Measurement of DC H₂O₂ with PF6-AM

Dendritic cells were cultured in $3cm^2$ plates. The DCs were then incubated in PBS with 5μM PF6-AM for 30min at 37°C (Basu, Rajakaruna et al. 2014). The SPOT ADVANCED software was used to set the microscope settings: 10x magnification, exposure time = 300msec, binning= none, brightness =1, gain =1, and measure full chip, multiple photos setting with exposure time on manual. The DCs incubated with the PF6-AM were then placed on a Zeiss fluorescent microscope. PBS with excess PF6-AM removed and a baseline photo of fluorescence was taken. SPOT ADVANCED was setup to take a photo every 0.5s for 30 min. Media containing treatments was added and photos were initiated simultaneously. Fluorescence was quantified using Image J and normalized to baseline fluorescence. Excitation/emission wavelengths for PF6 were 488 nm and 520 nm respectively.

Microscopy

Dendritic Cells were plated on 8-well chamber slides. After 24 hour treatment with 150uM BODIPY FL C-16 (Life Technologies) complexed 2:1 with BSA, the DCs were stained for microscopy as previously described (Zhu 2012). Antibodies used were

73

anti- human CD74, CD1a, CD1b, CD1c, and anti-mouse IgG1-APC (eBioscience). DCs were imaged on a Zeiss LSM 710 NLO at 40x magnification.

PA Treated DC Sample Preparation and Mass Spectrometry Analysis

After 24 hr treatment with 150 μM PA complexed 2:1 with BSA, the DCs were lysed on ice for 2 hours in radio-immunoprecipitation assay (RIPA) buffer (Santa Cruz Biotechnology, CA) containing 1% Nonidet P40, PMSF (0.2 mM), and protease inhibitor cocktail (Roche). The protein mixture was centrifuged at 10,000 rpm at 4°C for 15 minutes in a Beckman GS-15R centrifuge equipped with a F2402 rotor and the supernatant transferred into a clean tube. The protein concentration in the supernatant was determined by BCA Protein Assay (Thermo Scientific Pierce, Rockford, IL USA). Approximately 60 μg of each protein sample was resuspended in 25mM triethylammonium bicarbonate buffer, pH 7.8. The protein was reduced with a final concentration of 10 mM DTT and incubated at 50°C for 30 minutes, followed by carboxymethylation achieved by addition of 25 mM iodoacetamide (final concentration) and incubation of the mixture in the dark for 1 hour. The proteins were precipitated by addition of 4 volumes of precooled (-20°C) acetone and stored at -20°C overnight. The protein was pelleted at 14,000 rpm in the Beckman GS-15R centrifuge for 10 minutes at 4°C and the supernatant discarded. The protein pellet was dissolved in 25 mM triethylammonium bicarbonate buffer (100 μM GTP, 100 μM GDP in 8 mM PIPES pH 6.8) and partially digested by trypsin (Sigma-Aldrich, St. Louis, MO) at a protein / trypsin enzyme ratio of 25:1 (by mass) for 10 hours at 37°C.

A Tandem Mass Tagging isobaric (TMT) Kit (Thermo-Fisher Scientific) was used to label the peptides following the manufacturer's recommended conditions. Each TMT-labeled protein pool was acidified with 0.1% Formic Acid (FA) and fractionated by strong cation-exchange (SCX) chromatography on a Toptip column (Poly LC, MD). For fractionation, the column matrix was equilibrated with 0.1% FA in 20% acetonitrile (ACN) to facilitate peptide binding. After collection of the flow-through volume, 1.0 mL of each sub-fraction was eluted sequentially with 20% ACN, 0.05 M KCl, 0.2 M KCl, 0.5 M KCL, and 5% ammonium hydroxide in 20% ACN. Next, the fractions were dried under vacuum to remove the ACN, reconstituted in 1% formic acid, and desalted using a Toptip column with C18/hypercarb mixed materials (Poly LC, MD). The eluted peptides were once again vacuum-dried, reconstituted in 30 µl of 0.1% FA, and subjected to LC-MS/MS analysis. The peptides were separated by online reversed phase liquid chromatography (RPLC) using an Easy-nLC equipped with an auto-sampler (Thermo Scientific). A 10 cm, 75 µm id, 3-µm particle size, C18-A2 analytical column (Thermo Scientific) was used for the RPLC separations. Quantitation of the SCX fractionated TMT-6 labeled peptides was carried out on the Thermo LTQ-Orbitrap Velos Pro mass spectrometer. Approximately 2 µg of peptide sample was injected in the analytical column. A pre-column (Thermo, 0.1 × 2 cm, 5 µm C18-A1) was brought in line with the analytical column and a 250-min gradient (solvent A, 0.1% FA in water; solvent B, 0.1% FA in ACN) from 5–30% solvent B was used for separating the peptides. The Orbitrap mass analyzer was set to acquire data at R = 60,000 resolution for the parent full-scan mass spectrum, followed by data-dependent high collision-energy dissociation (HCD) MS/MS spectra for the top 12 most abundant ions acquired at R = 7500 resolution.

DC Proteome Data Analysis

PA treated DC proteins were identified and quantified by analysis with the Proteome Discoverer 1.4 platform (Thermo) and the Mascot search engine (Mascot Darmon 2.2.2; Matrix Science, London, UK) employing the International Protein Index (IPI) Homo sapiens database (version 3.73, June 2010, containing 89739 entries). Mascot searching parameters were used as follows: Carbamidomethylation of cysteine and TMT-6 modification of the peptide N-terminus and lysine were set as fixed modifications and oxidation of methionine and deamination of asparagine and glutamine were set as variable modifications. Trypsin was the protease selected and preparations containing up to two missed cleavages were used. Mass tolerance for the precursor ions was 10 ppm and for the MS/MS 0.2 Da. The peptides were filtered for a maximum false discovery rate of 1%. At least one unique peptide with a posterior error probability of less than 0.05 was accepted for quantification using the grouped TMT-reporter ions and proteins.

Ingenuity Pathway Analysis of the PA Treated DC Proteome

The Ingenuity Pathway Analysis program (IPA, Ingenuity Systems, www.ingenuity.com) (Qiagen, USA) is an intuitive web-based application for rapid and accurate analysis and interpretation of the biological meaning in genomic and proteomic data. Analysis of pathways were made using log2 fold-changes and p-values between two-group comparisons. The ratios of significant protein expression levels were determined at r = 1.25. Multivariate statistics analysis using the "R" program has previously been utilized for metabolic profiling (Reitman, Jin et al. 2011). We have adapted this method for protein expression statistics analysis. Multivariate statistics and

associated graphics were performed in R, version 64.25.1. Heat maps were drawn using the heatmap.2 function found in the g-plots package.

Statistical Analysis

One or two way-ANOVA was performed with GraphPad Prism 6.00 software (GraphPad, San Diego, CA), and values at P <0.05 were deemed significant (**=p<0.01, ***=p<0.001, ****=p<0.0001).

Results

Palmitic Acid Induces Dendritic Cell Secretion of Pro-inflammatory Cytokines

Our lab previously demonstrated that PA matures and activates DCs as measured by upregulation of CD86 and CD80 surface expression. In addition, we have also shown that PA binds TLR4 and induces signaling that results in secretion of IL-1β. Preliminary data from our laboratory indicated that other TLR4 dependent pro-inflammatory cytokines may also be released from DCs upon exposure to PA. We therefore evaluated the cytokine profile of PA treated DCs. We first incubated DCs with 300μM PA for either 3 or 6 hours. Following the incubation, we isolated mRNA from the cells and performed RT-PCR to identify the presence of mRNA of the following inflammatory and anti-inflammatory cytokines or their subunits: IL-8, IL-10, IFN-γ, IL-12/23p40, IFN-γ, IFN-α, IL-6, and IL-1β. We also cultured DCs with PA for 24hrs and assessed the supernatant for secreted cytokines using cytometric bead array. Our results confirmed our previous finding that IL-1β is induced by PA treatment (Figure 20A, D, H, and K). Additionally, we found that both IL-12/23p40 and IFN-α are secreted by DCs in response

to PA (Figure 20I and J). The p40 cytokine subunit detected is assumed to be from IL-23

rather than IL-12 due to failure to detect active IL-12p70 (Figure 15) and will be referred

to as IL-23 for the remainder of this chapter.
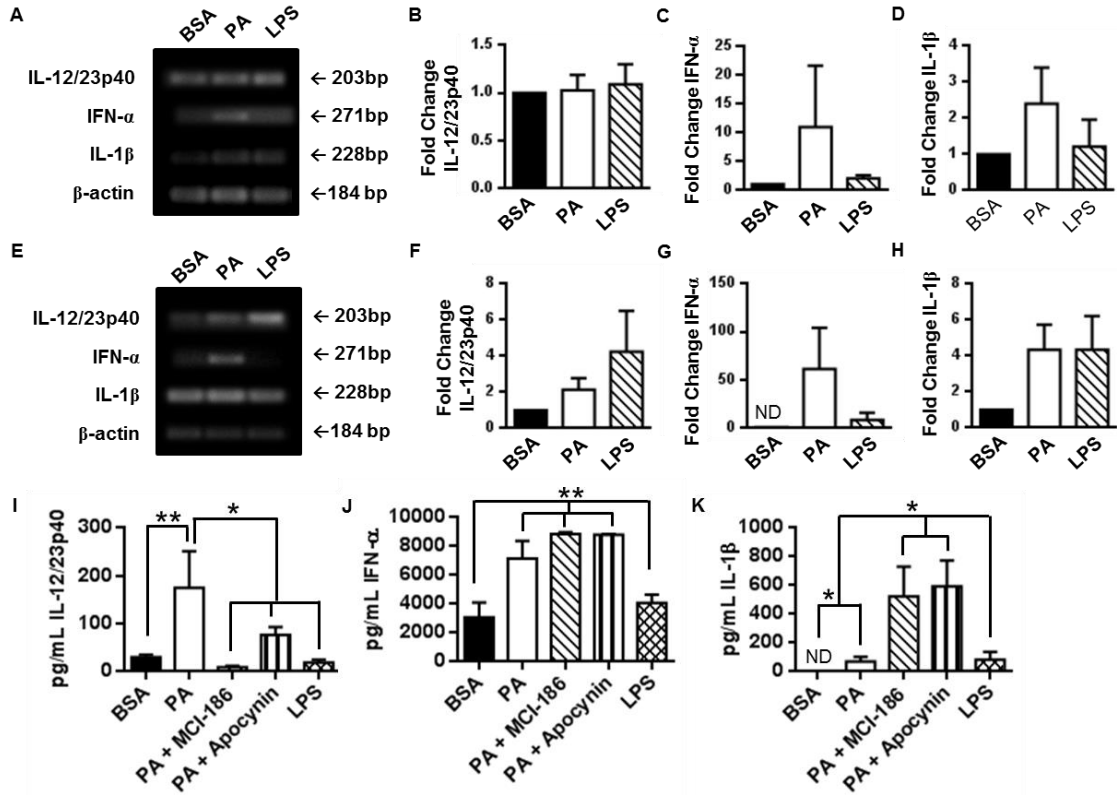
Figure 20. Palmitic acid upregulates dendritic cell pro-inflammatory cytokines. Immature DCs were treated with 300μM PA complexed 2:1 with BSA for 3 or 6 hrs. After palmitic acid incubation, mRNA was isolated from the cells and reverse transcribed into cDNA. Semi quantitative RT-PCR was performed for the cytokines indicated above. (A) acrylamide gel images of RT-PCR results after 3 hours of PA treatment. (B,C, and D) Bar graph representation of semi-quantitative analysis of PCR gel from (A). (E) acrylamide gel images of RT-PCR results after 3 hours of PA treatment. (F,G, and H) Bar graph representation of semi-quantitative analysis of PCR gel from (E). The DCs were incubated with 150μM palmitic acid for 24 hrs (I,J, and K). The cell supernatants were collected and analyzed for the levels of the indicated cytokines after PA and PA + ROS inhibitors MCI-186 and Apocynin treatment by cytometric bead array. Statistical analysis of the data was performed using One way ANOVA (*=p<0.05, **=p<0.01).

Palmitic Acid Induces Dendritic Cell Death

Apoptosis in macrophages was shown to be TLR4 dependent (Haase, Kirschning et al. 2003). Because PA was identified as a TLR4 ligand and has been documented to cause lipotoxicity, we assessed its effects on DC viability. To determine DC viability, a modified Annexin V and PI assay for apoptosis was used (Figure 21A-C). We measured the viability of DCs treated with physiological doses (high = 300uM, medium = 150uM, and low = 75uM, representing PA serum levels in a fasting autoimmune patient or type 2 diabetic, in a fed-state autoimmune patient, and in a normal individual, respectively (Fraser, Thoen et al. 1999)) of PA and found that all concentrations of PA caused significant cell death at 48 hours. However, none of these doses induced significant cell death at time points up to 24 hrs. Thus, all doses up to 24 hours can be used for functional assays. Additionally, we found that PA induced DC death was accompanied by activation of caspase 3/7 (Figure 21D).

ROS has been demonstrated to be important in TLR4 signaling (Maloney, Sweet et al. 2009). Moreover, it is well documented that addition of PA to cells results in increased ROS (Maloney, Sweet et al. 2009). To characterize the role PA generated ROS plays in TLR4 dependent apoptosis in DCs, we co-treated DCs with PA and MCI-186, a non-specific ROS scavenger. We found that blocking ROS completely inhibited caspase 3/7 activity, indicating a role for ROS in PA-induced cell death (Figure 21D). However, blocking ROS with MCI-186 could not rescue DCs from PA-induced cell death. Thus, ROS may have other roles to play in DC function. We found that blocking ROS with MCI-186 or with Apocynin (an inhibitor of NADPH oxidase activity) inhibits IL-23p40 secretion and amplifies IL-1β secretion (Figure 20I, J, and K). To assess whether ROS is

involved in regulating DC activation, we co-treated DCs with PA and MCI-186 and measured co-stimulatory factor expression. We found that blocking ROS resulted in the inhibition of PA-upregulated CD86 and CD80 (Figure 22). These results implicate ROS in PA mediated DC activation. In addition, we previously showed PA-induced NF-κB activation through TLR4 is dependent on ROS. Together, this data led us to further investigate the role of ROS in PA-mediated DC activation.

Palmitic Acid Induces ROS in Dendritic Cells

To confirm PA generation of ROS in DCs, we first directly measured ROS in PA treated DCs. As expected, PA increased the levels of ROS after 24 hrs of treatment (Figure 23A). Ingenuity pathway analysis of proteome changes induced by PA in DCs after 24 hrs supported this finding (Figure 23B, C and D). Because PA stimulates TLR4 and TLR4 has been shown to activate NOX4 (Park, Jung et al. 2004), we were also interested in PA generated H_2O_2 oxidative bursts that may contribute to regulation of TLR4 signaling in dendritic cells (Asehnoune, Strassheim et al. 2004).
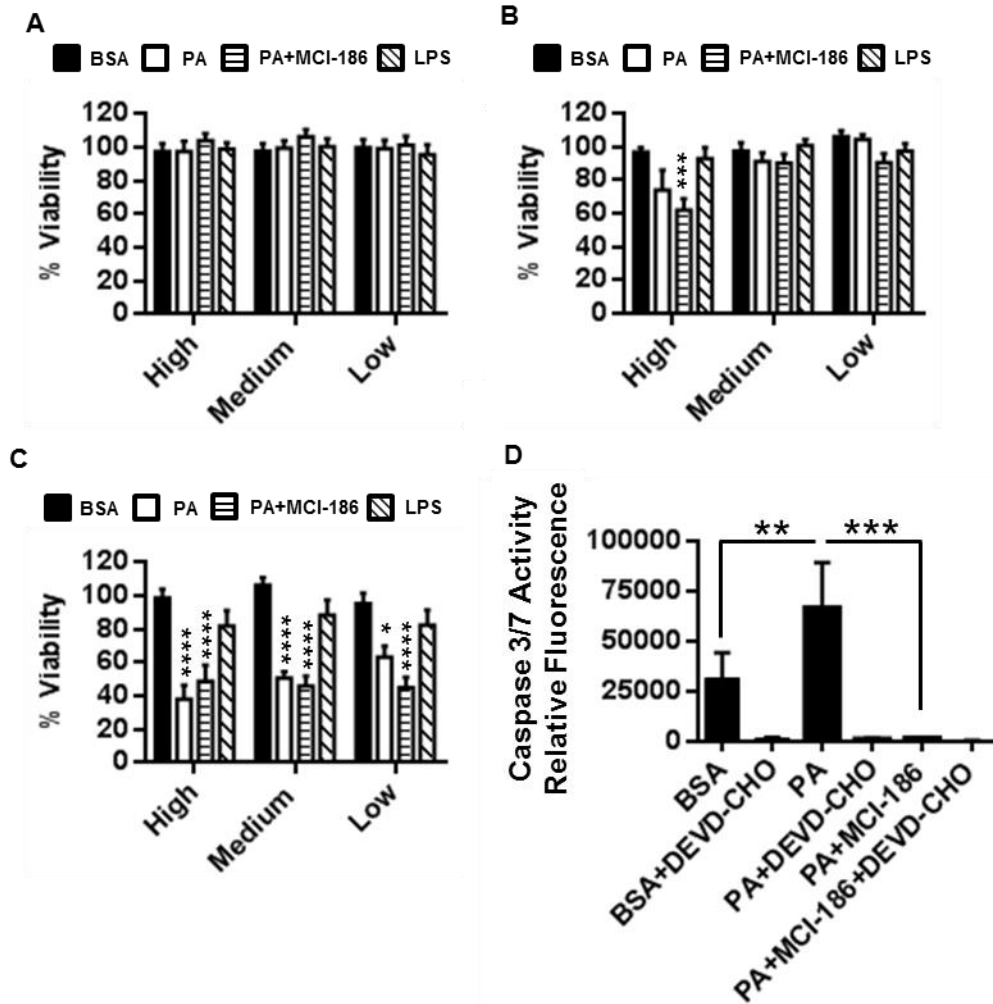
Figure 21. Dendritic cell viability following high (300μM), medium (150μM) and, low (75μM) dose PA treatment. Monocyte-derived dendritic cells were inoculated with PA in a 2:1 molar ratio with BSA for (A) 12 hrs, (B) 24 hrs, or (C) 48 hrs. The cells were analyzed for loss of viability by flow cytometry using Annexin V and propidium iodide (PI) staining. Lipopolysaccaride (LPS) was used as a control to assess DC activation while MCI-186, a free radical scavenger, was used to determine if PA mediated adverse effects were ROS dependent. The data is represented as the percent of total DCs negative for both Annexin V and PI normalized to the BSA negative control. (D) PA induces caspase 3/7 activity. DCs were treated with PA complexed 2:1 with BSA for 36 hrs. Caspase 3/7 activity was measured by the emitted fluorescence of cleaved DEVD-AMC. Graphs are representative of 3 separate patient samples assayed in duplicate. Statistical analysis was calculated based on one way ANOVA (**=$p<0.01$, ***=$p<0.001$, ****=$p<0.0001$).
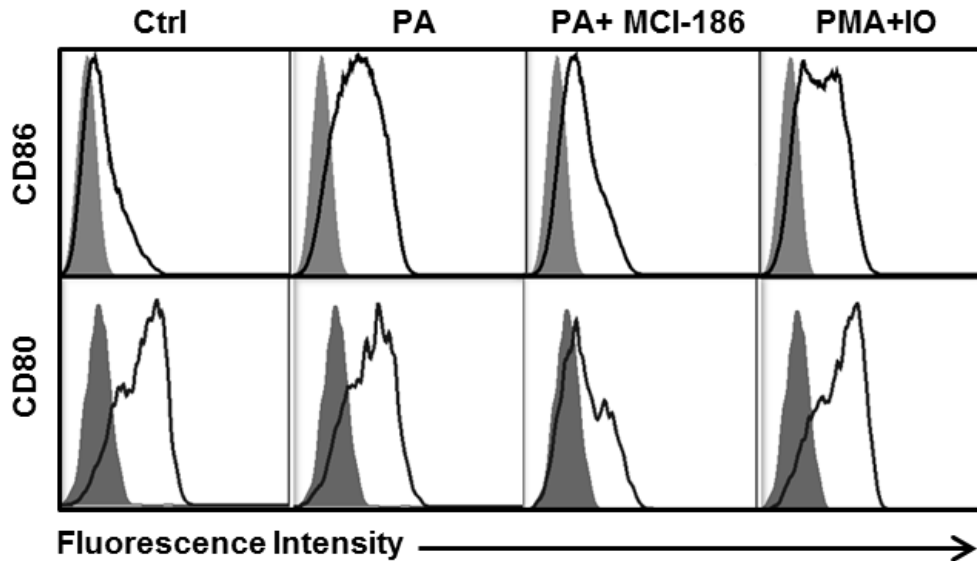
Figure 22. PA induced DC activation is attenuated by MCI-186. Dendritic cells were treated with 300μM PA complexed 2:1 with BSA for 36 hrs. Cells were then stained and analyzed by flow cytometry. DCs were gated by the phenotype (CD14^{low}CD11c^{high}) and histograms for the indicated marker was plotted. The shaded histogram is the isotype control and the open histogram is the experimental sample. Data is representative of three separate experiments.

H$_2$O$_2$ oxidative bursts would be observed at very early time points. Using fluorescence microscopy and the selective H$_2$O$_2$ probe PF6, we showed, similar to LPS the natural ligand for TLR4, that PA can induce H$_2$O$_2$ in dendritic cells in seconds (Figure 23E) (Basu, Rajakaruna et al. 2014).

Palmitic Acid Impairs Dendritic Cell Antigen Presentation

After demonstrating that PA-induced ROS is involved in DC activation, we set out to characterize the effects of PA on DC function. We used mass spectrometry to measure the levels of proteome changes in PA treated DCs. The significance of these
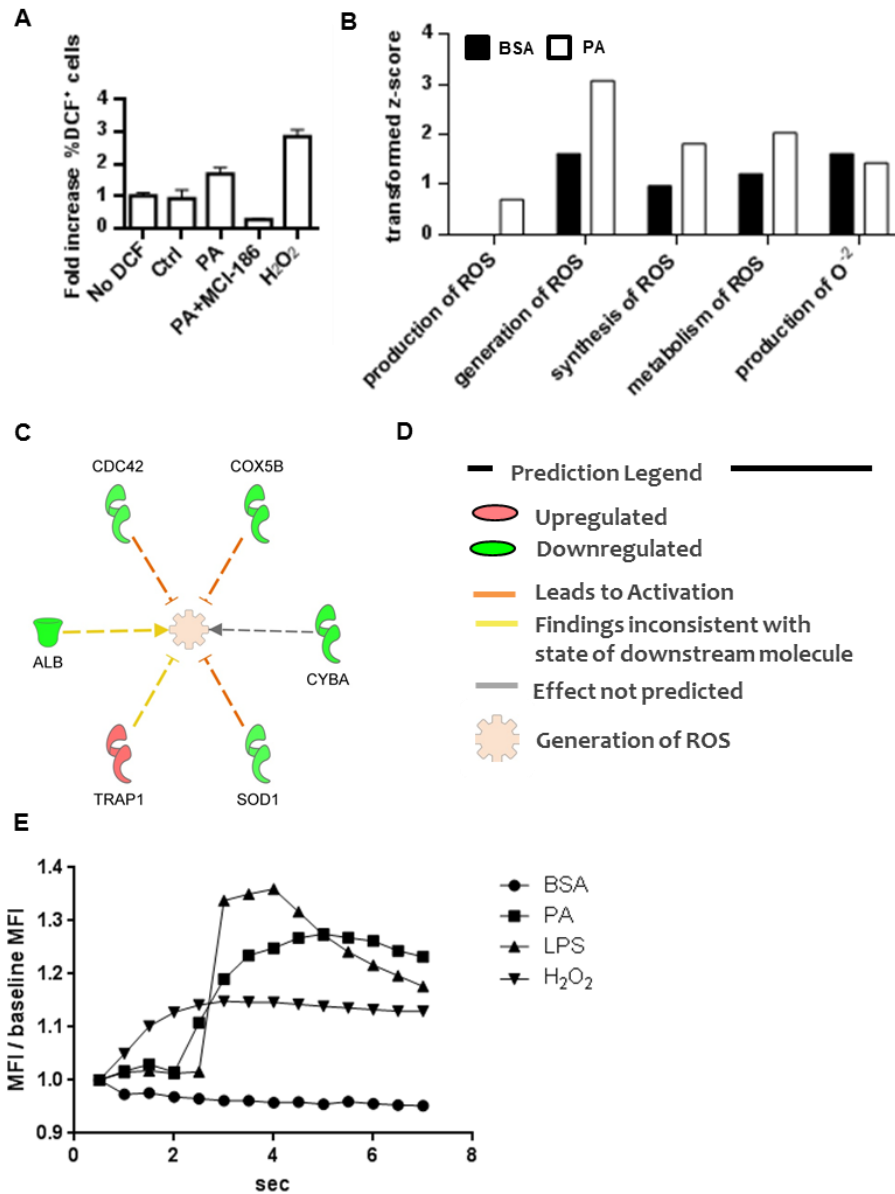
Figure 23. Palmitic Acid induces ROS in dendritic cells. (A) Monocyte derived DCs were treated for 24 hrs with PA. The induction of ROS was determined by measurement of DCF fluorescence and expressed as fold increase relative to DCs not incubated with DCF. The addition of the ROS scavenger MCI-186 was included as an additional control. The data represents three individual experiments performed in duplicate. (B) Comparison of activation z-scores for cellular functions related to ROS production. After 24hr treatment, the DC proteome was assessed by mass spectrometry and protein changes were further analyzed using Ingenuity Pathway analysis. Transformed z-scores derived from this analysis are displayed on the bar graph. The z-scores indicate whether the proteome changes in the DC after treatment are associated with the indicated cellular functions. (z-score = statistical measurement of a score's relationship to the mean of a group of scores. A z-score of 0 indicates the score is identical to the mean) (C) Network display of the cellular function "generation of ROS." (D) Prediction legend for interpretation of network in panel (C).(E) DCs were pre-incubated with the specific H_2O_2 probe PF6-AM. Upon addition of the indicated stimuli, PF6 fluorescence was dected by rapid-fire snap shots by the digital camera on a Zeiss fluorescent microscope. The mean fluorescence intensity of PF6 was normalized to baseline and plotted against time.

83

protein changes were then further assessed using ingenuity pathway analysis (IPA). The

IPA program uses an algorithm to determine if a canonical signaling pathway is

associated with the proteome changes caused by PA a treatment. The significance of

these associations are indicated by assigned p-values, and with these p-values we

generated a heat map (Figure 24A). Based on the proteins detected during mass

spectrometer analysis, the antigen presentation pathway is the canonical pathway most

significantly associated with the control DCs (BSA treatment only). PA treatment greatly

reduced this association. In addition, PA treatment decreased the association of DCs with

three signaling pathways: "Lipid Antigen Presentation by CD1," "Leukocyte

Extravasation Signaling," and "Communication between Innate and Adaptive Immune

Cells" (Figure 24A). According to IPA, PA increases "Clathrin-mediated Endocytosis

Signaling" but not "Calveolar-mediated Endocytosis Signaling." The influence of PA on

these signaling pathways was validated by the activation of pathways previously

associated with PA treatment such as "Mitochondrial Dysfunction" (Padilla, Descorbeth

et al. 2011), "Fatty Acid Oxidation I," and "Ketogenesis." To determine the correlations

of canonical signaling pathways with PA treatment of DCs, we subjected the p-values

from the heat map in Figure 24A to principal component analysis (PCA) (Figure 24B).

The PCA biplot shows that pathway #5 (EIF2 signaling) is the canonical pathway most

correlated with PA treatment of DCs. EIF2 signaling occurs in response to cellular stress

and leads to regulation of both global and specific mRNA translation. These results

suggest that PA is processed by DCs as a stress signal, which as supported by our data,

results in DC activation and secretion of pro-inflammatory cytokines.
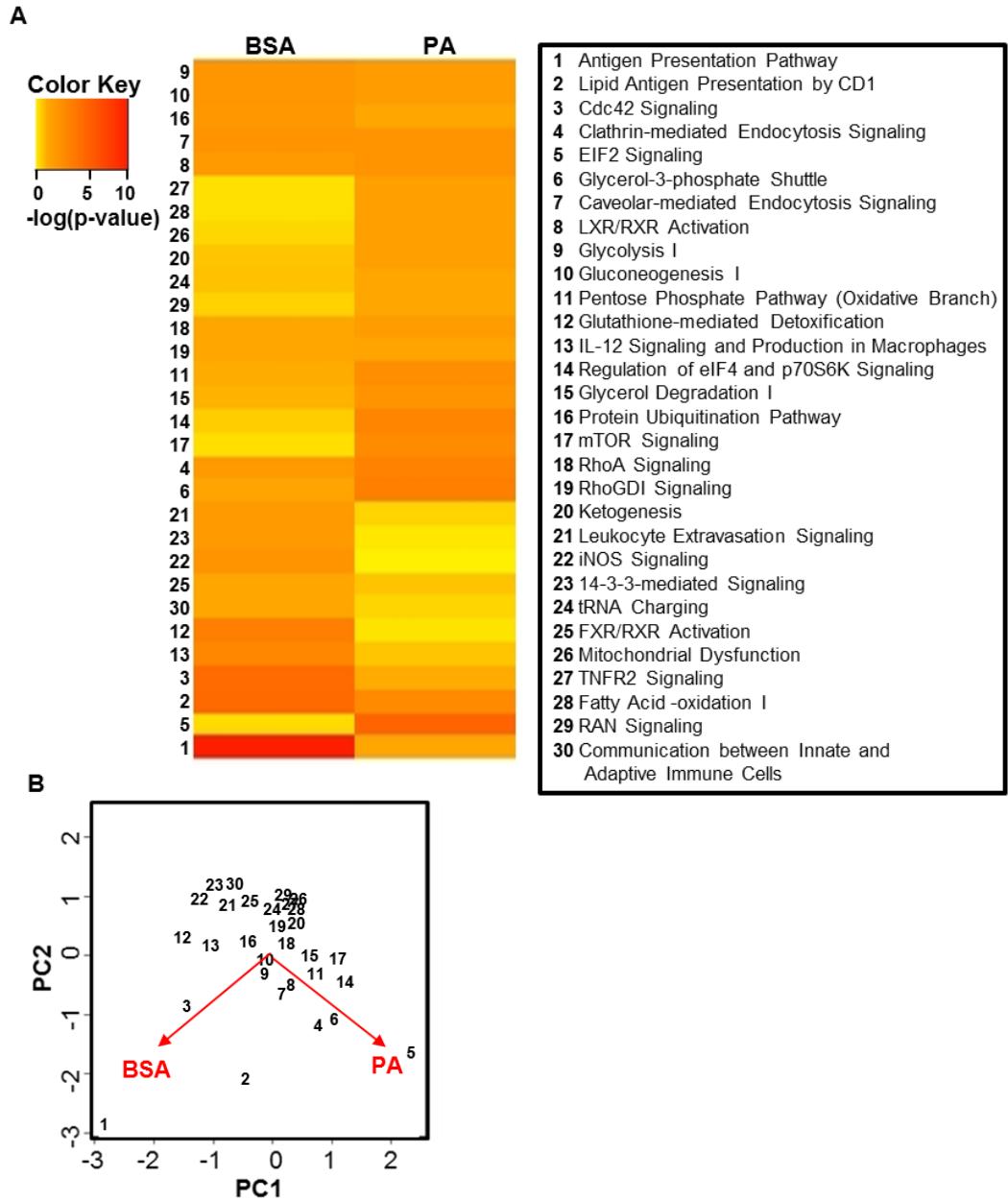
Figure 24. Dendritic cell function is downregulated in PA treated DCs. (A) Heat map representing canonical pathways [-log(p-values)] identified in PA treated DCs. Increasing intensity of red color indicates a higher probability that the indicated pathway is regulated. (B) Principal component analysis (PCA) of DC canonical pathways, -log(p-values). The Bi-plot correlates dendritic cell regulation of indicated pathways with PA treatment or control. These correlations are indicated by the proximity of individual pathways (numbers) to either vector arrowhead. Numbers further from the center of the plot in the direction of the vector indicates increased correlation of the indicated pathway with the designated treatment. Example: Pathway #5 is highly correlated with PA treated DCs, and Function #12 is poorly correlated with PA treated DCs. Zero (0) on the x and y axis is the weighted mean of the multivariate dataset. The values on the (x; y) axis represent (+/-) deviation from the mean of the dataset (0).

Palmitic Acid Colocalizes with CD1b and Induces its Downregulation in DCs

As previously indicated, DCs require 3 signals in order to direct naïve T cell morphogenesis. We have demonstrated that PA affects 2 of these 3 signals: co-stimulatory factors and cytokines. Our mass spectrometry data indicates that the third signal, antigen presentation, is downregulated by PA after 24hrs.

This data corroborates earlier findings indicating that saturated fatty acids impair protein antigen presentation and that serum lipids and mycobacteria regulate the CD1 molecules involved in lipid antigen presentation (Leslie, Dascher et al. 2008, Gagliardi, Teloni et al. 2009). Although antigen presentation seems to be impaired in PA treated DCs, we speculated that lipid antigen presentation via CD1 pathways may still be utilized similar to mycolic acid (Cohen, Garg et al. 2009). Therefore, we assessed changes in surface expression of CD1 molecules on DCs in response to PA treatment by flow cytometry. We found that CD1b and CD1c were significantly downregulated on the surface of DCs in response to PA (Figure 25A). Our mass spectrometry proteome data corroborated these findings (Figure 25B) and showed that all proteins identified in the CD1 lipid antigen presentation pathway were partially downregulated (Figure 25C). To further investigate whether PA could be presented as an autoantigen on CD1 molecules, we determined the spatial relationship between PA and CD1 using fluorescence microscopy (Figure 25D). Because PA structure is similar to a side chain of mycolic acid, a group 1 CD1 antigen, we only assessed the expression of group 1 CD1 molecules on DCs in response to PA (Cohen, Garg et al. 2009). Dendritic cells were incubated with 150uM BODIPY FL C-16 (a fluorescent PA analog) for 24hrs prior to analysis for colocalization with CD1 molecules. The cell images showed a distinct colocalization of
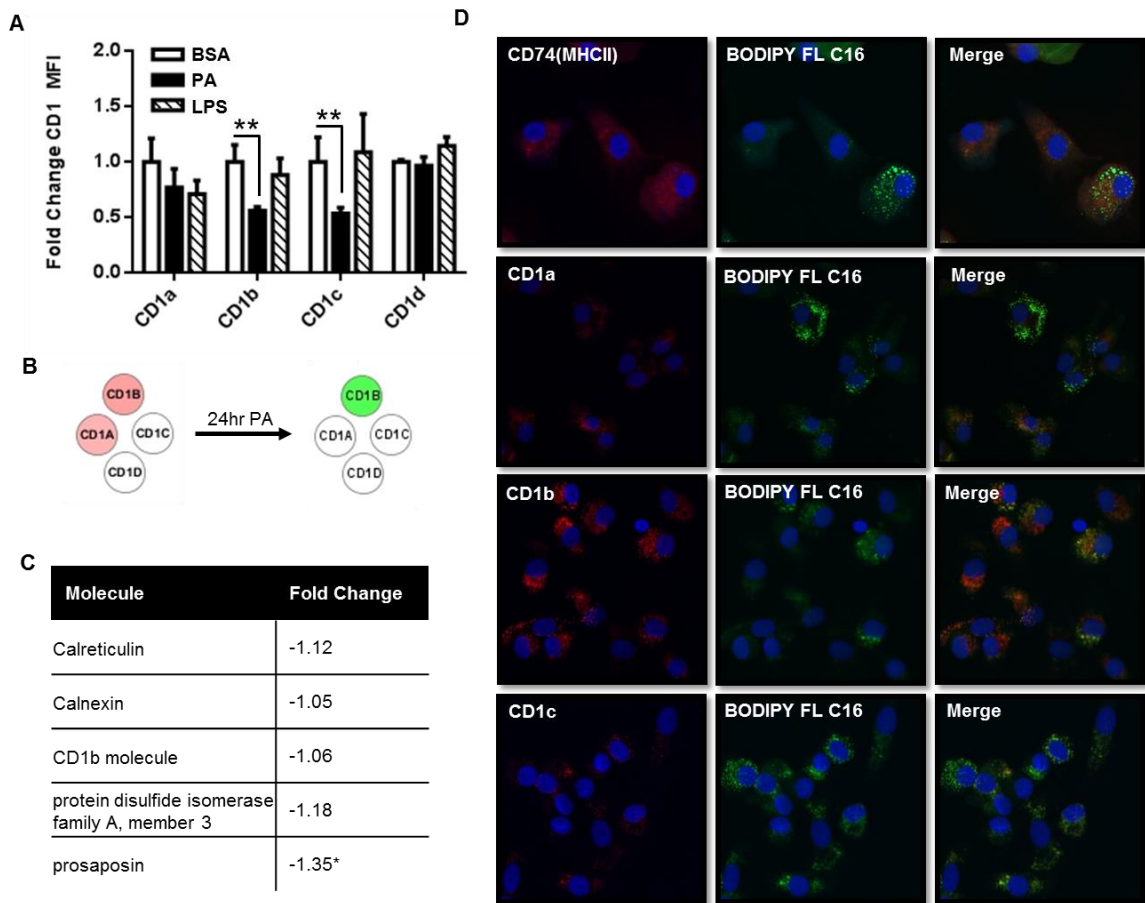
Figure 25. PA treatment affects CD1 expression on DCs. (A) DCs were treated with 150μM PA complexed 2:1 with BSA for 24hrs. Following incubation, the cells were stained for surface receptors and analyzed by flow cytometry. DCs were gated according to the phenotype (CD14^{low}CD11c^{high}HLA-DR^{high}) and the normalized MFI for the indicated marker was plotted. Statistical analysis was performed using One way ANOVA (**=$p<0.01$, ***=$p<0.001$). N=3. (B) Mass spectrometry analysis of class I CD1 molecule expression in DCs. Compared to monocytes, DCs display increased CD1a and CD1b (red circles). Upon 24hr treatment with PA, CD1b is downregulated (green circle). (C) IPA output of downregulated molecules in the lipid antigen presentation pathway in PA treated DCs. (D) The PA analogue (BODIPY FL C-16) colocalizes with CD1b in DCs. Immature DCs were incubated with 150uM BODIPY FL C-16 complexed 2:1 with BSA for 24 hrs. Following incubation, the cells were stained with DAPI and CD74 APC, CD1a-APC, or CD1b-APC. The cells were imaged at 40x. Colors identifying colocalization: Blue is DAPI stain, green is BODIPY FL C-16, red is designated marker, and yellow indicates colocalization. The images presented are representative of 4 separate experiments.

BODIPY FL C-16 with CD1b, but not with the negative control CD74, or with CD1a and CD1c (Figure 25C). The data suggests that PA may be presented as a lipid antigen on dendritic cell CD1b.

Discussion

In this study, we have identified two potential mechanisms by which PA may activate DCs and subsequently induce an inflammatory T cell response. The first mechanism is that of ROS production in PA treated DCs. Figure 23 definitively shows PA induces ROS, and more specifically H_2O_2, in dendritic cells. PA activates TLR4 and Park et al. demonstrated that TLR4 directly associates with NADPH oxidase 4 (Park, Jung et al. 2004). This association results in production of superoxide and downstream ROS that is necessary for TLR4 signaling (Maloney, Sweet et al. 2009). Upon blocking ROS in DCs with either an ROS scavenger or an NADPH oxidase inhibitor, PA induced upregulation of CD86 and secretion of IL-23 is diminished (Figure 20 and 22). Because TLR4 signaling requires ROS, reduced secretion of IL-23 is likely due to transcription not being initiated. ROS inhibitors had no effect on IFN-α secretion (Figure 20). Transcription of IFN-α is regulated by the transcription factors IRF-3 and IRF-7 (Barnes, Lubyova et al. 2002). TLR4 activation of IRF-3 and IRF-7 is through TRIF/TRAM dependent signaling mechanism which is likely independent of ROS regulation (Palsson-McDermott and O'Neill 2004, Kawasaki and Kawai 2014). Therefore, blocking ROS in PA treated DCs should not affect the transcription and secretion of IFN-α.

In the presence of ROS inhibitors, we showed that PA induced IL-1β secretion is enhanced (Figure 20). IL-1β secretion is dependent on both TLR4 signaling and active

caspase-1 which cleaves pro-IL-1β into active IL-1β. The ROS scavenger MCI-186 inhibits TLR4 activation of NF-κB, but not completely (Figure 16). Therefore, transcription and translation of pro-IL-1β would still occur in the presence of MCI-186. We speculate that the ability of ROS scavengers to enhance IL-1β secretion lies in the activation of caspase-1. High levels of ROS oxidizes cysteines in the active site of caspase-1 and inhibit its activity (Meissner, Molawi et al. 2008). Therefore, reducing ROS would allow for maximal caspase-1 activity and enhanced processing of pro-IL-1β to active IL-1β.

The second mechanism by which PA may activate DCs and subsequently induce an inflammatory T cell response is based on CD1b antigen presentation of PA. Dendritic cells treated with PA show increased CD86 and CD83 levels (Figure 15) and secrete IL-1β, IL-23p40, and IFN-α (Figures 15 and 20). This phenotype and cytokine profile is consistent with support of pro-inflammatory T cell development. In addition, IL-1β may synergize with IL-2 to promote CTL proliferation (Baxevanis, Dedoussis et al. 1994). The pro-inflammatory cytokine IL-23 has a role in inducing CTL secretion of IL-17 and promotion of diabetes (Ciric, El-behi et al. 2009).   IFN-α was shown to support the maintenance of CTLs (Pennock, White et al. 2013). In addition to costimulation and cytokine secretion, DCs also need to present antigen in order to activate T cells. Our fluorescence microscopy data shows a pattern of colocalization of the BODIPY analog of PA with CD1b. We therefore hypothesize that DCs can present PA to T cells on CD1b receptors. However, it is important to first know if PA treated DCs have any pro-inflammatory effect on T cells before a role for CD1b in this process can be determined.

Understanding how lipids or other components of our diet can affect the immune system is key to the treatment of metabolic diseases and especially those diseases affected by diet such as type 2 diabetes. Although the area of lipid immunology is still in its infancy, it is becoming clear that lipids' influence on the immune system may be just as important as the role protein antigens play. Further research is essential to uncover the role fatty acids play in immune regulation.

CHAPTER FIVE

IDENTIFICATION OF ANTI-PALMITIC ACID IGG AUTOANTIBODIES IN SERUM OF PATIENTS WITH TYPE 2 DIABETES

Abstract

High levels of serum saturated fatty acids (SFAs) interfere with cellular functions and have been associated with type 2 diabetes. Dietary SFAs can promote inflammation and secretion of IgG autoantibodies and the pro-inflammatory cytokine IL-1β. This chapter explores the presence of anti-palmitic acid (PA) IgG autoantibodies in patients with type 2 diabetes and correlates these antibodies with diabetes health parameters. We retrospectively analyzed serum samples from several cohorts of patients with and without type 2 diabetes, some of whom participated in a health education intervention that resulted in improved diabetes management. Anti-PA IgG was identified in several patients in all cohorts. Specifically, all patients in one cohort with unmanaged diabetes tested positive for anti-PA IgG and showed a significant reduction in anti-PA IgG following a 3 month educational intervention. Serum anti-PA autoantibodies demonstrated high avidity, were specific for long-chain SFAs, and correlated with serum FAs in patients with managed type 2 diabetes. Interestingly, we found that anti-PA IgG neutralized PA-induced IL-1β secretion from dendritic cells. Taken together, our data shows that non-esterified SFAs can be recognized by IgG autoantibodies from human sera. Identification of anti-PA IgG autoantibodies in human serum opens avenues of research for identification of lipid induced immune responses.

.

Introduction

Growing evidence in the literature supports the role of increased dietary intake of saturated fats in the initiation of inflammation (Munoz and Costa 2013, Santos, Oliveira et al. 2013). Although elevated plasma levels of non-esterified FAs have been extensively correlated to insulin resistance, the role of specific FAs, such as palmitic acid (PA), is not well understood (Cascio, Schiera et al. 2012, Martins, Nachbar et al. 2012). Obesity is closely associated with increased levels of pro-inflammatory cytokines (Esser, Legrand-Poels et al. 2014). Visceral adipose tissue is a major site of obesity-induced inflammation, and dyslipidemia is a major factor in the recruitment of activated immune cells such as macrophages, T cells, NK cells, dendritic cells, and B cells to visceral adipose tissue. Infiltrating adipose immune cells are a major source of pro-inflammatory cytokines in obesity-induced inflammation and type 2 diabetes (Oliver, McGillicuddy et al. 2010, Wong, Kyle et al. 2011, Esser, Legrand-Poels et al. 2014). In particular, the pro-inflammatory cytokine IL-1β can directly cause insulin resistance in insulin-sensitive cells (Ehses, Lacraz et al. 2009, Dinarello, Donath et al. 2010, Kawai and Akira 2010, Grishman, White et al. 2012, Esser, Legrand-Poels et al. 2014). Moreover, PA has been shown to activate Toll-like receptor 4 on immune cells and induce secretion of IL-1β (Luo, Yang et al. 2012).

Recently, B cells have been recognized as a major contributor to obesity-induced inflammation (Olefsky and Glass 2010, Winer and Winer 2012, Esser, Legrand-Poels et al. 2014, Sam and Mazzone 2014). B cells are recruited to adipose tissue in response to a high fat diet (Duffaut, Galitzky et al. 2009, Winer, Winer et al. 2014). The importance of IgG antibodies secreted by B cells has been established in a mouse model of type 2

diabetes. For example, depletion of B cells results in protection against diabetes in mice fed a high fat diet (Winer, Winer et al. 2011). In addition, the transfer of IgG antibodies from obesity-induced diabetic mice to non-diabetic mice rapidly induces insulin resistance and glucose intolerance (Winer, Winer et al. 2011). These findings suggest that B cell secretion of autoantibodies may be critical regulators of insulin resistance. Parallel to mice studies, humans with type 2 diabetes have disease-associated changes in B cell function, but the role of these changes in disease pathogenesis is not well established. Insulin resistance in obese individuals is linked to autoantibodies directed against intracellular protein antigens such as Golgi snap receptor complex 1 and Bruton's tyrosine kinase (Winer, Winer et al. 2011). There is the possibility that autoantibodies to lipids are generated in response to a high fat diet because the authors of that study only screened for protein antigens. For instance, autoantibodies to cholesterol have been detected in human serum (Horvath and Biro 2003). Moreover, IgM antibodies against FAs have been reported in multiple sclerosis as well as in human immunodeficiency virus (HIV) patients (Amara, Chaugier et al. 1994, Amara, Chaugier et al. 1994, Boullerne, Petry et al. 1996).

The purpose of the present study was to investigate whether humans produce class switched IgG autoantibodies that recognize saturated FAs such as PA. To answer this question, we retrospectively analyzed serum from 2 different cohorts of obese individuals, including patients with and without type 2 diabetes and patients who participated in the diabetes intervention program, *En Balance* (Wheeler, Montgomery et al. 2012). Our results show that autoantibodies to PA are indeed detectable in human serum.

Materials and Methods

Research Design and Methods

This study consisted of analysis of serum samples from the BioServe biorepository in addition to serum samples from a 3-month diabetes education intervention (*En Balance*) designed to promote improved type 2 diabetes management in Hispanic adults (Metghalchi, Rivera et al. 2008, Ojo, Beeson et al. 2010, Peterson, Beeson et al. 2010, Salto, Cordero-MacIntyre et al. 2011). We measured IL-1β and antibodies to palmitic acid in these samples and correlated the values obtained from the *En Balance* samples with the original primary outcomes of that study. These outcomes included fasting blood glucose, hemoglobin A1c, and body composition. A total of 73 Hispanic males and females with type 2 diabetes met the *En Balance* participation criteria as previously described (Ojo, Beeson et al. 2010, Salto, Cordero-MacIntyre et al. 2011).

Ethics and Informed Consent (En Balance Study)

The Loma Linda University Institutional Review Board (IRB) approved the *En Balance* study protocol and all participants gave written informed consent to participate. Signed consent forms for the study are stored in locked filing cabinets and cannot be linked to participant data according to Loma Linda University IRB protocol.

Evaluative Measures (En Balance Study)

Glucose, A1C, and insulin

Two blood samples (12-14 hr fasting) were drawn from the participants at both baseline and 3 months and analyzed for glucose, A1C, and insulin. Additional samples

were stored frozen at -80°C for future analysis.

Anthropometric measures and body fat composition

Anthropometric measures (height, weight, waist circumference, hip circumference, and waist/hip ratio) were assessed at baseline and 3 months as previously described (Metghalchi, Rivera et al. 2008, Chukwueke, Firek et al. 2012). Body composition was assessed at baseline and at 3 months using a TANITA scale (Detecto, Web City, Missouri), bioelectric impedance technology, and a fan beam dual X-ray absorptiometry (DXA) Hologic Discovery A software version 12.6 (Waltham, MA) as previously described (Ojo, Beeson et al. 2010, Salto, Cordero-MacIntyre et al. 2011).

Serum Samples for Detection of anti-PA IgG and IL-1β

Serum samples from 46 *En Balance* participants were available for anti-PA antibody and IL-1β testing. The baseline characteristics of these participants are presented in Table 3 with the exception of missing participant data. Twenty-one of these participants had paired serum samples from baseline and 3 months available for longitudinal analysis. Twelve participants had serum samples from only baseline and 13 participants had serum samples from only 3 months.

Serum samples (four groups with 20 serum samples each: Hispanic control, Hispanics with type 2 diabetes, Caucasian control, and Caucasians with type 2 diabetes) purchased from the BioServe biorepository (Beltsville, MD) were also tested for anti-PA antibody and IL-1β. The samples were gender, age, and BMI matched against the 21 *En Balance* participants with paired samples. Exclusion criteria consisted of history of renal

disease, self-declared diabetic complications, tobacco use, and other medical histories

including cancer history.

Table 3. Study Participant Characteristics at Baseline (n valid and missing cases = 46; n valid cases = 37, n missing cases = 9)

	Males (n = 8)	Females (n = 33)
Age (years)		
25-39	- - -	4
40-59	5	22
60+	3	7
Mean ±SD	56.25 ± 8.94	53.94 ± 10.17
Weight (kg)		
50-75	1	16
76-99	6	8
100+	1	3
Mean ±SD	88.98 ± 16.28	75.79 ± 18.55
Height (cm)		
145-159	- - -	22
160-169	4	5
170+	4	- - -
Mean ±SD****	168.43 ± 4.60	153.83 ± 5.78
BMI (kg/m^2)		
20-29	3	13
30-39	4	10
40+	1	4
Mean ±SD	31.41 ± 6.43	31.61 ± 7.11

**** = $p < 0.0001$

Synthesis of Palmitoylated Bovine Serum Albumin

Palmitoylation of BSA was performed by modifying a protocol developed by the Geffard laboratory (Amara, Chaugier et al. 1994, Amara, Chaugier et al. 1994, Boullerne, Petry et al. 1996). For this reaction, 10 mg of PA was dissolved in 10 mL of anhydrous methanol (Sigma-Aldrich) containing 100 μl of triethylamine (Sigma-Aldrich). To activate the carboxylic acid group, 200 mL of anhydrous dimethylformamide (DMF) solution containing ethylchloroformate (ETOCOCl) (Sigma-Aldrich) diluted 1/16 was added. The solution was incubated for 3 min at 4°C. Next, 200 mg FA-free BSA (Gemini Bio-Products) was dissolved in 10 mL of 1 mM CaCl2 1M phosphate buffer (pH 6.8) containing 100 μl of triethylamine (Sigma-Aldrich). The BSA solution was added to the PA solution and stirred for 1 hr at room temperature. The conjugates were purified by dialysis against 150 mL of dimethylformamide, methanol, and 1 mM CaCl2 phosphate buffer (pH 6.8), vol/vol/vol overnight at room temperature (RT), then against 1 mM CaCl2 1M phosphate buffer (pH 6.8) for 24 hours at RT. The mixture was dialyzed against PBS (pH 7.2) until precipitated phosphate became soluble, and filtered to remove any remaining precipitate. BSA-PA concentration was determined by measuring the optical density (OD) at 280 nm.

ELISA

An ELISA was developed for determining PA specific IgG autoantibodies in human serum using the Ready-Set-Go ELISA IgG kit (eBioscience) according to manufacturer protocol with the following exceptions. Plates were coated with 100 μL of

50 μg/mL PA-BSA or BSA. Serum samples were diluted 1:100 before use in ELISA. All samples were analyzed in triplicate.

Antibody avidity was determined by a competition ELISA as previously described (Boullerne, Petry et al. 1996). Purified IgG at 2 μg/mL in PBS was pre-incubated for 16 hrs at 4°C with BSA-PA at concentrations varying between 10-4 and 10-11 M. After centrifugation at 10,000 x g for 30 min, 100 μL of the supernatants was analyzed by ELISA as described above. The avidity was defined as the concentration of BSA-PA required for 50% inhibition (IC_{50}) of antibody binding to immobilized BSA-PA.

Isolation of anti-PA IgG antibodies

Total IgG from 7 participant sera was isolated and purifed on PierceTM Protein G Chromatography Cartridges (Thermo Scientific) according to the manufacturer's protocol. IgG that recognized BSA-PA was purified using the SulfoLink® Immobilization Kit for Proteins (Thermo Scientific) according to manufacturer's instructions. BSA-PA was immobilized to resin via covalent thioester bonds, and this resin was used to pack the chromatography column. The anti-PA antibodies were then purified by affinity chromatography.

Determination of anti-PA IgG Specificity

A lipid dot blot method was established to determine the reactivity of a panel of non-esterified FAs (from Sigma-Aldrich) and esterified palmitic acid (glycerol tripalmitate from Sigma-Aldrich and N-palmitoyl phosphytidyl ethanolamine from Enzo Life Sciences) to purified anti-PA IgG. Two μL of 0.2 M FAs dissolved in 100%

chloroform + 0.1% HCl were spotted onto nitrocellulose. After allowing the samples to completely dry, the membrane was blocked in Odyssey blocking buffer for 2 hrs. The lipid blots were probed with purified anti-PA antibodies overnight at 4°C. After washing the blot with PBS, anti-Human IgG conjugated to alkaline phosphatase (Sigma) was used as the secondary Ab.

Anti-PA IgG Neutralization Assay

Monocytes (CD14+) were isolated from human peripheral blood (Lifestream blood bank) and cultured in 96-well plates at a density of 200,000 per well in RPMI-1640 supplemented with 10% FBS, 1,000 U penicillin and streptomycin, 50 ng/mL GM-CSF, and 10 ng/mL IL-4 for 6 days to differentiate them into dendritic cells (DCs). The DCs were treated with 150 uM PA in a 1:1 ratio with BSA for 24 hrs in the presence of IgG Ab containing anti-PA IgG. A mixture of total IgG isolated from 5 Hispanics with type 2 diabetes with high anti-PA IgG levels or a mixture of total IgG isolated from 2 samples which tested negative for anti-PA IgG was used at a concentration of 1.4 mg/mL. Preadsorption of PA was performed at 37°C for 2 hrs. The culture supernatant (50 ul), was analyzed for IL-1β by cytometric bead array.

Determination of Serum Non-esterifed Fatty Acid Concentration

Using the Free Fatty Assay Colorimetric Kit (Cell Biolabs, Inc.), the concentration of free fatty acid in the serum samples diluted 1:2 was determined in duplicate following the manufacturer's recommendations.

Cytometric Bead Array

En Balance serum samples and cell culture supernatants were analyzed with human IL-1β flex set as described by the manufacturer (BD Biosciences) on MACSQuant flow cytometer (Miltenyi Biotecc). Data analysis was accomplished with FACP array v3 software.

Statistical Analysis

Statistical analyses were calculated using SPSS for Windows Version 22 (SPSS, Inc, Chicago, Illinois) with type I error set at $\alpha = 0.05$. The data are presented as means ± SD. Univariate and bivariate analyses were reported at baseline and at 3 months. Spearman's correlation coefficient was used to determine associations between body composition, glucose, and insulin levels with IL-1β and anti-PA antibodies. The Wilcoxon signed-rank test was used to identify baseline to 3-month paired differences. The Mann-Whitney test was used for nonparametric unpaired data analysis of changes in anti-PA autoantibody and FFA levels. GraphPad Prism 6 non-linear regression with outliers automatically excluded was used to determine IC_{50}.

Results

Detection of anti-PA IgG autoantibodies by ELISA

Lipids are generally considered poor immunogens, and immunoassays targeting lipids like PA are rare. We detected anti-PA IgM (data not shown) and IgG antibodies in serum by using a specialized ELISA (Figure 26) (Amara, Chaugier et al. 1994).
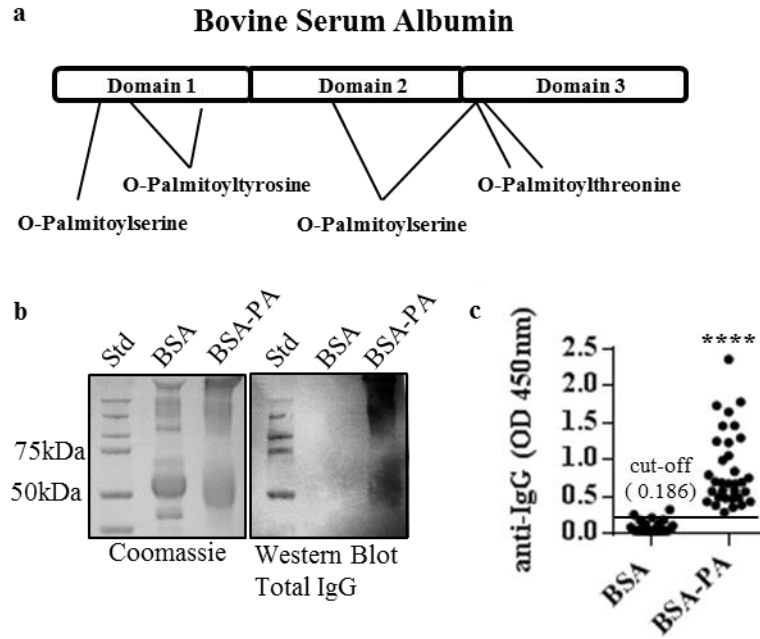
Figure 26. IgG antibodies from patient serum react with palmitoylated BSA. (A) Diagram of BSA palmitoylation sites. Seven accessible hydroxyl groups that can be palmitoylated are present on serine, tyrosine, or threonine of BSA. (B) Coomasie stained gel and SDS-PAGE western blot of palmitoylated BSA (BSA-PA). Palmitoylated BSA migrates faster on the gel than BSA (66kDa) due to an increased (-) charge contributed by SDS association with the palmitoyl group. Total IgG antibodies isolated from Hispanics with type 2 diabetes bind to BSA-PA but not to BSA (C) ELISA identification of anti-PA IgG. *En Balance* baseline serum samples from Hispanic diabetic patients were tested by ELISA for IgG Abs that react with BSA or BSA-PA. The cut-off value for positive antibody reactivity against BSA-PA (>0.186) was defined as an absorbance greater than two standard deviations above the mean value for BSA. Statistical analysis was accomplished with a Wilcoxon-ranked sign test. **** = p < 0.0001.

Because adsorbent 96-well plates bind protein and not FAs, we conjugated the FA of

interest, PA, to BSA in order to stably coat the plates with PA. The acylation reaction of

BSA with PA occurs via an SN2 mechanism which results in O-palmitoylation of serine,

tyrosine, and threonine in BSA (Figure 26A, B and Figure 27A and B). Due to the

orientation of the palmitoyl groups on BSA, only the carbon chain is an accessible

epitope for Ab binding (Figure 27B). We adopted this published approach with slight

modifications and demonstrated that class switched IgG antibodies which recognize PA can be identified in human serum (Figure 26C) (Boullerne, Petry et al. 1996).
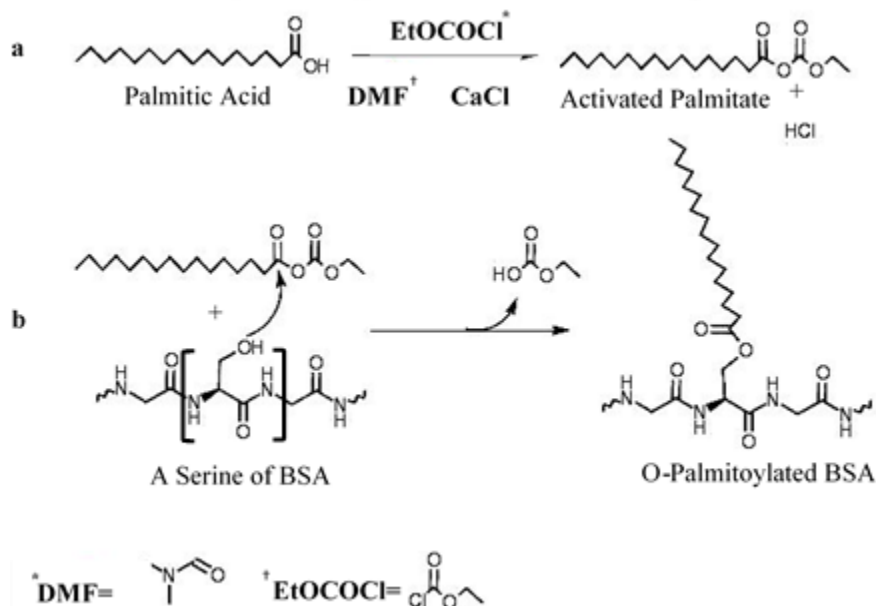
Figure 27. O-Palmitoylation of BSA. (A) The donated hydrogen from PA associates with Cl⁻ to form HCl and two palmitate anions associate with Ca^{2+} to form calcium palmitate. The negatively charged palmitate allows a nucleophilic attack on ethylchloroformate (EtOCOCl). The Cl⁻ is removed as a leaving group and an activated palmitate (anhydride) is formed. DMF = Dimethylformamide. (B) Available hydroxyl groups on BSA perform a nucleophilic attack on the activated palmitate via an SN2 mechanism. The leaving group is removed and the BSA is O-palmitoylated.

Anti-PA IgG Autoantibody Specificity for Long Chain Saturated FAs

To further characterize the antibodies which recognize BSA-PA, we isolated the total IgG fraction and anti-PA IgG autoantibodies from 5 *En Balance* participants with the highest antibody levels to determine Ab specificity and avidity. Using a novel lipid dot blot method constructed in our laboratory and a panel of fatty acids (Table 4), we found that anti-PA IgG can recognize non-esterified palmitic acid (16:0).

Table 4. Panel of Fatty acids tested against anti-PA IgG.

Fatty Acid	Degree of Saturation	Carbon Chain Length	Double bond position
Butyric Acid	saturated	6	N/A
Palmitic Acid	saturated	16	N/A
Stearic Acid	saturated	18	N/A
Lignoceric Acid	saturated	24	N/A
Palmitoleic Acid	monounsaturated	16:1	cis-Δ9
Oleic Acid	monounsaturated	18:1	cis-Δ9
Elaidic Acid	monounsaturated	19:1	trans-Δ9
Linoleic Acid	polyunsaturated	18:2	cis,cis-Δ9,Δ12
Arachidonic	polyunsaturated	20:4	cis,cis,cis,cis-Δ5Δ8,Δ11,Δ14
Docosahexaenoic Acid	polyunsaturated	22:6	cis,cis,cis,cis,cis,cis-Δ4,Δ7,Δ10,Δ13,Δ16,Δ19

In addition, we found the PA autoantibodies cross react with stearic acid (18:0), lignoceric acid (24:0), and elaidic acid (19:1) (Figure 28A).We also determined that the anti-PA IgG recognizes palmitic acid esterified to glycerol but not to phosphate (Figure 28B). Both total IgG fractions and the purified anti-PA IgG reacted with the same fatty acids. Next, we modified this dot blot approach to determine whether the anti-PA antibodies could bind to non-esterified PA in the presence of physiological concentrations of BSA. Figure 28C indicates that a PA dot blot probed with total IgG fraction containing anti-PA IgG still binds to PA in the presence of 750μM BSA. In addition, we determined the avidity of the anti-PA IgG autoantibodies for BSA-PA. Following the protocol published by Boullerne et al. (Boullerne, Petry et al. 1996), we used a competition ELISA to determine that the avidity of anti-PA IgG to BSA-PA was

approximately 2.07×10^{-9} (Figure 28D).
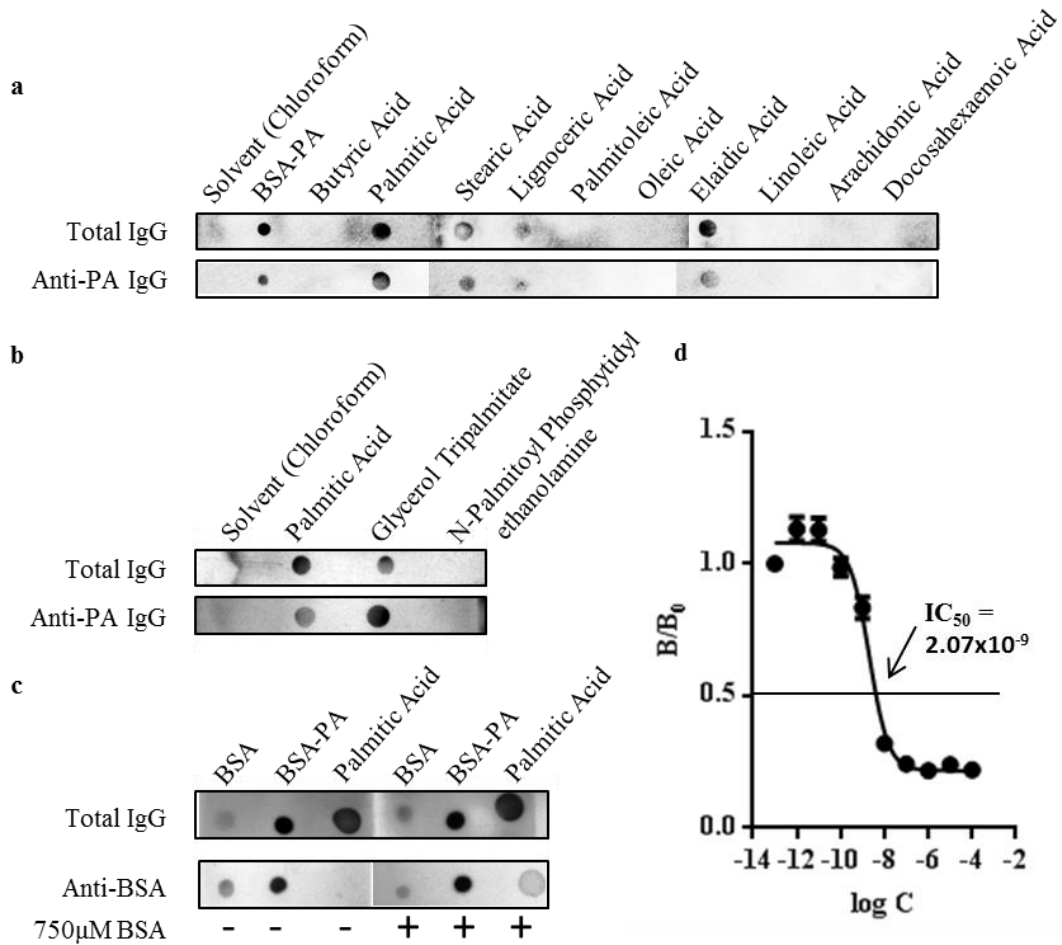
Figure 28. Specificity of anti-PA IgG autoantibodies for long chain saturated FAs. (A) Lipid dot blot of a panel of non-esterified FAs. The indicated FAs were probed with purified IgG or purified anti-PA IgG as the primary antibody. Anti-human IgG conjugated to alkaline phosphatase was the secondary Ab. The blots represent Abs isolated from the sera of 5 *En Balance* participants positive for anti-PA IgG. (B) Lipid dot blot comparison of non-esterified and esterified palmitic acid. The indicated molecules were probed with purified IgG or purified anti-PA IgG as the primary Ab. Anti-human IgG conjugated to alkaline phosphatase was the secondary Ab. The blots are representative of 3 experiments. (C) Dot blot binding assay. The ability of anti-PA to bind to palmitic acid in the presence of physiological levels of BSA (750uM) was tested. (D) Competition ELISA determination of anti-PA IgG avidity. Log C is the $\log_{10}$ of the concentration of the competitor BSA-PA in mol/L. The ratio between the absorbances with competition (B) and without competition (B_0) is plotted. Each data point represents the mean ratio of absorbances $\pm$ SEM of antibodies from 5 participant sera.

Anti-PA IgG Autoantibodies Are Detectable in Both Diabetic and Non-diabetic

Cohorts

After validation of the ELISA technique to identify anti-PA autoantibodies, we set out to determine if these antibodies play a role in type 2 diabetes. We tested for the presence of PA autoantibodies in the sera of 46 Hispanics with type 2 diabetes and assessed the impact of their participation in the *En Balance* program on antibody levels. Out of a total of 67 serum samples, paired samples (baseline vs. 3 month intervention) were available for only 21 participants. The remaining 26 participants had only a baseline or three month serum sample. We found that 100% (36/36) of the Hispanics with type 2 diabetes tested positive for anti-PA IgG autoantibodies before undergoing the diabetes education program (Figure 29A).

Interestingly, the frequency of participants in the *En Balance* program which tested positive for anti-PA autoantibodies was significantly decreased to 49% (20/41) after 3 months (Figure 29A).More importantly, the relative levels of anti-PA autoantibodies in individual participants (N = 21) from baseline (mean ± SEM = 1.05 ± 0.121) to 3 months (mean ± SEM = 0.25 ± 0.030) were significantly reduced (Figure 29B). This reduction in anti-PA autoantibodies coincided with improved diabetes control as described in previous publications (Table 5) (Metghalchi, Rivera et al. 2008, Ojo, Beeson et al. 2010, Salto, Cordero-MacIntyre et al. 2011, Chukwueke, Firek et al. 2012, Wheeler, Montgomery et al. 2012).

To determine whether these results are cohort, disease, or ethnicity specific, we tested serum samples from the BioServe biorespository. We found that approximately 30% of Caucasian control samples (7/21) and 33% of samples from Caucasians with type
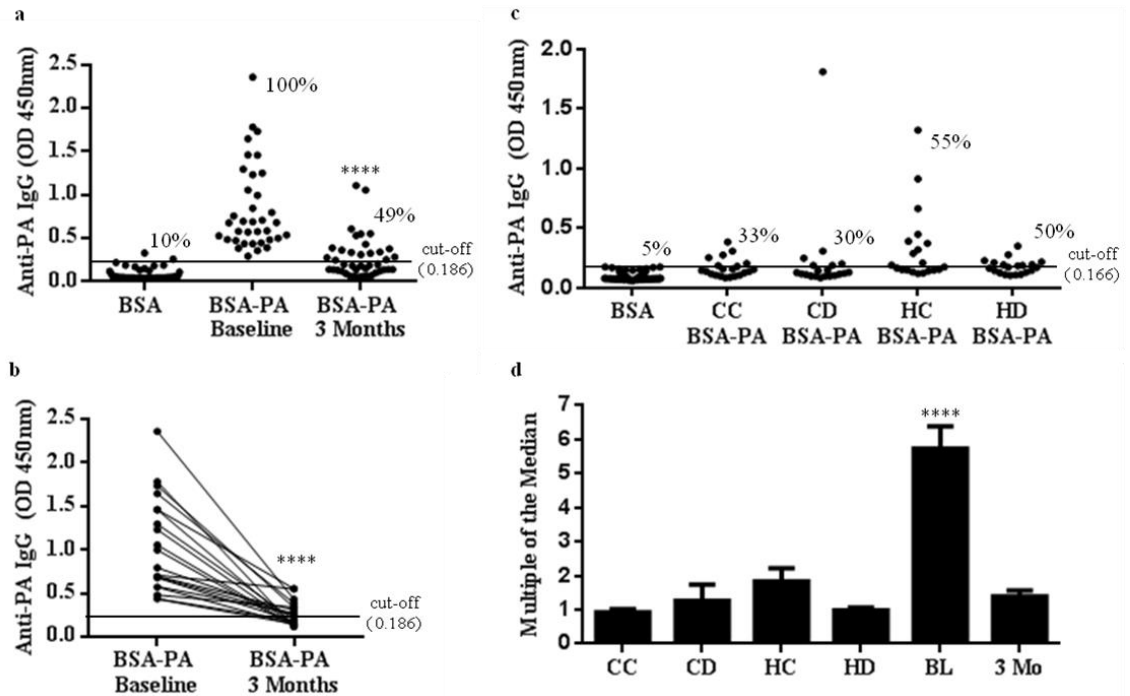
Figure 29. Detection of anti-PA autoantibodies in human serum. (A) Anti-PA IgG in serum of Hispanic *En Balance* participants with type 2 diabetes is reduced following 3 months of diabetes education. Each data point represents the mean optical density of anti-PA IgG antibodies detectable by ELISA. The cut-off value for positive antibody reactivity against BSA-PA (>0.186) was defined as an absorbance greater than two standard deviations above the mean value for BSA. The frequency of sera positive for each group is indicated as a percent on the graph. (B) Paired data from the 21 *En Balance* participants with both baseline (mean ± SEM = 1.05 ± 0.121) and 3 month serum (mean ± SEM = 0.25 ± 0.030) samples. The black lines connect data points belonging to the same participant. Data was analyzed by Mann-Whitney (for A) and Wilcoxon test (for B). (C) Frequency of anti-PA IgG Abs in serum samples from Bioserve biorepository. CC= Caucasian control; CD= Caucasian diabetic; HC = Hispanic control; HD= Hispanic diabetic. The cut-off value for positive antibody reactivity against BSA-PA (>0.166) was defined as an absorbance greater than two standard deviations above the mean value for BSA. (D) Comparison of anti-PA IgG levels among *En Balance* serum samples and Bioserve biorepository serum samples. The median of all corrected OD values (OD450 of BSA-PA reactivity − OD450 of BSA reactivity) for each sample was determined. The corrected OD value for each sample was divided by the median to obtain the Multiple of the Median (MoM). A MoM value of 1 is considered the "normal" range for the anti-PA autoantibody. BL= *En Balance* baseline samples; 3 Mo= *En Balance* 3 month samples. Data was analyzed by Mann-Whitney. $****$ = p < 0.0001.

2 diabetes (6/20) tested positive for anti-PA IgG by ELISA (Figure 29C). Overall, samples from Hispanic cohorts showed an increased frequency of patients who tested positive for anti-PA IgG. Serum from Hispanic controls were 55% positive (11/20) while serum from Hispanics with type 2 diabetes were 50% positive (10/20). The frequencies of serum samples positive for anti-PA IgG in the Hispanic cohorts from the BioServe biorepository (55% and 50%) are similar to that of serum samples from the *En Balance* (49%) cohort after 3 months of intervention.

Lastly, to compare anti-PA autoantibody levels across all groups, we performed multiple of the median (MoM) analysis. This type of analysis normalizes data with "1" corresponding to "normal" levels and also measures how far an individual test result deviates from the median. MoM is commonly used to report the results of medical screening test that tend to be highly variable (Bishop, Dunstan et al. 1993). First, we corrected the anti-PA IgG optical density values at OD_{450} by subtracting out the OD_{450} values obtained by reacting each serum sample with BSA alone. We then found the median of the all the corrected OD_{450} values from both the Bioserve and the *En Balance* samples. Each sample's OD_{450} value was divided by this median to obtain the MoM value. We found that only the baseline serum samples from the *En Balance* study significantly deviated from "normal" values in this data set (Figure 29C). This may indicate that high anti-PA antibody titers are related to how well type 2 diabetes is managed.

Table 5. Study Participant Clinical Characteristics with complete datasets at Baseline and 3 months, n = 13. Values are presented as the Mean ± SD.

Variables	Baseline	3 Months	Mean Difference	p-value
Anti-Palmitic Acid IgG (corrected OD[a])	0.79 ± 0.40	0.17 ± 0.09	0.71 ± 0.44	0.001
IL-1β (pg/mL)	1.09 ± 0.46	0.98 ± 0.38	0.100 ± 0.44	0.442
Fasting Glucose (mg/dL)	153.77 ± 65.12	143.62 ± 61.95	10.15 ± 19.36	0.050
HbA1c (%)	7.70 ± 2.16	6.76 ± 1.36	0.94 ± 1.18	0.005
HbA1c (mmol/mol)	61.00 ± 23.60	50.00 ± 14.90	11.00 ± 12.90	0.005
Insulin (pmol/L)	90.48 ± 74.88	99.30 ± 115.68	-8.88 ± 64.74	1.00
Cholesterol (mg/dL)	170.23 ± 33.51	158.54 ± 38.40	11.69 ± 31.60	0.184
HDL Cholesterol (mg/dL)	45.00 ± 8.19	48.00 ± 7.916	-3.00 ± 4.43	0.049
LDL Cholesterol (mg/dL)	98.62 ± 25.92	93.15 ± 25.35	5.46 ± 21.89	0.382
Cholesterol/HDL ratio (%)	3.86 ±0.85	3.35 ± 0.67	0.50 ± 0.63	0.023
Triglycerides (mg/dL)	249.38 ± 174.09	191.92 ± 36.15	57.46 ± 98.02	0.075
TANITA[b] Fat Mass (kg)	36.15 ± 12.40	33.98 ± 11.63	2.16 ± 2.45	0.013
TANITA[b] Fat Percent (%)	42.25 ± 7.27	40.56 ± 7.43	1.66 ± 1.97	0.034
Scale Weight (kg)	83.74 ± 16.10	82.17 ± 15.38	1.56 ± 3.20	0.100
Waist Circumference (cm)	101.43 ± 9.73	99.89 ± 10.33	1.54 ± 5.36	0.196
Hip Circumference (cm)	111.05 ± 13.91	111.94 ± 12.76	-0.89 ± 3.82	0.294
BMI (kg/m^2)	32.33 ± 6.33	32.11 ± 5.54	0.22 ± 2.64	0.039
DXA[c]-Trunk Fat (kg)	16.60 ± 43.79	15.66 ± 41.20	0.94 ± 1.06	0.007
DXA[c]-Trunk Percent Fat (%)	37.55 ± 6.78	36.36 ± 6.49	1.18 ± 1.68	0.041
DXA[c]-Total Fat (kg)	31.81 ± 11.06	30.27 ± 10.21	1.53 ± 1.86	0.013
DXA[c]-Total Percent Fat (%)	36.94 ± 8.11	35.90 ± 7.85	1.04 ± 1.18	0.012

[a]Optical Density
[b]A brand of bioelectric impedance technology which measures body composition. TANITA scales
  measure within 5% of DXA
[c]DXA-Dual-energy X-ray absorptiometry

Anti-PA Autoantibodies Neutralize PA-induced Secretion of Dendritic Cell IL-1β

To further understand what functions anti-PA autoantibodies have in the body, we determined anti-PA effects on PA-induced secretion of IL-1β from dendritic cells in the presence of BSA (Figure 30A). We found that pre-absorption of PA with IgG antibodies from patients with high levels of anti-PA but not from patients who tested negative for anti-PA IgG, significantly reduced secretion of IL-1β (Figure 30A). This result suggests that anti-PA IgG sequester non-esterified FAs in the blood. In support of this hypothesis, we found that anti-PA antibodies negatively correlate with serum IL-1β in the *En Balance* cohort at baseline (spearman r= -0.34, p=0.026) and at 3 months (spearman r=-0.26, p= 0.05).
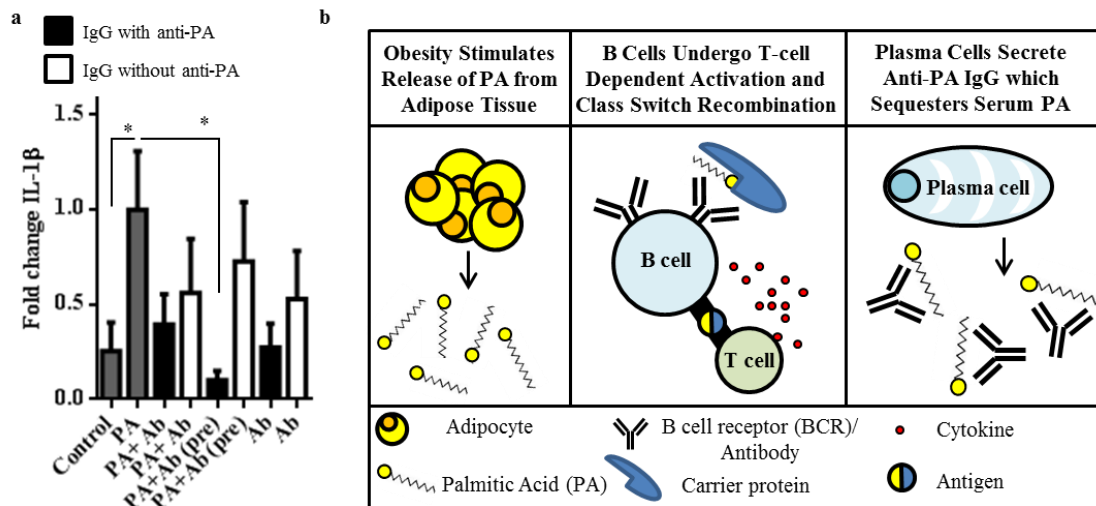
Figure 30. Anti-PA IgG neutralizes PA induced IL-β secretion from DCs in the presence of BSA. (A) Dendritic cells were cultured with 150μM PA (in 1:1 ratio with BSA) in the presence of a mixture of IgG antibody isolated from 5 *En Balance* participants who tested positive for anti-PA IgG (black bars) or in the presence of a mixture of IgG antibody isolated from 2 *En Balance* participants who tested negative for the antibody after the 3 month intervention (white bars). PA+Ab(pre) indicates dendritic cells that were treated with PA preadsorbed for 2 hrs with total IgG from the two groups described. After 24 hrs, media from the cell cultures was analyzed by cytometric bead array for IL-1β. Data was analyzed by One-Way Anova. * = p < 0.05. (B) Illustration of the potential mechanism for the generation of anti-PA IgG.

Anti-PA Autoantibodies and Serum IL-1β from Hispanic Participants with Type 2

Diabetes Correlates with Diabetes Health Variables

In addition to measuring PA autoantibodies, we determined the concentration of IL-1β present in the serum of *En Balance* participants. We found that serum IL-1β levels did not change from baseline to 3 months (Table 5). Next, we performed multivariate analysis of anti-PA autoantibodies, IL-1β, and the health variables collected from each participant at baseline and at 3 months. Surprisingly, we found that anti-PA autoantibodies negatively correlated with body fat (Table 6). In addition, the levels of IL-1β correlated to HbA1c values (Table 6).

Table 6. Anti-PA autoantibodies and IL-1β from serum of Hispanics with type 2 diabetes correlate with body composition and HbA1c respectively.

Variables	N	Spearman Correlation	p-value
Correlated with Anti-PA IgG			
DXA[a]- Total Fat (kg)	27	-0.429	0.025
DXA[a]-Trunk Percent Fat (%)	27	-0.404	0.003
Correlated with IL-1β			
HbA1c (%)	27	0.383	0.048

[a]DXA-Dual-energy X-ray absorptiometry

Total Non-esterified Fatty Acids Correlate with Anti-PA IgG Levels.

Finally, we measured the concentration of total non-esterified fatty acid (both bound and free) in all serum samples. As expected, total FA in serum was significantly

higher in the diabetic cohorts as compared to the non-diabetic controls (Figure 31B). In

the ethnic and T2D combined group, the levels of serum FA did not correlate with the

levels of anti-PA IgG detected in the serum samples (Figure 31A). Because no significant

correlations of anti-PA autoantibodies with improved diabetes control (Table 5) or serum

FA were found, we analyzed the data according to the published American Diabetes

Association target ranges for fasting blood glucose (FBG). We found that the levels of

FFA correlate with anti-PA IgG levels (n= 24, Spearman's rho 0.4862, p = 0.16) for

individuals whose FBG was in the target range of 70-130 mg/dL. However, the levels of

FFA do not correlate with anti-PA IgG levels for individuals whose diabetes is

unmanaged (FBG > 130 mg/dL).
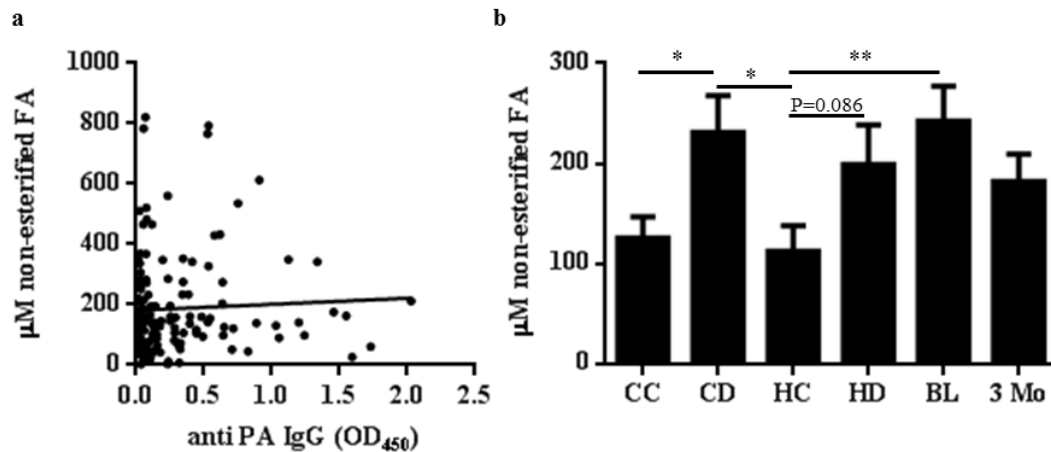
Figure 31. Serum non-esterified serum FA. (A) XY plot of anti-PA IgG and non-esterified serum FA for all serum samples in this study. (B) Bar graph of serum non-esterified FA among diabetic and non-diabetic cohorts. CC= Caucasian control; CD= Caucasian diabetic; HC = Hispanic control; HD= Hispanic diabetic. Data was analyzed by Mann-Whitney. * = p < 0.05, * = p < 0.01.

Discussion

In this chapter, IgG autoantibodies against PA were shown to be detectable in human serum (Figures 26 and 28). IgG antibodies are principally active during a secondary antibody response driven by T cells. Therefore, the emergence of anti-PA IgG autoantibodies coincides with maturation of an antibody response, which occurs upon repeated exposure to an antigen. We also demonstrated that conjugation to the carrier protein BSA is not necessary for anti-PA IgG to recognize PA (Figures 28A and 29). The anti-PA antibodies we found can recognize non-esterified palmitic acid as well as palmitic acid esterified to glycerol (Figure 29B), indicating that these antibodies could potentially function both in the blood and in the tissue where saturated fatty acids are stored as triglycerides.

Characterization of anti-PA IgG autoantibodies revealed that they are not specific for PA, but rather bind to long chain saturated FAs (Figure 28 and Table 4). Anti-PA IgG did not recognize butyric acid (6:0), indicating that these antibodies do not recognize short chain saturated FAs. Interestingly, we found that anti-PA did not recognize oleic acid (18:1) but did recognize elaidic acid (19:1). Both oleic and elaidic acid are monounsaturated long chain FAs, but only elaidic acid is recognized. We speculate that this result is due to the double bond being in the trans- rather than cis- configuration (Table 4), therefore structurally mimicking a saturated FA (Figure 27A). Further, we did not detect any IgG antibodies which bind to polyunsaturated FAs, supporting the notion that polyunsaturated FAs are anti-inflammatory (30).

Of particular significance is that our data clearly show that anti-PA autoantibodies were reduced in serum samples obtained from Hispanics with type 2 diabetes after 3

112

months of culturally sensitive diabetes education (Figure 29). In this same cohort of participants, blood glucose, hemoglobin A1c, body fat, and dietary fat were also significantly reduced, indicating that managing diabetes through diet and exercise can result in a reduction of PA autoantibodies (Table 4 and (23, 25-28)). However, we could not correlate any one parameter to the levels of anti-PA IgG or to the change in antibody levels. We speculate that a mechanism indirectly related to serum FA or dietary intake of saturated fat may underlie the generation of the anti-PA antibody.

Our data also showed that anti-PA IgG are found both in the diabetic and non-diabetic condition. Interestingly, Hispanic participants presented with the anti-PA antibody about 20% more frequently than Caucasian subjects (Figure 29C). Another point to note is that the amount of antibody in the Caucasian cohort did not differ between diabetic and non-diabetic. On the other hand, the serum from BioServe Hispanic controls had statistically significant higher levels of anti-PA IgG than the serum from BioServe Hispanic diabetes samples (Figure 29C). The only group that had serum levels of anti-PA IgG above control or "normal" levels were from the *En Balance* participants at baseline (Figure 29D). These participants not only had type 2 diabetes, but at baseline, their diabetes was unmanaged (Table 4). Further characterization of the relationship between diabetes management and anti-PA IgG, antibody levels could potentially lead to using anti-PA antibody as an additional biological indicator in the management of type 2 diabetes.

Table 6 demonstrates that anti-PA autoantibodies negatively correlate with body fat and that IL-1β positively correlates with HbA1c. These correlations seem counterintuitive because increased adiposity is associated with low-grade chronic

113

inflammation. However, obesity and increased BMI were shown to be associated with impaired antibody responses (Sheridan, Paich et al. 2012, Paich, Sheridan et al. 2013, Young, Gray et al. 2013). Our study shows that increased fat is associated with reduced production of anti-PA autoantibodies, a result which corroborates the literature observations (Sheridan, Paich et al. 2012, Paich, Sheridan et al. 2013, Young, Gray et al. 2013). The correlation of serum IL-1β with HbA1c supports current convention that IL-1β is strongly associated with insulin resistance and type 2 diabetes (Lagathu, Yvan-Charvet et al. 2006, Esser, Legrand-Poels et al. 2014).

We found that IgG from Hispanics with type 2 diabetes neutralized the secretion of IL-1β from DCs (Figure 30A). Previous studies have determined that IgG autoantibodies generated in type 2 diabetes are pathogenic (Winer, Winer et al. 2011, Winer, Winer et al. 2014). An alternative possibility requiring further exploration is that anti-PA IgG are generated as a protective mechanism against increased plasma non-esterified saturated FAs and subsequent inflammation and insulin resistance (Figure 30B). In "managed" diabetes, total serum non-esterified FAs correlate with the levels of anti-PA IgG. However, they do not correlate in "unmanaged" diabetes, indicating possible dysregulation of what may be a normal process of antibody production. Further research is necessary to determine what mechanisms link saturated fatty acids to the production of anti-PA IgG. Based on the available data, our current hypothesis is that increased non-esterified PA resulting from excess calories (or overeating) and obesity stimulates the production of anti-PA autoantibodies through an indirect mechanism such as palmitoylating serum proteins (Figure 30B). Because we observed class switched IgG autoantibodies (Figure 26, 28, and 29) we speculate that generation of anti-PA

autoantibodies is antigen and T cell dependent (MacLennan, Gulbranson-Judge et al. 1997). These autoantibodies may then sequester non-esterified SFAs and may help mitigate SFA induced inflammatory responses. The natural function of anti-PA IgG in the body remains unknown. If the role of anti-PA IgG in the healthy state and in unmanaged type 2 diabetes can be further validated, a new avenue in understanding and treatment of these conditions is possible. Potentially, these antibodies could be used as a therapeutic if they are found to be protective. Alternatively, they could be used as indicators of diabetes management. Understanding how poor type 2 diabetes management impacts anti-PA IgG production and lipid immunology could have an important impact on the future of type 2 diabetes research.

The main objective of the present study was to determine whether there are detectable levels of anti-PA autoantibodies in normal or diabetic patients and our findings support the existence of such autoantibodies. Future studies need to further explore the significance of this finding using larger cohorts of normal, pre-diabetic and diabetic patients. We propose that our findings raise the need to investigate the role of lipid autoantibodies in healthy conditions and in type 2 diabetes to further our understanding of lipid immunology.

CHAPTER SIX

CONCLUSIONS AND FUTURE DIRECTIONS

Summary

This body of research explored the relationships between palmitic acid and human immune cells and their possible implications in type 2 diabetes. Chapter 1 summarizes the role that fatty acids and immune cells play in the development of type 2 diabetes. From this review, it is clear that the recruitment of monocytes to visceral adipose tissue and subsequent differentiation into dendritic cells may play an important role in obesity-induced inflammation (Figure 31). Chapter 2 describes the necessity of histone H1 down-regulation and proper histone acetylation during monocyte differentiation into dendritic cells. Understanding epigenetic regulation of DC differentiation is the first step to defining what governs this process in the presence of palmitic acid, a likely scenario during diabetes inflammation. In chapter 3 and 4, the mechanism by which PA activates TLR4 on DCs and induces secretion of pro-inflammatory cytokines is discussed (Figure 31). Lastly, chapter 5 introduces a clinical aspect. Patients with unmanaged type 2 diabetes have high levels of antibodies that recognize PA. The precise role of these newly identified antibodies is unclear. Whether they are pathogenic or beneficial, it has become increasingly clear that they have a large implication for both diabetes research and lipid immunology.
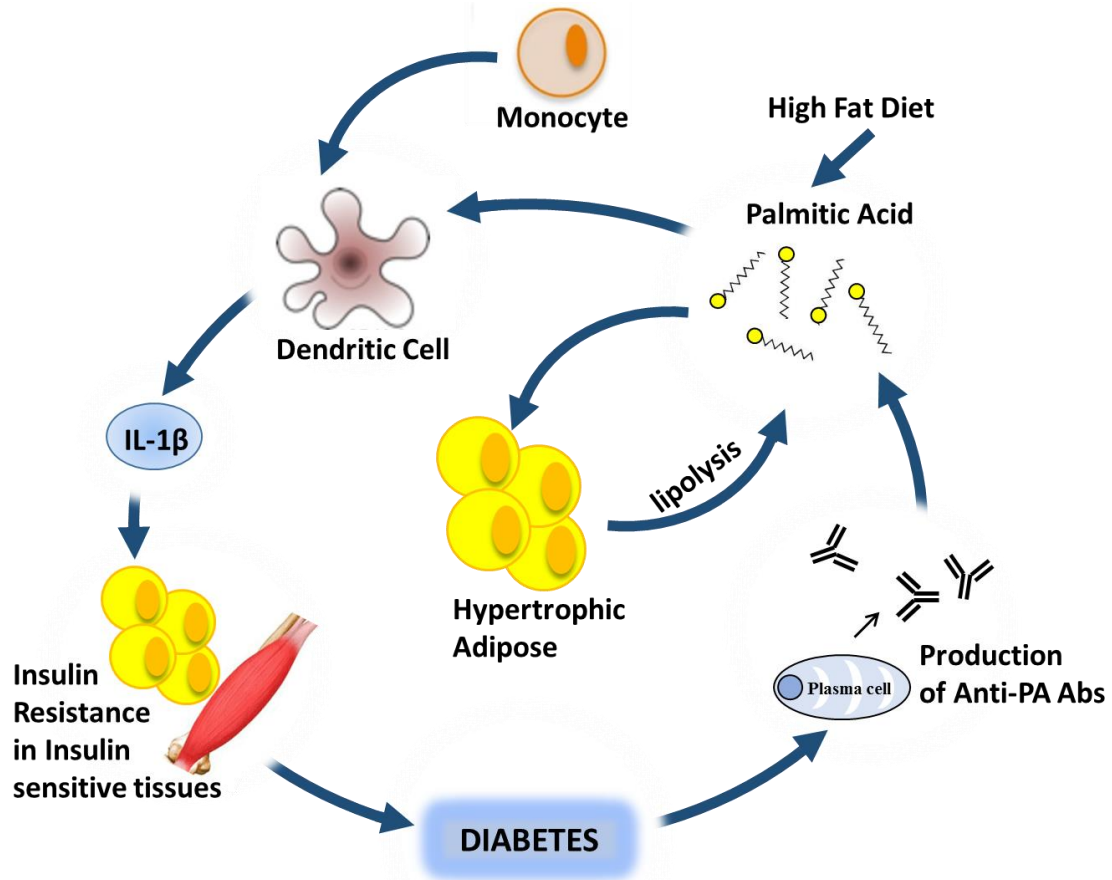
Figure 32. Summary. Diets high in palmitic acid lead to hypertrophic adipose tissue, increased lipolysis, and increased serum palmitic acid. Monocytes differentiate into DCs which can be affected by elevated concentrations of palmitic acid. PA activates DCs and induces secretion of IL-1β. Pro-inflammatory IL-1β is attributed to induction of insulin resistance and the onset of type 2 diabetes. In unmanaged type 2 diabetes, the production of anti-PA IgG antibodies are observed.

Future Directions

Aims

Saturated FAs, e.g. palmitic acid (PA), are pro-inflammatory and have been associated with metabolic syndrome, insulin resistance, and various immunological complications (Kim, Pham et al. 2007, Riserus 2008, Titov, Krylin et al. 2011). In

diabetes patients, serum saturated FAs are correlated with inflammation (Riserus 2008, Unger and Parkin 2010, Virtanen, Niinisto et al. 2010). Our laboratory has shown that the impact of PA on the immune system in type 2 diabetes can be partially attributed to their interaction with DCs and possibly B cells. While our laboratory has shown the pro-inflammatory effects of PA on DC function, complete elucidation of the molecular mechanisms by which PA impact DCs requires further investigation.

Our long-term goal is to understand how high fat diets may drive obesity-induced inflammation in order to identify targets for the development of new diabetes therapeutics. The overall objective of future research is to define the molecular mechanisms underlying palmitic acid induction of inflammation. Our central hypothesis is that monocytes differentiate into mature (activated) DCs in the presence of PA, and that these activated DCs can mount not only an innate but also an adaptive immune response. This hypothesis is based on data from this dissertation and current literature showing that (1) PA binds TLR4 on DCs and induces secretion of pro-inflammatory cytokines associated with chronic inflammation in adipocytes; (2) Obesity-induced inflammation increases the numbers of pro-inflammatory T cells in the visceral adipose tissue (Nishimura, Manabe et al. 2009), and PA-treated DCs seem to activate $CD8^+$ T cells (Figure 33). (3) Lastly, antibodies that recognize PA are present at high levels in patients with unmanaged type 2 diabetes (Figure 29). The rationale behind the proposed research is that understanding mechanisms of PA induced inflammation will aid the design of pharmacological agents which target inflammatory pathways responsible for obesity-induced inflammation and subsequent type 2 diabetes. Therefore, we will test our central hypothesis according to the following aims:

Aim 1: Characterize PA Modulation of DC Differentiation from Monocytes

Working Hypothesis: In the presence of PA, monocytes differentiate into mature, activated DCs. We will use mass spectrometry and Ingenuity Pathway Analysis to determine changes in the DC proteome as well as monitor post-translational modifications that occur in response to differentiation in the presence of PA.

Aim 2: Determine the Mechanism of PA Induced T Cell Activation

Working hypothesis: PA activated DCs may produce a pro-inflammatory response in T cells. To test this hypothesis, we will determine T cell phenotypic and cytokine profiles by flow cytometry after DC/T cell co-cultures in the presence of PA. Furthermore, we will use neutralizing antibodies against CD1 to determine if PA mediated T cell activation is CD1 dependent.

Aim 3: Determine the Role of Anti-PA Antibodies in Type 2 Diabetes

Our working hypothesis is that anti-PA antibodies are natural protective antibodies that reduce the level of free PA in the body. To determine whether anti-PA antibodies are protective or pathogenic, we will analyze and correlate the levels of anti-PA IgG, pro-inflammatory cytokines, palmitoylated proteins, and serum lipids before and after a lipid challenge in healthy and diabetic subjects. We will also use mass spectrometry and immunoprecipitation with anti-PA antibodies to determine all antigens recognized by the antibody.

Experimental Approach

Aim 1: Characterize PA Modulation of DC Differentiation from Monocytes

In vivo, the differentiation of dendritic cells from monocytes occurs in a microenvironment. In type 2 diabetes, this microenvironment is likely to be high in saturated free fatty acids. Therefore, it is important to understand how DC differentiation in a microenvironment with high concentrations of PA may affect downstream function. It is known that DCs differentiated in the presence of PA are hyper responsive to LPS stimulation (Zeyda, Saemann et al. 2005, Wang, Hao et al. 2007, Kong, Yen et al. 2010). Therefore, we hypothesize that, in the presence of PA, monocytes differentiate into mature, activated DCs.

To test this hypothesis we will differentiate monocytes using either GM-CSF + IL-4 or with GM-CSF + IL-4 + PA. Once differentiated, we will isolate the protein from the cells and label them with TMT-reagents for quantification by mass spectrometry. The changes in the DC proteome will be assessed and specific attention will be given to histone changes and post translational modifications we previously determined to be important in DC differentiation (Chapter 2, Figures 8 and 9). Ingenuity Pathway Analysis will be used to assess if PA differentiated DCs have a pro-inflammatory phenotype. Lastly, *in vitro* assays will be used to assess the effects of PA on DC differentiation. Levels of costimulatory factors, MHC molecules, CD1 molecules, and secreted cytokines will be analyzed.

Aim 2: Determine the Mechanism of PA Induced T Cell Activation

Preliminary data show that human peripheral blood treated with PA have

increased numbers of CD8$^+$CD127$^+$ T cells and that CD5$^+$ on CD8$^+$ T cell proliferation is increased (Figure 33). In addition, PA treated DCs have a pro-inflammatory phenotype manifested by increased surface CD86 and secretion of IL-1β, IFN-α, and IL-23 that would support the differentiation of pro-inflammatory T cells (Figures 15 and 20). Because this pro-inflammatory cytokine profile could support Th17 and CTL development, we will use PA modulated DC-T cell co-cultures to assess whether PA treated DCs can stimulate the differentiation of pro-inflammatory T cells. Using flow cytometry and cytometric bead array, we will measure markers of Th17 and CTLs to determine their relative abundance and activation in response to PA treated DCs after 5 days of co-culture.

Upon determining whether PA treated DCs can stimulate pro-inflammatory T cell development, we will assess the role of CD1b, an MHC-like molecule, in this interaction. Because antigen presentation and stimulation of the T cell receptor is a requirement for T cell activation, we believe that excess PA is presented on DCs as a CD1b bound lipid antigen. Proteins and lipoproteins are presented on MHCI and MHCII, but this is not possible for lipids. Lipids are presented exclusively on a family of MHC-like proteins called CD1 molecules (Schiefner and Wilson 2009). Our preliminary data showed that PA may associate with CD1b on DCs (Figure 25C).
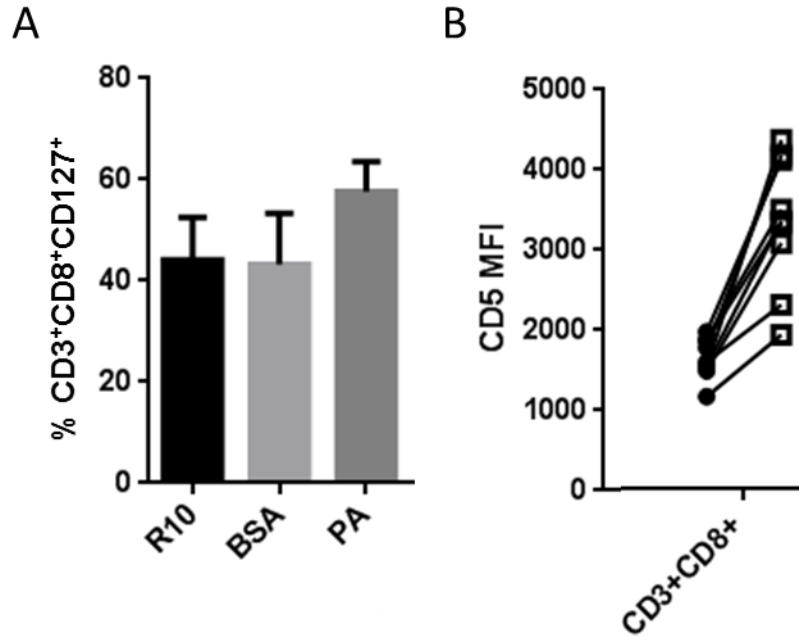
Figure 33. Effects of PA on CD8$^+$ T cells in Human Peripheral Blood. Peripheral blood was treated with 300uM PA complexed 2:1 with BSA for 5 days. Samples were stained and analyzed by flow cytometry. (A) The percent of total lymphocytes CD3, CD8, and CD127 positive. (B) The Mean fluorescent intensity (MFI) of CD5 on CD3$^+$CD8$^+$ cells (CTLs).

Initially, the special relationship of the PA analog (BODIPY C-16) to CD1b will be confirmed by confocal microscopy. To determine the cellular location of the CD1b molecules, we will perform Z-stack analysis in addition to comparing surface staining with intracellular staining. In a second set of experiments, we will assess whether PA-induced DC stimulation of T cells is dependent on CD1 presentation of PA. During 5 day DC-T cell cultures in the presence of PA, a neutralizing Ab against CD1b will be used assess the role of CD1b in DC mediated T cell activation. The T cells will be harvested and prepared for analysis by flow cytometry as mentioned in the above paragraph.

Aim 3: Determine the Role of Anti-PA Antibodies in Type 2 Diabetes

Our preliminary data indicates that anti-PA antibodies may be protective due to their ability to inhibit secretion of IL-1β from DCs exposed to PA *in vitro* (Figure 30). To determine whether these antibodies have a beneficial function *in vivo*, a prospective clinical study will be designed in which palmitate turnover will be measured in patients with and without type 2 diabetes after a bolus injection of ^{13}C-labeled palmitate as described in previous studies (Jensen, Haymond et al. 1989). Palmitate turnover will then be correlated with measured levels of anti-PA antibodies as well as assessment of clinical parameters to determine whether anti-PA antibodies play a role in enhancing PA metabolism. Additionally, we will isolate these antibodies (see Chapter 5) and use them for immunoprecipitation of serum antigens followed by mass spectrometry to identify other possible antigens or immunogens responsible for generating the antibody response.

Conclusions

The body of work presented here, in addition to the proposed future research, will begin to fill the void in the field of lipid immunology. Understanding lipid immunology will shed light on mechanisms by which diet derived saturated fatty acids induce inflammation. This dissertation has produced two key findings that have great potential to assist our understanding of the pathophysiology of type 2 diabetes and the approach taken to treat the disease.

The first major finding is that palmitic acid is a ligand for TLR4. This ligand – receptor interaction provides a direct link for the reported association between increased serum fatty acids in type 2 diabetes and inflammation and insulin resistance (See Chapter

1). Over-consumption of saturated fats leads to obesity which results in high levels of lipolysis and increased serum saturated free fatty acid levels. Palmitic acid, the most abundant of these saturated fatty acids can interact directly with cells expressing TLR4. These include but are not limited to DCs, macrophages, and B cells. If this type of innate immune activation is an early event in type 2 diabetes development, then targeting PA induced TLR4 signaling would be a promising prospect. The knowledge of how strongly PA binds TLR4 can aid in the design of small molecule inhibitors that would interfere with this interaction but preserve binding of natural ligands such as LPS. Therefore, immune responses to invading pathogens could be preserved.

The second key finding produced by this dissertation is the existence of antibodies that recognize PA in patients with unmanaged type 2 diabetes. This finding implies that a high fat diet can either directly, or indirectly induce an adaptive immune response, a concept supported in the literature (Lee and Lee 2014). Although the role these FA antibodies play in type 2 diabetes is currently unknown, their potential use in the field of diabetes is immense. To begin with, if anti-PA antibodies are highly produced when diabetes is unmanaged, they can serve as a good biomarker for physicians to assess disease management. Second, if anti-PA antibodies are protective and aid in the clearance of serum saturated fatty acids, it could potentially be used as a therapeutic. A monoclonal Ab against saturated fatty acids with an Fc portion that facilitates degradation by macrophages could be an approach to regulate serum lipids and subsequent chronic inflammatory signaling. Alternatively, anti-PA antibodies may be pathogenic, enhance inflammation through FcR signaling, or form antibody complexes that promote diabetic

nephropathy. Defining a pathogenic role for this antibody could provide an additional target for treatment of diabetes inflammation and its complications.

Overall, this dissertation has enhanced the knowledge of mechanisms underlying fatty acid mediated inflammation. The basic concept that a simple fatty acid can be a potent dietary immune modulator sets the stage for expansion of lipid immunology and general application of this knowledge to various systemic disease conditions such as lupus erythematosus, arthritis, spinal cord injury, and type 2 diabetes.

REFERENCES

Akashi, S., S. Saitoh, Y. Wakabayashi, T. Kikuchi, N. Takamura, Y. Nagai, Y. Kusumoto, K. Fukase, S. Kusumoto, Y. Adachi, A. Kosugi and K. Miyake (2003). "Lipopolysaccharide interaction with cell surface Toll-like receptor 4-MD-2: higher affinity than that with MD-2 or CD14." <u>J Exp Med</u> **198**(7): 1035-1042.

Amara, A., C. Chaugier and M. Geffard (1994). "Autoantibodies directed against conjugated fatty acids in sera of HIV-1-infected patients." <u>AIDS</u> **8**(5): 711-713.

Amara, A., C. Chaugier, J. M. Ragnaud and M. Geffard (1994). "Circulating autoantibodies directed against conjugated fatty acids in sera of HIV-1-infected patients." <u>Clin Exp Immunol</u> **96**(3): 379-383.

American Diabetes, A. (2013). "Economic costs of diabetes in the U.S. in 2012." <u>Diabetes Care</u> **36**(4): 1033-1046.

Asehnoune, K., D. Strassheim, S. Mitra, J. Y. Kim and E. Abraham (2004). "Involvement of reactive oxygen species in Toll-like receptor 4-dependent activation of NF-kappa B." <u>J Immunol</u> **172**(4): 2522-2529.

Baek, Y. S., S. Haas, H. Hackstein, G. Bein, M. Hernandez-Santana, H. Lehrach, S. Sauer and H. Seitz (2009). "Identification of novel transcriptional regulators involved in macrophage differentiation and activation in U937 cells." <u>BMC Immunol</u> **10**: 18.

Barnes, B., B. Lubyova and P. M. Pitha (2002). "On the role of IRF in host defense." <u>J Interferon Cytokine Res</u> **22**(1): 59-71.

Barreira da Silva, R. and C. Munz (2011). "Natural killer cell activation by dendritic cells: balancing inhibitory and activating signals." <u>Cell Mol Life Sci</u> **68**(21): 3505-3518.

Basu, S., S. Rajakaruna, B. C. Dickinson, C. J. Chang and A. S. Menko (2014). "Endogenous hydrogen peroxide production in the epithelium of the developing embryonic lens." <u>Mol Vis</u> **20**: 458-467.

Baxevanis, C. N., G. V. Dedoussis, A. D. Gritzapis, G. P. Stathopoulos and M. Papamichail (1994). "Interleukin 1 beta synergises with interleukin 2 in the outgrowth of autologous tumour-reactive CD8+ effectors." <u>Br J Cancer</u> **70**(4): 625-630.

Belfort, R., L. Mandarino, S. Kashyap, K. Wirfel, T. Pratipanawatr, R. Berria, R. A. Defronzo and K. Cusi (2005). "Dose-response effect of elevated plasma free fatty acid on insulin signaling." <u>Diabetes</u> **54**(6): 1640-1648.

Bell, D., J. W. Young and J. Banchereau (1999). "Dendritic cells." <u>Adv Immunol</u> **72**: 255-324.

Bernstein, L. E., J. Berry, S. Kim, B. Canavan and S. K. Grinspoon (2006). "Effects of etanercept in patients with the metabolic syndrome." <u>Arch Intern Med</u> **166**(8): 902-908.

Bertola, A., T. Ciucci, D. Rousseau, V. Bourlier, C. Duffaut, S. Bonnafous, C. Blin-Wakkach, R. Anty, A. Iannelli, J. Gugenheim, A. Tran, A. Bouloumie, P. Gual and A. Wakkach (2012). "Identification of adipose tissue dendritic cells correlated with obesity-associated insulin-resistance and inducing Th17 responses in mice and patients." <u>Diabetes</u> **61**(9): 2238-2247.

Bishop, J. C., F. D. Dunstan, B. J. Nix, T. M. Reynolds and A. Swift (1993). "All MoMs are not equal: some statistical properties associated with reporting results in the form of multiples of the median." <u>Am J Hum Genet</u> **52**(2): 425-430.

Boden, G., X. Chen, J. Rosner and M. Barton (1995). "Effects of a 48-h fat infusion on insulin secretion and glucose utilization." <u>Diabetes</u> **44**(10): 1239-1242.

Boden, G., P. Cheung, T. P. Stein, K. Kresge and M. Mozzoli (2002). "FFA cause hepatic insulin resistance by inhibiting insulin suppression of glycogenolysis." <u>Am J Physiol Endocrinol Metab</u> **283**(1): E12-19.

Bornstein, S. R., M. Abu-Asab, A. Glasow, G. Path, H. Hauner, M. Tsokos, G. P. Chrousos and W. A. Scherbaum (2000). "Immunohistochemical and ultrastructural localization of leptin and leptin receptor in human white adipose tissue and differentiating human adipose cells in primary culture." <u>Diabetes</u> **49**(4): 532-538.

Boullerne, A., K. G. Petry and M. Geffard (1996). "Circulating antibodies directed against conjugated fatty acids in sera of patients with multiple sclerosis." <u>J Neuroimmunol</u> **65**(1): 75-81.

Bryan, C. P. (2010). <u>Ancient Egyptian medicine : the papyrus ebers</u>. Chicago, IL, Research Associates School Times Publications & Frontline Distribution International Inc.

Cascio, G., G. Schiera and I. Di Liegro (2012). "Dietary fatty acids in metabolic syndrome, diabetes and cardiovascular diseases." <u>Curr Diabetes Rev</u> **8**(1): 2-17.

Cavallero, C., B. Malandra and G. Galansino (1954). "Diabetogenic action of pancreatic glucagon." Nature **173**(4404): 585-586.

Cella, M., A. Engering, V. Pinet, J. Pieters and A. Lanzavecchia (1997). "Inflammatory stimuli induce accumulation of MHC class II complexes on dendritic cells." Nature **388**(6644): 782-787.

Charles, M. A., E. Eschwege, N. Thibult, J. R. Claude, J. M. Warnet, G. E. Rosselin, J. Girard and B. Balkau (1997). "The role of non-esterified fatty acids in the deterioration of glucose tolerance in Caucasian subjects: results of the Paris Prospective Study." Diabetologia **40**(9): 1101-1106.

Chukwueke, I., A. Firek, L. Beeson, M. Brute, E. Shulz, M. De Leon and Z. R. Cordero-MacIntyre (2012). "The En Balance Spanish diabetes education program improves apolipoproteins, serum glucose and body composition in Hispanic diabetics." Ethn Dis **22**(2): 215-220.

Cinti, S., G. Mitchell, G. Barbatelli, I. Murano, E. Ceresi, E. Faloia, S. Wang, M. Fortier, A. S. Greenberg and M. S. Obin (2005). "Adipocyte death defines macrophage localization and function in adipose tissue of obese mice and humans." J Lipid Res **46**(11): 2347-2355.

Ciric, B., M. El-behi, R. Cabrera, G. X. Zhang and A. Rostami (2009). "IL-23 drives pathogenic IL-17-producing CD8+ T cells." J Immunol **182**(9): 5296-5305.

Clausell, J., N. Happel, T. K. Hale, D. Doenecke and M. Beato (2009). "Histone H1 subtypes differentially modulate chromatin condensation without preventing ATP-dependent remodeling by SWI/SNF or NURF." PLoS One **4**(10): e0007243.

Cohen, N. R., S. Garg and M. B. Brenner (2009). "Antigen Presentation by CD1 Lipids, T Cells, and NKT Cells in Microbial Immunity." Adv Immunol **102**: 1-94.

D'Autreaux, B. and M. B. Toledano (2007). "ROS as signalling molecules: mechanisms that generate specificity in ROS homeostasis." Nat Rev Mol Cell Biol **8**(10): 813-824.

Davis, J. E., N. K. Gabler, J. Walker-Daniels and M. E. Spurlock (2008). "Tlr-4 deficiency selectively protects against obesity induced by diets high in saturated fat." Obesity (Silver Spring) **16**(6): 1248-1255.

De Toma, I., G. Rossetti, S. Zambrano, M. E. Bianchi and A. Agresti (2014). "Nucleosome loss facilitates the chemotactic response of macrophages." J Intern Med **276**(5): 454-469.

Demarse, N. A., C. F. Quinn, D. L. Eggett, D. J. Russell and L. D. Hansen (2011). "Calibration of nanowatt isothermal titration calorimeters with overflow reaction vessels." Anal Biochem **417**(2): 247-255.

Deng, T., C. J. Lyon, L. J. Minze, J. Lin, J. Zou, J. Z. Liu, Y. Ren, Z. Yin, D. J. Hamilton, P. R. Reardon, V. Sherman, H. Y. Wang, K. J. Phillips, P. Webb, S. T. Wong, R. F. Wang and W. A. Hsueh (2013). "Class II major histocompatibility complex plays an essential role in obesity-induced adipose inflammation." Cell Metab **17**(3): 411-422.

Dinarello, C. A., M. Y. Donath and T. Mandrup-Poulsen (2010). "Role of IL-1beta in type 2 diabetes." Curr Opin Endocrinol Diabetes Obes **17**(4): 314-321.

Donath, M. Y. and S. E. Shoelson (2011). "Type 2 diabetes as an inflammatory disease." Nat Rev Immunol **11**(2): 98-107.

Duffaut, C., J. Galitzky, M. Lafontan and A. Bouloumie (2009). "Unexpected trafficking of immune cells within the adipose tissue during the onset of obesity." Biochem Biophys Res Commun **384**(4): 482-485.

Eberlin, A., C. Grauffel, M. Oulad-Abdelghani, F. Robert, M. E. Torres-Padilla, R. Lambrot, D. Spehner, L. Ponce-Perez, J. M. Wurtz, R. H. Stote, S. Kimmins, P. Schultz, A. Dejaegere and L. Tora (2008). "Histone H3 tails containing dimethylated lysine and adjacent phosphorylated serine modifications adopt a specific conformation during mitosis and meiosis." Mol Cell Biol **28**(5): 1739-1754.

Ehses, J. A., G. Lacraz, M. H. Giroix, F. Schmidlin, J. Coulaud, N. Kassis, J. C. Irminger, M. Kergoat, B. Portha, F. Homo-Delarche and M. Y. Donath (2009). "IL-1 antagonism reduces hyperglycemia and tissue inflammation in the type 2 diabetic GK rat." Proc Natl Acad Sci U S A **106**(33): 13998-14003.

Elgazar-Carmon, V., A. Rudich, N. Hadad and R. Levy (2008). "Neutrophils transiently infiltrate intra-abdominal fat early in the course of high-fat feeding." J Lipid Res **49**(9): 1894-1903.

Engelhardt, D. v. (1989). Diabetes, its medical and cultural history : outlines, texts, bibliography. Berlin ; New York, Springer-Verlag.

Esser, N., S. Legrand-Poels, J. Piette, A. J. Scheen and N. Paquot (2014). "Inflammation as a link between obesity, metabolic syndrome and type 2 diabetes." Diabetes Res Clin Pract.

Fan, Y., T. Nikitina, E. M. Morin-Kensicki, J. Zhao, T. R. Magnuson, C. L. Woodcock and A. I. Skoultchi (2003). "H1 linker histones are essential for mouse

development and affect nucleosome spacing in vivo." <u>Mol Cell Biol</u> **23**(13): 4559-4572.

Fan, Y., T. Nikitina, J. Zhao, T. J. Fleury, R. Bhattacharyya, E. E. Bouhassira, A. Stein, C. L. Woodcock and A. I. Skoultchi (2005). "Histone H1 depletion in mammals alters global chromatin structure but causes specific changes in gene regulation." <u>Cell</u> **123**(7): 1199-1212.

Fangradt, M., M. Hahne, T. Gaber, C. Strehl, R. Rauch, P. Hoff, M. Lohning, G. R. Burmester and F. Buttgereit (2012). "Human monocytes and macrophages differ in their mechanisms of adaptation to hypoxia." <u>Arthritis Res Ther</u> **14**(4): R181.

Ferraz-Amaro, I., M. Arce-Franco, J. Muniz, J. Lopez-Fernandez, V. Hernandez-Hernandez, A. Franco, J. Quevedo, J. Martinez-Martin and F. Diaz-Gonzalez (2011). "Systemic blockade of TNF-alpha does not improve insulin resistance in humans." <u>Horm Metab Res</u> **43**(11): 801-808.

Feuerer, M., L. Herrero, D. Cipolletta, A. Naaz, J. Wong, A. Nayer, J. Lee, A. B. Goldfine, C. Benoist, S. Shoelson and D. Mathis (2009). "Lean, but not obese, fat is enriched for a unique population of regulatory T cells that affect metabolic parameters." <u>Nat Med</u> **15**(8): 930-939.

Finkel, T. (1999). "Signal transduction by reactive oxygen species in non-phagocytic cells." <u>J Leukoc Biol</u> **65**(3): 337-340.

Franks, P. W., R. L. Hanson, W. C. Knowler, M. L. Sievers, P. H. Bennett and H. C. Looker (2010). "Childhood obesity, other cardiovascular risk factors, and premature death." <u>N Engl J Med</u> **362**(6): 485-493.

Fraser, D. A., J. Thoen, A. C. Rustan, O. Forre and J. Kjeldsen-Kragh (1999). "Changes in plasma free fatty acid concentrations in rheumatoid arthritis patients during fasting and their effects upon T-lymphocyte proliferation." <u>Rheumatology (Oxford)</u> **38**(10): 948-952.

Fujiwara, S. and T. Amisaki (2008). "Identification of high affinity fatty acid binding sites on human serum albumin by MM-PBSA method." <u>Biophys J</u> **94**(1): 95-103.

Gagliardi, M. C., R. Teloni, F. Giannoni, S. Mariotti, M. E. Remoli, V. Sargentini, M. Videtta, M. Pardini, G. De Libero, E. M. Coccia and R. Nisini (2009). "Mycobacteria exploit p38 signaling to affect CD1 expression and lipid antigen presentation by human dendritic cells." <u>Infect Immun</u> **77**(11): 4947-4952.

Garcia, B. A., C. M. Barber, S. B. Hake, C. Ptak, F. B. Turner, S. A. Busby, J. Shabanowitz, R. G. Moran, C. D. Allis and D. F. Hunt (2005). "Modifications of human histone H3 variants during mitosis." <u>Biochemistry</u> **44**(39): 13202-13213.

Gonzalez-Gay, M. A., C. Gonzalez-Juanatey, T. R. Vazquez-Rodriguez, J. A. Miranda-Filloy and J. Llorca (2010). "Insulin resistance in rheumatoid arthritis: the impact of the anti-TNF-alpha therapy." Ann N Y Acad Sci **1193**: 153-159.

Grishman, E. K., P. C. White and R. C. Savani (2012). "Toll-like receptors, the NLRP3 inflammasome, and interleukin-1beta in the development and progression of type 1 diabetes." Pediatr Res **71**(6): 626-632.

Haase, R., C. J. Kirschning, A. Sing, P. Schrottner, K. Fukase, S. Kusumoto, H. Wagner, J. Heesemann and K. Ruckdeschel (2003). "A dominant role of Toll-like receptor 4 in the signaling of apoptosis in bacteria-faced macrophages." J Immunol **171**(8): 4294-4303.

Halberg, N., T. Khan, M. E. Trujillo, I. Wernstedt-Asterholm, A. D. Attie, S. Sherwani, Z. V. Wang, S. Landskroner-Eiger, S. Dineen, U. J. Magalang, R. A. Brekken and P. E. Scherer (2009). "Hypoxia-inducible factor 1alpha induces fibrosis and insulin resistance in white adipose tissue." Mol Cell Biol **29**(16): 4467-4483.

Halliwell, B. (2002). "Vitamin E and thetreatment and prevention of diabetes: a case for a controlled clinical trial." Singapore Med J **43**(9): 479-484.

Han, J. W., S. H. Ahn, S. H. Park, S. Y. Wang, G. U. Bae, D. W. Seo, H. K. Kwon, S. Hong, H. Y. Lee, Y. W. Lee and H. W. Lee (2000). "Apicidin, a histone deacetylase inhibitor, inhibits proliferation of tumor cells via induction of p21WAF1/Cip1 and gelsolin." Cancer Res **60**(21): 6068-6074.

Hashimoto, D., J. Miller and M. Merad (2011). "Dendritic cell and macrophage heterogeneity in vivo." Immunity **35**(3): 323-335.

Hashimoto, H., Y. Takami, E. Sonoda, T. Iwasaki, H. Iwano, M. Tachibana, S. Takeda, T. Nakayama, H. Kimura and Y. Shinkai (2010). "Histone H1 null vertebrate cells exhibit altered nucleosome architecture." Nucleic Acids Res **38**(11): 3533-3545.

Hashimoto, S., T. Suzuki, H. Y. Dong, S. Nagai, N. Yamazaki and K. Matsushima (1999). "Serial analysis of gene expression in human monocyte-derived dendritic cells." Blood **94**(3): 845-852.

Hass, R., H. Gunji, R. Datta, S. Kharbanda, A. Hartmann, R. Weichselbaum and D. Kufe (1992). "Differentiation and retrodifferentiation of human myeloid leukemia cells is associated with reversible induction of cell cycle-regulatory genes." Cancer Res **52**(6): 1445-1450.

Hempel, S. L., G. R. Buettner, Y. Q. O'Malley, D. A. Wessels and D. M. Flaherty (1999). "Dihydrofluorescein diacetate is superior for detecting intracellular oxidants: comparison with 2',7'-dichlorodihydrofluorescein diacetate, 5(and 6)-carboxy-

2',7'-dichlorodihydrofluorescein diacetate, and dihydrorhodamine 123." <u>Free Radic Biol Med</u> **27**(1-2): 146-159.

Hirasawa, A., T. Hara, S. Katsuma, T. Adachi and G. Tsujimoto (2008). "Free fatty acid receptors and drug discovery." <u>Biol Pharm Bull</u> **31**(10): 1847-1851.

Hong, J., K. Ishihara, K. Yamaki, K. Hiraizumi, T. Ohno, J. W. Ahn, O. Zee and K. Ohuchi (2003). "Apicidin, a histone deacetylase inhibitor, induces differentiation of HL-60 cells." <u>Cancer Lett</u> **189**(2): 197-206.

Horvath, A. and A. Biro (2003). "Anti-cholesterol antibodies in human sera." <u>Autoimmun Rev</u> **2**(5): 272-277.

Hosogai, N., A. Fukuhara, K. Oshima, Y. Miyata, S. Tanaka, K. Segawa, S. Furukawa, Y. Tochino, R. Komuro, M. Matsuda and I. Shimomura (2007). "Adipose tissue hypoxia in obesity and its impact on adipocytokine dysregulation." <u>Diabetes</u> **56**(4): 901-911.

Hotamisligil, G. S., N. S. Shargill and B. M. Spiegelman (1993). "Adipose expression of tumor necrosis factor-alpha: direct role in obesity-linked insulin resistance." <u>Science</u> **259**(5091): 87-91.

Hu, F. B. (2011). "Globalization of diabetes: the role of diet, lifestyle, and genes." <u>Diabetes Care</u> **34**(6): 1249-1257.

Hummasti, S. and G. S. Hotamisligil (2010). "Endoplasmic reticulum stress and inflammation in obesity and diabetes." <u>Circ Res</u> **107**(5): 579-591.

Igoillo-Esteve, M., L. Marselli, D. A. Cunha, L. Ladriere, F. Ortis, F. A. Grieco, F. Dotta, G. C. Weir, P. Marchetti, D. L. Eizirik and M. Cnop (2010). "Palmitate induces a pro-inflammatory response in human pancreatic islets that mimics CCL2 expression by beta cells in type 2 diabetes." <u>Diabetologia</u> **53**(7): 1395-1405.

Illana, V. and R. Farhaeus (2012). "Purification of His-ubiquitin Proteins from Mammalian Cells." <u>bio-protocol</u> **2**(17).

Iwamoto, S., S. Iwai, K. Tsujiyama, C. Kurahashi, K. Takeshita, M. Naoe, A. Masunaga, Y. Ogawa, K. Oguchi and A. Miyazaki (2007). "TNF-alpha drives human CD14+ monocytes to differentiate into CD70+ dendritic cells evoking Th1 and Th17 responses." <u>J Immunol</u> **179**(3): 1449-1457.

Iwata, Y., T. Matsushita, M. Horikawa, D. J. Dilillo, K. Yanaba, G. M. Venturi, P. M. Szabolcs, S. H. Bernstein, C. M. Magro, A. D. Williams, R. P. Hall, E. W. St Clair and T. F. Tedder (2011). "Characterization of a rare IL-10-competent B-cell subset in humans that parallels mouse regulatory B10 cells." <u>Blood</u> **117**(2): 530-541.

Jaensson, E., H. Uronen-Hansson, O. Pabst, B. Eksteen, J. Tian, J. L. Coombes, P. L. Berg, T. Davidsson, F. Powrie, B. Johansson-Lindbom and W. W. Agace (2008). "Small intestinal CD103+ dendritic cells display unique functional properties that are conserved between mice and humans." J Exp Med **205**(9): 2139-2149.

Jagannathan, M., M. McDonnell, Y. Liang, H. Hasturk, J. Hetzel, D. Rubin, A. Kantarci, T. E. Van Dyke, L. M. Ganley-Leal and B. S. Nikolajczyk (2010). "Toll-like receptors regulate B cell cytokine production in patients with diabetes." Diabetologia **53**(7): 1461-1471.

Jager, J., T. Gremeaux, M. Cormont, Y. Le Marchand-Brustel and J. F. Tanti (2007). "Interleukin-1beta-induced insulin resistance in adipocytes through down-regulation of insulin receptor substrate-1 expression." Endocrinology **148**(1): 241-251.

Jensen, M. D., M. W. Haymond, R. A. Rizza, P. E. Cryer and J. M. Miles (1989). "Influence of body fat distribution on free fatty acid metabolism in obesity." J Clin Invest **83**(4): 1168-1173.

Jin, D., J. Sun, J. Huang, Y. He, A. Yu, X. Yu and Z. Yang (2014). "TNF-alpha reduces g0s2 expression and stimulates lipolysis through PPAR-gamma inhibition in 3T3-L1 adipocytes." Cytokine **69**(2): 196-205.

Kang, K., S. M. Reilly, V. Karabacak, M. R. Gangl, K. Fitzgerald, B. Hatano and C. H. Lee (2008). "Adipocyte-derived Th2 cytokines and myeloid PPARdelta regulate macrophage polarization and insulin sensitivity." Cell Metab **7**(6): 485-495.

Karpe, F., J. R. Dickmann and K. N. Frayn (2011). "Fatty acids, obesity, and insulin resistance: time for a reevaluation." Diabetes **60**(10): 2441-2449.

Kawai, T. and S. Akira (2010). "The role of pattern-recognition receptors in innate immunity: update on Toll-like receptors." Nat Immunol **11**(5): 373-384.

Kawasaki, T. and T. Kawai (2014). "Toll-like receptor signaling pathways." Front Immunol **5**: 461.

Kendall, M. R. and C. J. Hupfeld (2008). "FTY720, a sphingosine-1-phosphate receptor modulator, reverses high-fat diet-induced weight gain, insulin resistance and adipose tissue inflammation in C57BL/6 mice." Diabetes Obes Metab **10**(9): 802-805.

Kiertscher, S. M. and M. D. Roth (1996). "Human CD14+ leukocytes acquire the phenotype and function of antigen-presenting dendritic cells when cultured in GM-CSF and IL-4." J Leukoc Biol **59**(2): 208-218.

Kim, F., M. Pham, I. Luttrell, D. D. Bannerman, J. Tupper, J. Thaler, T. R. Hawn, E. W. Raines and M. W. Schwartz (2007). "Toll-like receptor-4 mediates vascular inflammation and insulin resistance in diet-induced obesity." Circ Res **100**(11): 1589-1596.

Kim, J. Y., K. Tillison, J. H. Lee, D. A. Rearick and C. M. Smas (2006). "The adipose tissue triglyceride lipase ATGL/PNPLA2 is downregulated by insulin and TNF-alpha in 3T3-L1 adipocytes and is a target for transactivation by PPARgamma." Am J Physiol Endocrinol Metab **291**(1): E115-127.

Kolb, H. and T. Mandrup-Poulsen (2010). "The global diabetes epidemic as a consequence of lifestyle-induced low-grade inflammation." Diabetologia **53**(1): 10-20.

Kong, W., J. H. Yen, E. Vassiliou, S. Adhikary, M. G. Toscano and D. Ganea (2010). "Docosahexaenoic acid prevents dendritic cell maturation and in vitro and in vivo expression of the IL-12 cytokine family." Lipids Health Dis **9**: 12.

Kraakman, M. J., A. J. Murphy, K. Jandeleit-Dahm and H. L. Kammoun (2014). "Macrophage polarization in obesity and type 2 diabetes: weighing down our understanding of macrophage function?" Front Immunol **5**: 470.

Lagathu, C., L. Yvan-Charvet, J. P. Bastard, M. Maachi, A. Quignard-Boulange, J. Capeau and M. Caron (2006). "Long-term treatment with interleukin-1beta induces insulin resistance in murine and human adipocytes." Diabetologia **49**(9): 2162-2173.

Larsen, C. M., M. Faulenbach, A. Vaag, J. A. Ehses, M. Y. Donath and T. Mandrup-Poulsen (2009). "Sustained effects of interleukin-1 receptor antagonist treatment in type 2 diabetes." Diabetes Care **32**(9): 1663-1668.

Larsen, C. M., M. Faulenbach, A. Vaag, A. Volund, J. A. Ehses, B. Seifert, T. Mandrup-Poulsen and M. Y. Donath (2007). "Interleukin-1-receptor antagonist in type 2 diabetes mellitus." N Engl J Med **356**(15): 1517-1526.

Latz, E., T. S. Xiao and A. Stutz (2013). "Activation and regulation of the inflammasomes." Nat Rev Immunol **13**(6): 397-411.

Le Naour, F., L. Hohenkirk, A. Grolleau, D. E. Misek, P. Lescure, J. D. Geiger, S. Hanash and L. Beretta (2001). "Profiling changes in gene expression during differentiation and maturation of monocyte-derived dendritic cells using both oligonucleotide microarrays and proteomics." J Biol Chem **276**(21): 17920-17931.

Lechmann, M., S. Berchtold, J. Hauber and A. Steinkasserer (2002). "CD83 on dendritic cells: more than just a marker for maturation." Trends Immunol **23**(6): 273-275.

Lee, B. C. and J. Lee (2014). "Cellular and molecular players in adipose tissue inflammation in the development of obesity-induced insulin resistance." Biochim Biophys Acta **1842**(3): 446-462.

Lee, J. Y., N. A. Kim, A. Sanford and K. E. Sullivan (2003). "Histone acetylation and chromatin conformation are regulated separately at the TNF-alpha promoter in monocytes and macrophages." J Leukoc Biol **73**(6): 862-871.

Lee, J. Y., K. H. Sohn, S. H. Rhee and D. Hwang (2001). "Saturated fatty acids, but not unsaturated fatty acids, induce the expression of cyclooxygenase-2 mediated through Toll-like receptor 4." J Biol Chem **276**(20): 16683-16689.

Legrand-Poels, S., N. Esser, L. L'Homme, A. Scheen, N. Paquot and J. Piette (2014). "Free fatty acids as modulators of the NLRP3 inflammasome in obesity/type 2 diabetes." Biochem Pharmacol **92**(1): 131-141.

Leonarduzzi, G., P. Gamba, S. Gargiulo, F. Biasi and G. Poli (2012). "Inflammation-related gene expression by lipid oxidation-derived products in the progression of atherosclerosis." Free Radic Biol Med **52**(1): 19-34.

Leslie, D. S., C. C. Dascher, K. Cembrola, M. A. Townes, D. L. Hava, L. C. Hugendubler, E. Mueller, L. Fox, C. Roura-Mir, D. B. Moody, M. S. Vincent, J. E. Gumperz, P. A. Illarionov, G. S. Besra, C. G. Reynolds and M. B. Brenner (2008). "Serum lipids regulate dendritic cell CD1 expression and function." Immunology **125**(3): 289-301.

Liang, H., P. Tantiwong, A. Sriwijitkamol, K. Shanmugasundaram, S. Mohan, S. Espinoza, R. A. Defronzo, J. J. Dube and N. Musi (2013). "Effect of a sustained reduction in plasma free fatty acid concentration on insulin signalling and inflammation in skeletal muscle from human subjects." J Physiol **591**(Pt 11): 2897-2909.

Liu, J., A. Divoux, J. Sun, J. Zhang, K. Clement, J. N. Glickman, G. K. Sukhova, P. J. Wolters, J. Du, C. Z. Gorgun, A. Doria, P. Libby, R. S. Blumberg, B. B. Kahn, G. S. Hotamisligil and G. P. Shi (2009). "Genetic deficiency and pharmacological stabilization of mast cells reduce diet-induced obesity and diabetes in mice." Nat Med **15**(8): 940-945.

Lopez-Castejon, G. and D. Brough (2011). "Understanding the mechanism of IL-1beta secretion." Cytokine Growth Factor Rev **22**(4): 189-195.

Lumeng, C. N., J. L. Bodzin and A. R. Saltiel (2007). "Obesity induces a phenotypic switch in adipose tissue macrophage polarization." J Clin Invest **117**(1): 175-184.

Luo, X., Y. Yang, T. Shen, X. Tang, Y. Xiao, T. Zou, M. Xia and W. Ling (2012). "Docosahexaenoic acid ameliorates palmitate-induced lipid accumulation and inflammation through repressing NLRC4 inflammasome activation in HepG2 cells." Nutr Metab (Lond) **9**(1): 34.

MacLennan, I. C., A. Gulbranson-Judge, K. M. Toellner, M. Casamayor-Palleja, E. Chan, D. M. Sze, S. A. Luther and H. A. Orbea (1997). "The changing preference of T and B cells for partners as T-dependent antibody responses develop." Immunol Rev **156**: 53-66.

Macleod, J. J. R. and F. G. Banting (1923). The antidiabetic functions of the panereas and the successful isolation of the antidiabetic harmone--insulin. St. Louis,, Press of the C. V. Mosby company.

Maelfait, J., E. Vercammen, S. Janssens, P. Schotte, M. Haegman, S. Magez and R. Beyaert (2008). "Stimulation of Toll-like receptor 3 and 4 induces interleukin-1beta maturation by caspase-8." J Exp Med **205**(9): 1967-1973.

Maloney, E., I. R. Sweet, D. M. Hockenbery, M. Pham, N. O. Rizzo, S. Tateya, P. Handa, M. W. Schwartz and F. Kim (2009). "Activation of NF-kappaB by palmitate in endothelial cells: a key role for NADPH oxidase-derived superoxide in response to TLR4 activation." Arterioscler Thromb Vasc Biol **29**(9): 1370-1375.

Mantell, B. S., M. Stefanovic-Racic, X. Yang, N. Dedousis, I. J. Sipula and R. M. O'Doherty (2011). "Mice lacking NKT cells but with a complete complement of CD8+ T-cells are not protected against the metabolic abnormalities of diet-induced obesity." PLoS One **6**(6): e19831.

Mantovani, A., S. Sozzani, M. Locati, P. Allavena and A. Sica (2002). "Macrophage polarization: tumor-associated macrophages as a paradigm for polarized M2 mononuclear phagocytes." Trends Immunol **23**(11): 549-555.

Martinez, F. O., A. Sica, A. Mantovani and M. Locati (2008). "Macrophage activation and polarization." Front Biosci **13**: 453-461.

Martins, A. R., R. T. Nachbar, R. Gorjao, M. A. Vinolo, W. T. Festuccia, R. H. Lambertucci, M. F. Cury-Boaventura, L. R. Silveira, R. Curi and S. M. Hirabara (2012). "Mechanisms underlying skeletal muscle insulin resistance induced by fatty acids: importance of the mitochondrial function." Lipids Health Dis **11**: 30.

Mateescu, B., P. England, F. Halgand, M. Yaniv and C. Muchardt (2004). "Tethering of HP1 proteins to chromatin is relieved by phosphoacetylation of histone H3." EMBO Rep **5**(5): 490-496.

Mazitschek, R., V. Patel, D. F. Wirth and J. Clardy (2008). "Development of a fluorescence polarization based assay for histone deacetylase ligand discovery." Bioorg Med Chem Lett **18**(9): 2809-2812.

Mbongue, J. C., D. A. Nicholas, K. Zhang, N. S. Kim, B. N. Hamilton, M. Larios, G. Zhang, K. Umezawa, A. F. Firek and W. H. Langridge (2015). "Induction of indoleamine 2, 3-dioxygenase in human dendritic cells by a cholera toxin B subunit-proinsulin vaccine." PLoS One **10**(2): e0118562.

McGillicuddy, F. C., E. H. Chiquoine, C. C. Hinkle, R. J. Kim, R. Shah, H. M. Roche, E. M. Smyth and M. P. Reilly (2009). "Interferon gamma attenuates insulin signaling, lipid storage, and differentiation in human adipocytes via activation of the JAK/STAT pathway." J Biol Chem **284**(46): 31936-31944.

Meissner, F., K. Molawi and A. Zychlinsky (2008). "Superoxide dismutase 1 regulates caspase-1 and endotoxic shock." Nat Immunol **9**(8): 866-872.

Mellman, I. and R. M. Steinman (2001). "Dendritic cells: specialized and regulated antigen processing machines." Cell **106**(3): 255-258.

Metghalchi, S., M. Rivera, L. Beeson, A. Firek, M. De Leon, H. Balcazar and Z. R. Cordero-MacIntyre (2008). "Improved clinical outcomes using a culturally sensitive diabetes education program in a Hispanic population." Diabetes Educ **34**(4): 698-706.

Miao, F., Z. Chen, L. Zhang, Z. Liu, X. Wu, Y. C. Yuan and R. Natarajan (2012). "Profiles of epigenetic histone post-translational modifications at type 1 diabetes susceptible genes." J Biol Chem **287**(20): 16335-16345.

Millar, C. B., S. K. Kurdistani and M. Grunstein (2004). "Acetylation of yeast histone H4 lysine 16: a switch for protein interactions in heterochromatin and euchromatin." Cold Spring Harb Symp Quant Biol **69**: 193-200.

Misteli, T., A. Gunjan, R. Hock, M. Bustin and D. T. Brown (2000). "Dynamic binding of histone H1 to chromatin in living cells." Nature **408**(6814): 877-881.

Moon, J. S., S. Lee, M. A. Park, Siempos, II, M. Haslip, P. J. Lee, M. Yun, C. K. Kim, J. Howrylak, S. W. Ryter, K. Nakahira and A. M. Choi (2015). "UCP2-induced fatty acid synthase promotes NLRP3 inflammasome activation during sepsis." J Clin Invest.

Munoz, A. and M. Costa (2013). "Nutritionally mediated oxidative stress and inflammation." Oxid Med Cell Longev **2013**: 610950.

Nagy, L., A. Szanto, I. Szatmari and L. Szeles (2012). "Nuclear hormone receptors enable macrophages and dendritic cells to sense their lipid environment and shape their immune response." Physiol Rev **92**(2): 739-789.

Nakano, H., K. L. Lin, M. Yanagita, C. Charbonneau, D. N. Cook, T. Kakiuchi and M. D. Gunn (2009). "Blood-derived inflammatory dendritic cells in lymph nodes stimulate acute T helper type 1 immune responses." Nat Immunol **10**(4): 394-402.

Nathan, C. F., H. W. Murray, M. E. Wiebe and B. Y. Rubin (1983). "Identification of interferon-gamma as the lymphokine that activates human macrophage oxidative metabolism and antimicrobial activity." J Exp Med **158**(3): 670-689.

Nguyen, M. T., S. Favelyukis, A. K. Nguyen, D. Reichart, P. A. Scott, A. Jenn, R. Liu-Bryan, C. K. Glass, J. G. Neels and J. M. Olefsky (2007). "A subpopulation of macrophages infiltrates hypertrophic adipose tissue and is activated by free fatty acids via Toll-like receptors 2 and 4 and JNK-dependent pathways." J Biol Chem **282**(48): 35279-35292.

Nishimura, S., I. Manabe, M. Nagasaki, K. Eto, H. Yamashita, M. Ohsugi, M. Otsu, K. Hara, K. Ueki, S. Sugiura, K. Yoshimura, T. Kadowaki and R. Nagai (2009). "CD8+ effector T cells contribute to macrophage recruitment and adipose tissue inflammation in obesity." Nat Med **15**(8): 914-920.

Nishimura, S., I. Manabe, S. Takaki, M. Nagasaki, M. Otsu, H. Yamashita, J. Sugita, K. Yoshimura, K. Eto, I. Komuro, T. Kadowaki and R. Nagai (2013). "Adipose Natural Regulatory B Cells Negatively Control Adipose Tissue Inflammation." Cell Metab.

O'Rourke, R. W., M. D. Metcalf, A. E. White, A. Madala, B. R. Winters, Maizlin, II, B. A. Jobe, C. T. Roberts, Jr., M. K. Slifka and D. L. Marks (2009). "Depot-specific differences in inflammatory mediators and a role for NK cells and IFN-gamma in inflammation in human adipose tissue." Int J Obes (Lond) **33**(9): 978-990.

Ogata, A., A. Morishima, T. Hirano, Y. Hishitani, K. Hagihara, Y. Shima, M. Narazaki and T. Tanaka (2011). "Improvement of HbA1c during treatment with humanised anti-interleukin 6 receptor antibody, tocilizumab." Ann Rheum Dis **70**(6): 1164-1165.

Ohmura, K., N. Ishimori, Y. Ohmura, S. Tokuhara, A. Nozawa, S. Horii, Y. Andoh, S. Fujii, K. Iwabuchi, K. Onoe and H. Tsutsui (2010). "Natural killer T cells are involved in adipose tissues inflammation and glucose intolerance in diet-induced obese mice." Arterioscler Thromb Vasc Biol **30**(2): 193-199.

Ojo, E., L. Beeson, E. Shulz, A. Firek, M. De Leon, H. Balcazar and Z. Cordero-Macintyre (2010). "Effect of the EnBalance, a culturally and language-sensitive

diabetes education program, on dietary changes and plasma lipid profile in Hispanic diabetics." Int J Body Compos Res **8**(Supp): S69-S76.

Olefsky, J. M. and C. K. Glass (2010). "Macrophages, inflammation, and insulin resistance." Annu Rev Physiol **72**: 219-246.

Oliver, E., F. McGillicuddy, C. Phillips, S. Toomey and H. M. Roche (2010). "The role of inflammation and macrophage accumulation in the development of obesity-induced type 2 diabetes mellitus and the possible therapeutic effects of long-chain n-3 PUFA." Proc Nutr Soc **69**(2): 232-243.

Osborn, O., H. Gram, E. P. Zorrilla, B. Conti and T. Bartfai (2008). "Insights into the roles of the inflammatory mediators IL-1, IL-18 and PGE2 in obesity and insulin resistance." Swiss Med Wkly **138**(45-46): 665-673.

Padilla, A., M. Descorbeth, A. L. Almeyda, K. Payne and M. De Leon (2011). "Hyperglycemia magnifies Schwann cell dysfunction and cell death triggered by PA-induced lipotoxicity." Brain Res **1370**: 64-79.

Paich, H. A., P. A. Sheridan, J. Handy, E. A. Karlsson, S. Schultz-Cherry, M. G. Hudgens, T. L. Noah, S. S. Weir and M. A. Beck (2013). "Overweight and obese adult humans have a defective cellular immune response to pandemic H1N1 influenza A virus." Obesity (Silver Spring) **21**(11): 2377-2386.

Pal, M., M. A. Febbraio and M. Whitham (2014). "From cytokine to myokine: the emerging role of interleukin-6 in metabolic regulation." Immunol Cell Biol **92**(4): 331-339.

Palming, J., B. G. Gabrielsson, E. Jennische, U. Smith, B. Carlsson, L. M. Carlsson and M. Lonn (2006). "Plasma cells and Fc receptors in human adipose tissue--lipogenic and anti-inflammatory effects of immunoglobulins on adipocytes." Biochem Biophys Res Commun **343**(1): 43-48.

Palsson-McDermott, E. M. and L. A. O'Neill (2004). "Signal transduction by the lipopolysaccharide receptor, Toll-like receptor-4." Immunology **113**(2): 153-162.

Pankow, J. S., B. B. Duncan, M. I. Schmidt, C. M. Ballantyne, D. J. Couper, R. C. Hoogeveen, S. H. Golden and S. Atherosclerosis Risk in Communities (2004). "Fasting plasma free fatty acids and risk of type 2 diabetes: the atherosclerosis risk in communities study." Diabetes Care **27**(1): 77-82.

Paolisso, G., P. A. Tataranni, J. E. Foley, C. Bogardus, B. V. Howard and E. Ravussin (1995). "A high concentration of fasting plasma non-esterified fatty acids is a risk factor for the development of NIDDM." Diabetologia **38**(10): 1213-1217.

Papamokos, G. V., G. Tziatzos, D. G. Papageorgiou, S. D. Georgatos, A. S. Politou and E. Kaxiras (2012). "Structural role of RKS motifs in chromatin interactions: a molecular dynamics study of HP1 bound to a variably modified histone tail." Biophys J **102**(8): 1926-1933.

Park, B. S., D. H. Song, H. M. Kim, B. S. Choi, H. Lee and J. O. Lee (2009). "The structural basis of lipopolysaccharide recognition by the TLR4-MD-2 complex." Nature **458**(7242): 1191-1195.

Park, H. S., H. Y. Jung, E. Y. Park, J. Kim, W. J. Lee and Y. S. Bae (2004). "Cutting edge: direct interaction of TLR4 with NAD(P)H oxidase 4 isozyme is essential for lipopolysaccharide-induced production of reactive oxygen species and activation of NF-kappa B." J Immunol **173**(6): 3589-3593.

Patsouris, D., P. P. Li, D. Thapar, J. Chapman, J. M. Olefsky and J. G. Neels (2008). "Ablation of CD11c-positive cells normalizes insulin sensitivity in obese insulin resistant animals." Cell Metab **8**(4): 301-309.

Pennock, N. D., J. T. White, E. W. Cross, E. E. Cheney, B. A. Tamburini and R. M. Kedl (2013). "T cell responses: naive to memory and everything in between." Adv Physiol Educ **37**(4): 273-283.

Peterson, R. M., L. Beeson, E. Shulz, A. Firek, M. De Leon, H. Balcazar, S. Tonstad and Z. R. Cordero-Macintyre (2010). "Impacting obesity and glycemic control using a culturally-sensitive diabetes education program in Hispanic patients with type 2 diabetes." Int J Body Compos Res **8**(3): 85-94.

Pickup, J. C. and M. A. Crook (1998). "Is type II diabetes mellitus a disease of the innate immune system?" Diabetologia **41**(10): 1241-1248.

Piro, S., E. T. Maniscalchi, A. Monello, G. Pandini, L. G. Mascali, A. M. Rabuazzo and F. Purrello (2010). "Palmitate affects insulin receptor phosphorylation and intracellular insulin signal in a pancreatic alpha-cell line." Endocrinology **151**(9): 4197-4206.

Poggi, M., J. Jager, O. Paulmyer-Lacroix, F. Peiretti, T. Gremeaux, M. Verdier, M. Grino, A. Stepanian, S. Msika, R. Burcelin, D. de Prost, J. F. Tanti and M. C. Alessi (2009). "The inflammatory receptor CD40 is expressed on human adipocytes: contribution to crosstalk between lymphocytes and adipocytes." Diabetologia **52**(6): 1152-1163.

Porcelli, S., M. B. Brenner, J. L. Greenstein, S. P. Balk, C. Terhorst and P. A. Bleicher (1989). "Recognition of cluster of differentiation 1 antigens by human CD4-CD8-cytolytic T lymphocytes." Nature **341**(6241): 447-450.

Probst, H. C., J. Lagnel, G. Kollias and M. van den Broek (2003). "Inducible transgenic mice reveal resting dendritic cells as potent inducers of CD8+ T cell tolerance." Immunity **18**(5): 713-720.

Rausch, M. E., S. Weisberg, P. Vardhana and D. V. Tortoriello (2008). "Obesity in C57BL/6J mice is characterized by adipose tissue hypoxia and cytotoxic T-cell infiltration." Int J Obes (Lond) **32**(3): 451-463.

Reitman, Z. J., G. Jin, E. D. Karoly, I. Spasojevic, J. Yang, K. W. Kinzler, Y. He, D. D. Bigner, B. Vogelstein and H. Yan (2011). "Profiling the effects of isocitrate dehydrogenase 1 and 2 mutations on the cellular metabolome." Proc Natl Acad Sci U S A **108**(8): 3270-3275.

Reth, M. (2002). "Hydrogen peroxide as second messenger in lymphocyte activation." Nat Immunol **3**(12): 1129-1134.

Reynolds, C. M., F. C. McGillicuddy, K. A. Harford, O. M. Finucane, K. H. Mills and H. M. Roche (2012). "Dietary saturated fatty acids prime the NLRP3 inflammasome via TLR4 in dendritic cells-implications for diet-induced insulin resistance." Mol Nutr Food Res **56**(8): 1212-1222.

Riserus, U. (2008). "Fatty acids and insulin sensitivity." Curr Opin Clin Nutr Metab Care **11**(2): 100-105.

Riserus, U., W. C. Willett and F. B. Hu (2009). "Dietary fats and prevention of type 2 diabetes." Prog Lipid Res **48**(1): 44-51.

Rivollier, A., J. He, A. Kole, V. Valatas and B. L. Kelsall (2012). "Inflammation switches the differentiation program of Ly6Chi monocytes from antiinflammatory macrophages to inflammatory dendritic cells in the colon." J Exp Med **209**(1): 139-155.

Rocha, V. Z., E. J. Folco, G. Sukhova, K. Shimizu, I. Gotsman, A. H. Vernon and P. Libby (2008). "Interferon-gamma, a Th1 cytokine, regulates fat inflammation: a role for adaptive immunity in obesity." Circ Res **103**(5): 467-476.

Romani, N., S. Gruner, D. Brang, E. Kampgen, A. Lenz, B. Trockenbacher, G. Konwalinka, P. O. Fritsch, R. M. Steinman and G. Schuler (1994). "Proliferating dendritic cell progenitors in human blood." J Exp Med **180**(1): 83-93.

Romani, N., D. Reider, M. Heuer, S. Ebner, E. Kampgen, B. Eibl, D. Niederwieser and G. Schuler (1996). "Generation of mature dendritic cells from human blood. An improved method with special regard to clinical applicability." J Immunol Methods **196**(2): 137-151.

Rothstein, T. L., D. O. Griffin, N. E. Holodick, T. D. Quach and H. Kaku (2013). "Human B-1 cells take the stage." <u>Ann N Y Acad Sci</u> **1285**: 97-114.

Saberi, M., N. B. Woods, C. de Luca, S. Schenk, J. C. Lu, G. Bandyopadhyay, I. M. Verma and J. M. Olefsky (2009). "Hematopoietic cell-specific deletion of toll-like receptor 4 ameliorates hepatic and adipose tissue insulin resistance in high-fat-fed mice." <u>Cell Metab</u> **10**(5): 419-429.

Salgin, B., K. K. Ong, A. Thankamony, P. Emmett, N. J. Wareham and D. B. Dunger (2012). "Higher fasting plasma free fatty acid levels are associated with lower insulin secretion in children and adults and a higher incidence of type 2 diabetes." <u>J Clin Endocrinol Metab</u> **97**(9): 3302-3309.

Salsman, S. J., K. Hensley and R. A. Floyd (2005). "Sensitivity of protein tyrosine phosphatase activity to the redox environment, cytochrome C, and microperoxidase." <u>Antioxid Redox Signal</u> **7**(7-8): 1078-1088.

Salto, L. M., Z. Cordero-MacIntyre, L. Beeson, E. Schulz, A. Firek and M. De Leon (2011). "En Balance participants decrease dietary fat and cholesterol intake as part of a culturally sensitive Hispanic diabetes education program." <u>Diabetes Educ</u> **37**(2): 239-253.

Sam, S. and T. Mazzone (2014). "Adipose tissue changes in obesity and the impact on metabolic function." <u>Transl Res</u>.

Sancho, M., E. Diani, M. Beato and A. Jordan (2008). "Depletion of human histone H1 variants uncovers specific roles in gene expression and cell growth." <u>PLoS Genet</u> **4**(10): e1000227.

Santos, S., A. Oliveira and C. Lopes (2013). "Systematic review of saturated fatty acids on inflammation and circulating levels of adipokines." <u>Nutr Res</u> **33**(9): 687-695.

Schiefner, A. and I. A. Wilson (2009). "Presentation of lipid antigens by CD1 glycoproteins." <u>Curr Pharm Des</u> **15**(28): 3311-3317.

Seager Danciger, J., M. Lutz, S. Hama, D. Cruz, A. Castrillo, J. Lazaro, R. Phillips, B. Premack and J. Berliner (2004). "Method for large scale isolation, culture and cryopreservation of human monocytes suitable for chemotaxis, cellular adhesion assays, macrophage and dendritic cell differentiation." <u>J Immunol Methods</u> **288**(1-2): 123-134.

Segura, E., A. L. Albiston, I. P. Wicks, S. Y. Chai and J. A. Villadangos (2009). "Different cross-presentation pathways in steady-state and inflammatory dendritic cells." <u>Proc Natl Acad Sci U S A</u> **106**(48): 20377-20381.

Serbina, N. V., T. P. Salazar-Mather, C. A. Biron, W. A. Kuziel and E. G. Pamer (2003). "TNF/iNOS-producing dendritic cells mediate innate immune defense against bacterial infection." <u>Immunity</u> **19**(1): 59-70.

Shaikh, S. R., C. A. Jolly and R. S. Chapkin (2012). "n-3 Polyunsaturated fatty acids exert immunomodulatory effects on lymphocytes by targeting plasma membrane molecular organization." <u>Mol Aspects Med</u> **33**(1): 46-54.

Shen, L., M. H. Yen Chng, M. N. Alonso, R. Yuan, D. A. Winer and E. G. Engleman (2014). "B-1a lymphocytes attenuate insulin resistance." <u>Diabetes</u>.

Sheridan, P. A., H. A. Paich, J. Handy, E. A. Karlsson, M. G. Hudgens, A. B. Sammon, L. A. Holland, S. Weir, T. L. Noah and M. A. Beck (2012). "Obesity is associated with impaired immune response to influenza vaccination in humans." <u>Int J Obes (Lond)</u> **36**(8): 1072-1077.

Shi, H., M. V. Kokoeva, K. Inouye, I. Tzameli, H. Yin and J. S. Flier (2006). "TLR4 links innate immunity and fatty acid-induced insulin resistance." <u>J Clin Invest</u> **116**(11): 3015-3025.

Song, M. J., K. H. Kim, J. M. Yoon and J. B. Kim (2006). "Activation of Toll-like receptor 4 is associated with insulin resistance in adipocytes." <u>Biochem Biophys Res Commun</u> **346**(3): 739-745.

Stagakis, I., G. Bertsias, S. Karvounaris, M. Kavousanaki, D. Virla, A. Raptopoulou, D. Kardassis, D. T. Boumpas and P. I. Sidiropoulos (2012). "Anti-tumor necrosis factor therapy improves insulin resistance, beta cell function and insulin signaling in active rheumatoid arthritis patients with high insulin resistance." <u>Arthritis Res Ther</u> **14**(3): R141.

Stefanovic-Racic, M., X. Yang, M. S. Turner, B. S. Mantell, D. B. Stolz, T. L. Sumpter, I. J. Sipula, N. Dedousis, D. K. Scott, P. A. Morel, A. W. Thomson and R. M. O'Doherty (2012). "Dendritic cells promote macrophage infiltration and comprise a substantial proportion of obesity-associated increases in CD11c+ cells in adipose tissue and liver." <u>Diabetes</u> **61**(9): 2330-2339.

Steinman, R. M. and J. Swanson (1995). "The endocytic activity of dendritic cells." <u>J Exp Med</u> **182**(2): 283-288.

Storlien, L. H., A. B. Jenkins, D. J. Chisholm, W. S. Pascoe, S. Khouri and E. W. Kraegen (1991). "Influence of dietary fat composition on development of insulin resistance in rats. Relationship to muscle triglyceride and omega-3 fatty acids in muscle phospholipid." <u>Diabetes</u> **40**(2): 280-289.

Strissel, K. J., J. DeFuria, M. E. Shaul, G. Bennett, A. S. Greenberg and M. S. Obin (2010). "T-cell recruitment and Th1 polarization in adipose tissue during diet-induced obesity in C57BL/6 mice." Obesity (Silver Spring) **18**(10): 1918-1925.

Suganami, T., T. Mieda, M. Itoh, Y. Shimoda, Y. Kamei and Y. Ogawa (2007). "Attenuation of obesity-induced adipose tissue inflammation in C3H/HeJ mice carrying a Toll-like receptor 4 mutation." Biochem Biophys Res Commun **354**(1): 45-49.

Suganami, T., K. Tanimoto-Koyama, J. Nishida, M. Itoh, X. Yuan, S. Mizuarai, H. Kotani, S. Yamaoka, K. Miyake, S. Aoe, Y. Kamei and Y. Ogawa (2007). "Role of the Toll-like receptor 4/NF-kappaB pathway in saturated fatty acid-induced inflammatory changes in the interaction between adipocytes and macrophages." Arterioscler Thromb Vasc Biol **27**(1): 84-91.

Suganami, T., X. Yuan, Y. Shimoda, K. Uchio-Yamada, N. Nakagawa, I. Shirakawa, T. Usami, T. Tsukahara, K. Nakayama, Y. Miyamoto, K. Yasuda, J. Matsuda, Y. Kamei, S. Kitajima and Y. Ogawa (2009). "Activating transcription factor 3 constitutes a negative feedback mechanism that attenuates saturated Fatty acid/toll-like receptor 4 signaling and macrophage activation in obese adipose tissue." Circ Res **105**(1): 25-32.

Takashiba, S., T. E. Van Dyke, S. Amar, Y. Murayama, A. W. Soskolne and L. Shapira (1999). "Differentiation of monocytes to macrophages primes cells for lipopolysaccharide stimulation via accumulation of cytoplasmic nuclear factor kappaB." Infect Immun **67**(11): 5573-5578.

Talukdar, S., Y. Oh da, G. Bandyopadhyay, D. Li, J. Xu, J. McNelis, M. Lu, P. Li, Q. Yan, Y. Zhu, J. Ofrecio, M. Lin, M. B. Brenner and J. M. Olefsky (2012). "Neutrophils mediate insulin resistance in mice fed a high-fat diet through secreted elastase." Nat Med **18**(9): 1407-1412.

Terme, J. M., B. Sese, L. Millan-Arino, R. Mayor, J. C. Izpisua Belmonte, M. J. Barrero and A. Jordan (2011). "Histone H1 variants are differentially expressed and incorporated into chromatin during differentiation and reprogramming to pluripotency." J Biol Chem **286**(41): 35347-35357.

Tezuka, H., Y. Abe, M. Iwata, H. Takeuchi, H. Ishikawa, M. Matsushita, T. Shiohara, S. Akira and T. Ohteki (2007). "Regulation of IgA production by naturally occurring TNF/iNOS-producing dendritic cells." Nature **448**(7156): 929-933.

Thomas, C. C. and L. H. Philipson (2015). "Update on Diabetes Classification." Med Clin North Am **99**(1): 1-16.

Ting, J. P., R. C. Lovering, E. S. Alnemri, J. Bertin, J. M. Boss, B. K. Davis, R. A. Flavell, S. E. Girardin, A. Godzik, J. A. Harton, H. M. Hoffman, J. P. Hugot, N.

Inohara, A. Mackenzie, L. J. Maltais, G. Nunez, Y. Ogura, L. A. Otten, D. Philpott, J. C. Reed, W. Reith, S. Schreiber, V. Steimle and P. A. Ward (2008). "The NLR gene family: a standard nomenclature." Immunity **28**(3): 285-287.

Titov, V. N., V. V. Krylin and K. Shiriaeva Iu (2011). "[Prevention of atherosclerosis. Excess of palmitic acid in food--a cause of hypercholesterolemia, inflammatory syndrome, insulin resistance in myocytes, and apoptosis]." Klin Lab Diagn(2): 4-15.

Tripathy, D., P. Mohanty, S. Dhindsa, T. Syed, H. Ghanim, A. Aljada and P. Dandona (2003). "Elevation of free fatty acids induces inflammation and impairs vascular reactivity in healthy subjects." Diabetes **52**(12): 2882-2887.

Unger, J. and C. G. Parkin (2010). "Type 2 diabetes: an expanded view of pathophysiology and therapy." Postgrad Med **122**(3): 145-157.

Virtanen, S. M., S. Niinisto, J. Nevalainen, I. Salminen, H. M. Takkinen, S. Kaaria, L. Uusitalo, G. Alfthan, M. G. Kenward, R. Veijola, O. Simell, J. Ilonen and M. Knip (2010). "Serum fatty acids and risk of advanced beta-cell autoimmunity: a nested case-control study among children with HLA-conferred susceptibility to type I diabetes." Eur J Clin Nutr.

Wang, H., Q. Hao, Q. R. Li, X. W. Yan, S. Ye, Y. S. Li, N. Li and J. S. Li (2007). "Omega-3 polyunsaturated fatty acids affect lipopolysaccharide-induced maturation of dendritic cells through mitogen-activated protein kinases p38." Nutrition **23**(6): 474-482.

Wang, Z., D. Liu, F. Wang, S. Liu, S. Zhao, E. A. Ling and A. Hao (2012). "Saturated fatty acids activate microglia via Toll-like receptor 4/NF-kappaB signalling." Br J Nutr **107**(2): 229-241.

Weatherill, A. R., J. Y. Lee, L. Zhao, D. G. Lemay, H. S. Youn and D. H. Hwang (2005). "Saturated and polyunsaturated fatty acids reciprocally modulate dendritic cell functions mediated through TLR4." J Immunol **174**(9): 5390-5397.

Wersto, R. P., F. J. Chrest, J. F. Leary, C. Morris, M. A. Stetler-Stevenson and E. Gabrielson (2001). "Doublet discrimination in DNA cell-cycle analysis." Cytometry **46**(5): 296-306.

Wheeler, G., S. B. Montgomery, L. Beeson, K. Bahjri, E. Shulz, A. Firek, M. De Leon and Z. Cordero-MacIntyre (2012). "En Balance: the effects of Spanish diabetes education on physical activity changes and diabetes control." Diabetes Educ **38**(5): 723-732.

Winer, D. A., S. Winer, M. H. Y. Chng, L. Shen and E. G. Engleman (2014). "B Lymphocytes in obesity-related adipose tissue inflammation and insulin resistance." Cellular and Molecular Life Sciences **71**(6): 1033-1043.

Winer, D. A., S. Winer, L. Shen, P. P. Wadia, J. Yantha, G. Paltser, H. Tsui, P. Wu, M. G. Davidson, M. N. Alonso, H. X. Leong, A. Glassford, M. Caimol, J. A. Kenkel, T. F. Tedder, T. McLaughlin, D. B. Miklos, H. M. Dosch and E. G. Engleman (2011). "B cells promote insulin resistance through modulation of T cells and production of pathogenic IgG antibodies." Nat Med **17**(5): 610-617.

Winer, S., Y. Chan, G. Paltser, D. Truong, H. Tsui, J. Bahrami, R. Dorfman, Y. Wang, J. Zielenski, F. Mastronardi, Y. Maezawa, D. J. Drucker, E. Engleman, D. Winer and H. M. Dosch (2009). "Normalization of obesity-associated insulin resistance through immunotherapy." Nat Med **15**(8): 921-929.

Winer, S., G. Paltser, Y. Chan, H. Tsui, E. Engleman, D. Winer and H. M. Dosch (2009). "Obesity predisposes to Th17 bias." Eur J Immunol **39**(9): 2629-2635.

Winer, S. and D. A. Winer (2012). "The adaptive immune system as a fundamental regulator of adipose tissue inflammation and insulin resistance." Immunol Cell Biol **90**(8): 755-762.

Wong, B. X., R. A. Kyle, P. C. Myhill, K. D. Croft, C. M. Quinn, W. Jessup and B. B. Yeap (2011). "Dyslipidemic diabetic serum increases lipid accumulation and expression of stearoyl-CoA desaturase in human macrophages." Lipids **46**(10): 931-941.

Wong, S. W., M. J. Kwon, A. M. Choi, H. P. Kim, K. Nakahira and D. H. Hwang (2009). "Fatty acids modulate Toll-like receptor 4 activation through regulation of receptor dimerization and recruitment into lipid rafts in a reactive oxygen species-dependent manner." J Biol Chem **284**(40): 27384-27392.

Wu, D., A. B. Molofsky, H. E. Liang, R. R. Ricardo-Gonzalez, H. A. Jouihan, J. K. Bando, A. Chawla and R. M. Locksley (2011). "Eosinophils sustain adipose alternatively activated macrophages associated with glucose homeostasis." Science **332**(6026): 243-247.

Wu, H., S. Ghosh, X. D. Perrard, L. Feng, G. E. Garcia, J. L. Perrard, J. F. Sweeney, L. E. Peterson, L. Chan, C. W. Smith and C. M. Ballantyne (2007). "T-cell accumulation and regulated on activation, normal T cell expressed and secreted upregulation in adipose tissue in obesity." Circulation **115**(8): 1029-1038.

Wu, L., V. V. Parekh, J. Hsiao, D. Kitamura and L. Van Kaer (2014). "Spleen supports a pool of innate-like B cells in white adipose tissue that protects against obesity-associated insulin resistance." Proc Natl Acad Sci U S A.

Wueest, S., R. A. Rapold, D. M. Schumann, J. M. Rytka, A. Schildknecht, O. Nov, A. V. Chervonsky, A. Rudich, E. J. Schoenle, M. Y. Donath and D. Konrad (2010). "Deletion of Fas in adipocytes relieves adipose tissue inflammation and hepatic manifestations of obesity in mice." J Clin Invest **120**(1): 191-202.

Xu, F., K. Zhang and M. Grunstein (2005). "Acetylation in histone H3 globular domain regulates gene expression in yeast." Cell **121**(3): 375-385.

Xu, H., H. An, J. Hou, C. Han, P. Wang, Y. Yu and X. Cao (2008). "Phosphatase PTP1B negatively regulates MyD88- and TRIF-dependent proinflammatory cytokine and type I interferon production in TLR-triggered macrophages." Mol Immunol **45**(13): 3545-3552.

Yang, X., X. Zhang, B. L. Heckmann, X. Lu and J. Liu (2011). "Relative contribution of adipose triglyceride lipase and hormone-sensitive lipase to tumor necrosis factor-alpha (TNF-alpha)-induced lipolysis in adipocytes." J Biol Chem **286**(47): 40477-40485.

Young, K. M., C. M. Gray and L. G. Bekker (2013). "Is obesity a risk factor for vaccine non-responsiveness?" PLoS One **8**(12): e82779.

Zeyda, M., J. Huber, G. Prager and T. M. Stulnig (2011). "Inflammation correlates with markers of T-cell subsets including regulatory T cells in adipose tissue from obese patients." Obesity (Silver Spring) **19**(4): 743-748.

Zeyda, M., M. D. Saemann, K. M. Stuhlmeier, D. G. Mascher, P. N. Nowotny, G. J. Zlabinger, W. Waldhausl and T. M. Stulnig (2005). "Polyunsaturated fatty acids block dendritic cell activation and function independently of NF-kappaB activation." J Biol Chem **280**(14): 14293-14301.

Zhang, K., M. Schrag, A. Crofton, R. Trivedi, H. Vinters and W. Kirsch (2012). "Targeted proteomics for quantification of histone acetylation in Alzheimer's disease." Proteomics **12**(8): 1261-1268.

Zhang, Y., M. Cooke, S. Panjwani, K. Cao, B. Krauth, P. Y. Ho, M. Medrzycki, D. T. Berhe, C. Pan, T. C. McDevitt and Y. Fan (2012). "Histone h1 depletion impairs embryonic stem cell differentiation." PLoS Genet **8**(5): e1002691.

Zhu, H. (2012). "Immunofluorescence (Especially for cells growing on the coverglass)." Bio-protocol **2**(4).

Zietara, N., M. Lyszkiewicz, J. Puchalka, G. Pei, M. G. Gutierrez, S. Lienenklaus, E. Hobeika, M. Reth, V. A. Martins dos Santos, A. Krueger and S. Weiss (2013). "Immunoglobulins drive terminal maturation of splenic dendritic cells." Proc Natl Acad Sci U S A **110**(6): 2282-2287.